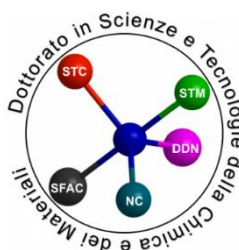


University of Genova



Department of Chemistry and Industrial Chemistry (DCCI)
**Doctorate in “Sciences and Technologies of Chemistry and
Materials” XXXII cycle (cod. 6200)**
Curriculum: *Chemical Sciences and Technologies*



**Benzo-fused nitroheterocycles *via* benzannulation with
nitro-1,3-butadienes: synthesis and application.**

Ph.D. Student
Angela Pagano

Supervisor
Professor Giovanni Petrillo

1st November the 2016 - 31st October 2019

Sarà pure la seconda pagina, ma è questa l'ultima pagina che ho scritto: quella che mi ha messo più in difficoltà. La pagina della dedica è forse l'unica pagina che tutti i tuoi amici e familiari leggono mentre stai stappando lo spumante e lo stai versando nei bicchieri.

Eppure, di tutti questi tre anni trascorsi, questo lavoro di dottorato ha rappresentato una piccola parte della mia esistenza. Lavoro di cui sono orgogliosa e fiera, ma che non ritengo così importante. Ripensando ai tre anni trascorsi, ho cambiato città allontanandomi dal posto che era stato il mio nido per anni, ho salutato la mia famiglia e i miei amici ignara che avrei dovuto iniziare a combattere contro il mostro della nostalgia. Ho imparato a sentire mio un altro posto, ho imparato a integrarmi in una città sicuramente non famosa per l'ospitalità.

Ho conosciuto nuovi amici, visitato molti posti, goduto della mia prima indipendenza, incontrato il mio primo grande amore, ho vissuto per sei mesi all'estero dove ho dovuto essere più forte di quanto non lo fossi mai stata prima. Sono diventata zia, imparando ad innamorarmi di manine e piedini piccolissimi e accettando che però sarebbero cresciuti lontano da me.

Insomma, sono cambiata e cresciuta così tanto che la tesi di dottorato rappresenta per me solo una delle tantissime esperienze nuove vissute.

Quindi dedicare la mia tesi non sarebbe tutto, quello che vorrei dedicare sono questi tre anni nella loro interezza con le trasformazioni e i cambiamenti che hanno reso me una persona diversa, si spera migliore.

A me

ACKNOWLEDGEMENTS

First and foremost, I would like to express my heartiest gratitude to my supervisor Prof. Giovanni Petrillo who expertly supported my Ph.D. study. His guidance and enthusiastic encouragement helped me in all the time, stimulating and directing me in academic research, conference communications and journal papers. He never doubted my capabilities and always had confidence in my ability bringing out the best in me. His dedication to students has been both admirable and inspirational. I feel honored to have had a chance to work with him and learn from him. My appreciation for his guidance and continuous support is immeasurable.

My sincere thanks also go to Dr. Cinzia Tavani, Dr. Lara Bianchi, Dr. Massimo Maccagno and Dr. Alice Benzi, for their feedback, cooperation and of course friendship.

I am thankful to Prof. Andrea Mazzanti and Dr. Michele Mancinelli for the interesting collaboration which improved my research.

Last but not the least, I am also grateful to Prof. Richard J. K. Taylor, Dr. William P. Unsworth and Dr. Hon E. P. Ho, who provided me an opportunity to join their team, and who gave access to their laboratories and research facilities.

ABSTRACT

Nitroindoles, despite their scanty occurrence in nature, are attractive reactive intermediates in organic synthesis thanks to the coupling of the properties of the nitro group and of the indole moiety.^[1] While nitration of the pyrrole nucleus can be easily achieved, nitration on the benzene ring represents a more challenging target. *Ex-novo* construction of the pyrrole onto a functionalized benzene derivative is, by far, the synthetic strategy most frequently exploited to access indole nitrated on the benzene ring. Herein, we expand the synthetic access to such nitroindoles reporting an original protocol based on the *ex-novo* construction of the benzene ring onto pyrrole employing mono- or dinitro-1,3-butadienes as powerful C₄ benzannulating agents. This appealing, metal-free process characterized by high atom economy and mild reaction conditions allows to synthesize nitroindoles characterized by patterns of substitution not easy to be obtained otherwise.^[2] Such unusual substitution patterns have demonstrated to be promising for further elaborations, *i.e.* the application of the classic Cadogan reaction conditions in order to access pyrrolocarbazoles with a rarely reported ring fusion.^[3]

A very interesting side project regarded the synthesis of a series of atropisomeric naphthyl nitroindoles with two stereogenic axes originated from steric hindrances forcing the naphthyl groups out of the indole plane; the asymmetry of the indole “spacer” makes both the *syn* and *anti* diastereoisomers entail an atropisomeric pair. A stereodynamic analysis of such new atropisomeric nitroindoles has been done resolving atropisomers by chiral HPLC and determining their absolute configuration and the rotational barriers of the indole–naphthyl axes.^[4]

This work, within an Erasmus+ project, demonstrates also the photochemical activity of electron donor-acceptor (EDA) complexes providing a way to generate radicals under mild conditions. This strategy has recently found application in chemical synthesis. Reported methods classically relied on the formation of intermolecular EDA complexes. Herein, we further expand the synthetic utility of this strategy demonstrating that indole-tethered ynones form an intramolecular electron donor-acceptor complex that can undergo visible-light-induced charge transfer to promote thiyl radical generation from thiols.^[5] This initiates a novel radical chain sequence, based on dearomatizing spirocyclization with concomitant C–S bond formation. Sulfur-containing spirocycles are formed in high yields using this simple and mild synthetic protocol, in which neither transition metal catalysts nor photocatalysts are required. The proposed mechanism is supported by various mechanistic studies, and the unusual radical initiation mode represents only the second report of the use of an intramolecular electron donor-acceptor complex in synthesis.

CONTENTS

1. INTRODUCTION.....	6
1.1. <i>N</i> -HETEROCYCLIC COMPOUNDS.	6
1.2. INDOLES: OCCURRENCE AND SIGNIFICANCE.	6
1.3. NITROINDOLES: OCCURRENCE AND SIGNIFICANCE.	8
1.4. NITROINDOLES: SYNTHESIS.	10
1.4.1. <i>Direct nitration of indoles.</i>	10
1.4.2. <i>Heteroannulation approach.</i>	12
1.4.3. <i>Benzannulation approach.</i>	18
2. SCOPE.....	19
3. RESULTS AND DISCUSSION.....	21
3.1. AN UNPRECEDENTED EASY ACCESS TO RARE NITROINDOLES.	21
3.1.1. <i>Atropisomerism.</i>	28
3.2. SEQUENTIAL ANNULATIONS TO NOVEL PYRROLO[3,2- <i>c</i>]CARBAZOLES.	33
4. ERASMUS PROJECT.....	38
4.1. SPIROINDOLES AND SPIROINDOLINES.....	38
4.2. RADICAL SPIROCYCLISATION OF INDOLE-TETHERED YNONES.....	40
4.3. MECHANISTIC INVESTIGATIONS.	44
5. CONCLUSIONS.....	47
6. EXPERIMENTAL SECTION	49
7. ABBREVIATION LIST	82
8. REFERENCES.....	84

1. INTRODUCTION

1.1. *N*-Heterocyclic compounds.

Heterocycles are cyclic structures with two or more different kinds of atoms in the ring; depending on the ring size, the nature and number of the heteroatoms, the possible heterocyclic systems are limitless: for this reason, it is not surprisingly that they constitute the largest and most varied family of organic compounds.^[6] Furthermore, a valuable balance between chemical stability and reactivity, the latter essentially due to the electronic distribution (polarization) within a C-Het bond, makes heterocycles very effective building-blocks in organic synthesis^[7] and most privileged final structures in, *e.g.*, the pharmacological or biological fields. Other important applications of heterocyclic compounds encompass their use as anticorrosive agents, agrochemicals, herbicides, fungicides, photostabilizers, photographic sensitizers and developers, copolymers, dyestuff, sensitizers, fluorescent whiteners, booster agents, flavouring agents, and antioxidants and vulcanization accelerators in the rubber industry.^[8]

Among heterocycles, a prominent role is undoubtedly played by *N*-heterocycles, which are, indeed, omnipresent in nature, playing essential roles in all living systems: pyrimidine and purine bases of DNA and RNA, heterocyclic rings contained in three of the essential amino acids (proline, histidine, and tryptophan) found in enzymes and proteins, several vitamins and cofactors (thiamine, nicotinamide, riboflavin, folic acid, biotin, just to cite some), pigments (chlorophyll) and hormones (serotonin and histamine) are noticeable examples of their vital roles.^[9]

This wide distribution in nature is strictly connected primarily to the broad spectrum of pharmacological activities that such compounds display. As a matter of fact, besides a vast and diversified natural production, nowadays, the large majority of pharmaceuticals are *N*-heterocyclic compounds synthesized by mimicking nature, with widespread use as anticancer agents, analeptics, analgesics, hypnotics, and vasopressor modifiers.^[10]

Conceivably enough, this range of applications has stimulated during the years the design of efficient synthetic methodologies.^[11] In this scenario, heterocyclic chemistry (and *N*-heterocyclic chemistry, in particular) represents one of the most valuable sources of novel compounds with the most diverse physical, chemical and biological properties.

1.2. Indoles: occurrence and significance.

In the general field of heterocycles, the possible fusion of two or more rings leads to a range of polycyclic structures. Indole is an example of an aromatic *N*-heterocyclic compound with a fused bicyclic structure, consisting of a six-membered benzene ring fused to a five-membered pyrrole ring.

Isolated the first time by Baeyer from the reaction of indigo with a mixture of sulfuric acid and sulfuric anhydride,^[12] indole (*indigo+oleum*) represents one of the most ubiquitous heterocyclic structures both in nature, where it is widely present in plants, and in industry, as an important core of agrochemicals, functional polymers/sensors, fragrances, and dyes.^[13] However, the significance of indole derivatives is best highlighted by their biological applications.^[14] To catalogue the complete biological activity range of indole derivatives is nearly impossible, and only some indications about the scope of such activities are reported in

Figure 1. Tryptophan is an essential amino acid. It is degraded by higher plants to heteroauxin, a plant growth-regulating hormone, and by bacteria to tryptamine, which is the start for some of the condensed ring alkaloids. Serotonin and melatonin are key neurotransmitters in the central nervous system. Ondansetron is an indole-based drug used for the suppression of nausea and vomiting caused by cancer chemotherapy and radiotherapy. Oxypertine is an antipsychotic and antidepressant used in the treatment of schizophrenia. Arbidol is an antiviral treatment for influenza infection. The hallucinogenic activity of lysergic acid diethylamide (LSD) is well known. Several anticancer drugs contain an indole core, the most famous of which are the pervinca alkaloids vinblastine and vincristine, both of which continue to be important drugs for the treatment of Hodgkin's disease, childhood leukemia, and other types of cancer.

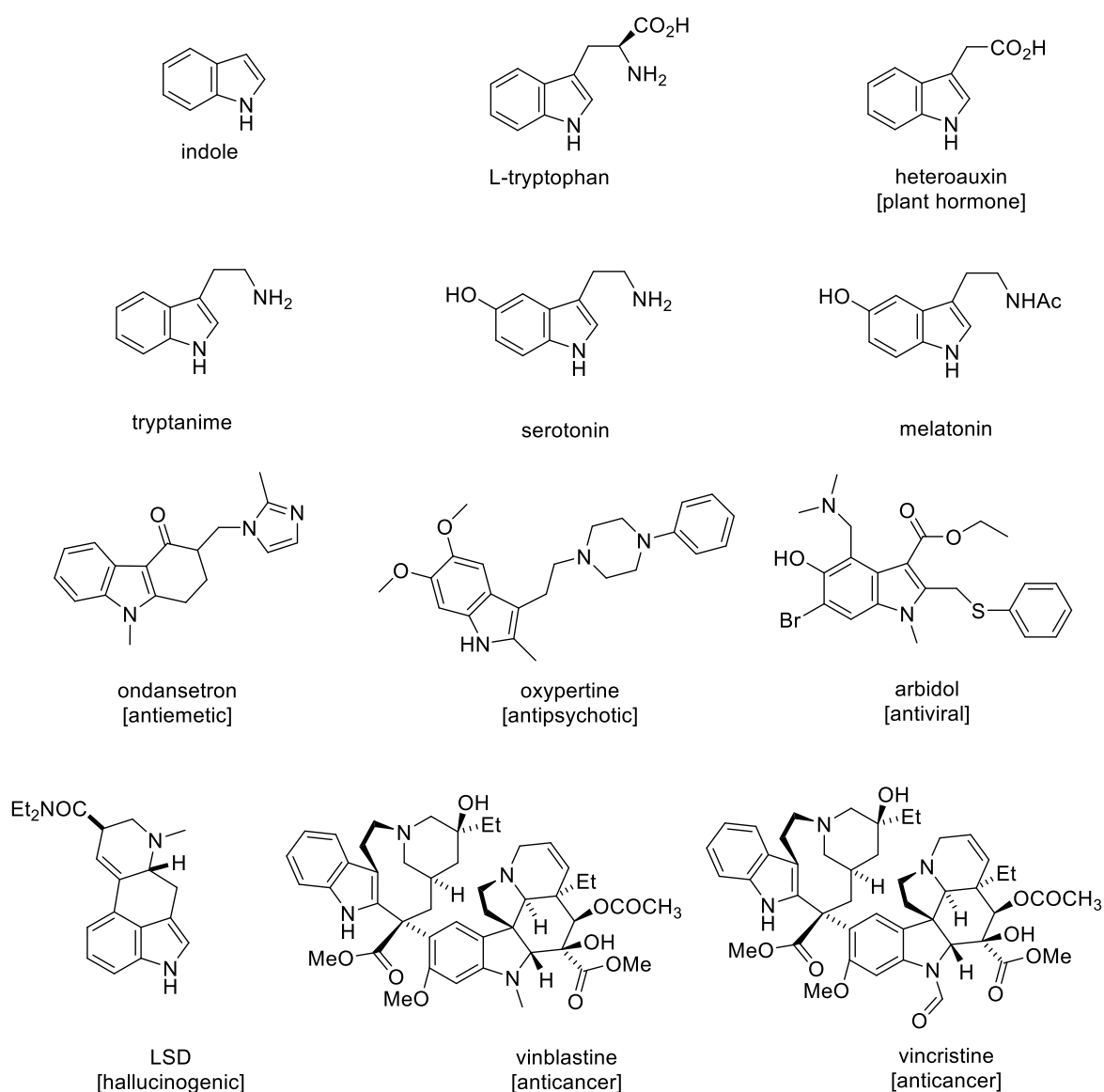


Figure 1. Biologically important indole derivatives.

1.3. Nitroindoles: occurrence and significance.

Although, as reported before, the indole motif can be considered one of the most widespread *N*-heterocycles in nature, the natural occurrence of nitrated indole is definitely scanty.^[1]

Thaxtomin phytotoxins, generated as microbial metabolites, are a rare example of natural compounds possessing a unique 4-nitroindole moiety, essential requirement for their phytotoxicity.^[15] They have been found in the common potato scab infected by the soil bacterium *Streptomyces scabies*.^[16] During the last year, thaxtomin A (Figure 2), the most predominant and active member of such a family, attracted attention due to its herbicidal activity.^[17]

The first total synthesis of thaxtomin A was reported in 2013,^[18] where the 4-nitroindole moiety was synthesized by Pd-catalyzed direct coupling of an aldehyde with 3-nitro-2-iodoaniline as reported later (Scheme 2, d).

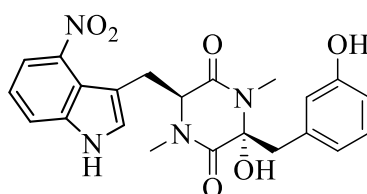


Figure 2. Thaxtomin A: a natural 4-nitroindole derivative.

Besides the thaxtomins discussed above, the only other naturally occurring nitroindole appears to be a 3-nitroindole isolated from the Arctic sea lice bacterium *Salgenticibacter* sp. T436 along with 18 other aromatic nitro compounds.^[19]

Despite the scanty presence of nitroindoles in nature, thanks to the coupling of the properties of the nitro group and of the indole moiety, nitroindoles are anyway attractive targets in organic synthesis as reactive intermediates, also due to the possible transformations of the nitro group into different other valuable functionalities, besides to its reactivity-affecting and group-orienting effects.^[1] Although reduction of the nitro group is a key transformation widely used to access the corresponding aminoindoles, often in turn precursors of other compounds^[20] (such as, *e.g.* biologically active compounds^[21]), nitroindoles have demonstrated during the years to be valuable precursor of fused nitrogenated polycycles *e.g.* via [3+2] dearomatizing annulation processes,^[22] multicomponent heteroannulations,^[23] and multicomponent domino cycloadditions.^[21]

Already since 1973, Garcia *et al.* transformed 1-methyl-3-nitroindole-2-carboxylic acid into several [1,4]diazepino[6,5-*b*]indoles **1** (Figure 3, a).^[24] 2-Methyl-4-nitro-1*H*-indole has been used for the first generation supply route of 2AZD1981 (Figure 3, a),^[25] an AstraZeneca inflammatory drug. In 2019, Liangce Rong *et al.* reported a novel method for the synthesis of nitrogen-containing spiro compounds **2** (Figure 3, a) directly from 5-nitroindole *via* an *in situ* reduction and multicomponent cyclization reaction.^[26] Moreover, derivatives of 5-nitroindole are used in the synthesis of nitrazepam (Figure 3, b),^[27] an hypnotic drug. On the other hand, derivatives of 6-nitroindole are used in the synthesis of arnoamine B (Figure 3, a),^[28] a biologically-active fused polycyclic aromatic alkaloid isolated from marine sources.

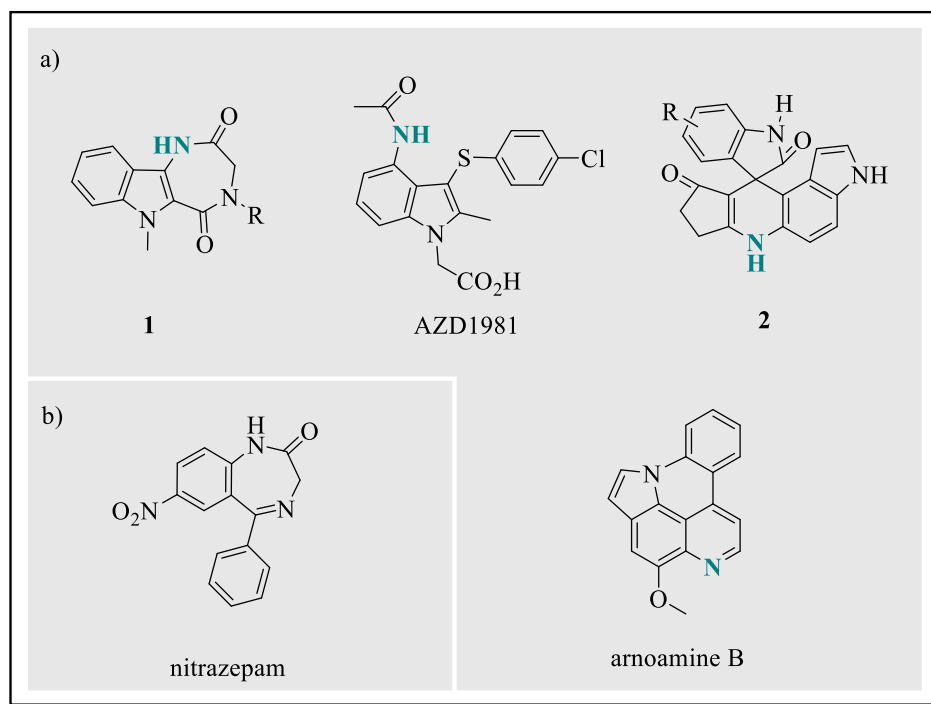


Figure 3. a) Fused nitrogenated polycycles synthesized from nitroindoles: nitrogen derived from the original nitro group being indicated in green; b) the hypnotic drug nitrazepam.

The nitro group has also proven to be a valuable pharmacophore,^[29] possibly thanks to partially reduced forms. Biological evaluation of 4-nitroindole derivatives has shown activity as 5HT_{2A} receptor agonist.^[30] 5-Nitroindole is used as a universal base analogue in oligonucleotides (Figure 4) thanks to its ability to replace any of the four natural bases without significantly destabilizing neighbouring base-pair interactions or disrupting the expected functional capability of the resulting modified oligonucleotide. Incorporation of universal bases into oligonucleotides is desirable in cases when either imprecise or random base-pairing is required, and the resulting mis-matched complements need to be stable.^[31]

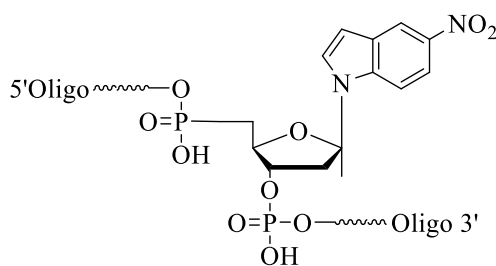


Figure 4. 5-Nitroindole as a universal base analogue in oligonucleotides.

In addition, in material science, electro polymerization of 6- and 5-nitroindoles has received increasing attention due to the potential applications of the resulting conducting films in various domains like electrochemical sensors, green-light-emitting materials, electro-catalysis, anode materials in battery and anticorrosion agents.^[32] Structural studies showed that the polymerization occurs mainly at 2,3-positions.^[33] Because the nitro group on the backbone can be easily reduced to amino group, the properties of inherently conducting polymers may be modified. Thus, the introduction of the nitro group on the main backbone will provide a novel approach for the post-functionalization of inherently conducting polymers.^[34]

1.4. Nitroindoles: synthesis.

Following the literature on the preparation of nitroindoles, it is possible to identify three main different approaches: 1) direct nitro functionalization of a pre-existing indole nucleus (Figure 5, pathway *a*); 2) *ex-novo* construction of the pyrrole ring onto a pre-existing benzene ring (Figure 5, pathway *b*: heteroannulation); 3) *ex-novo* construction of the benzene ring onto a pre-existing pyrrole ring (Figure 5, pathway *c*: benzannulation).

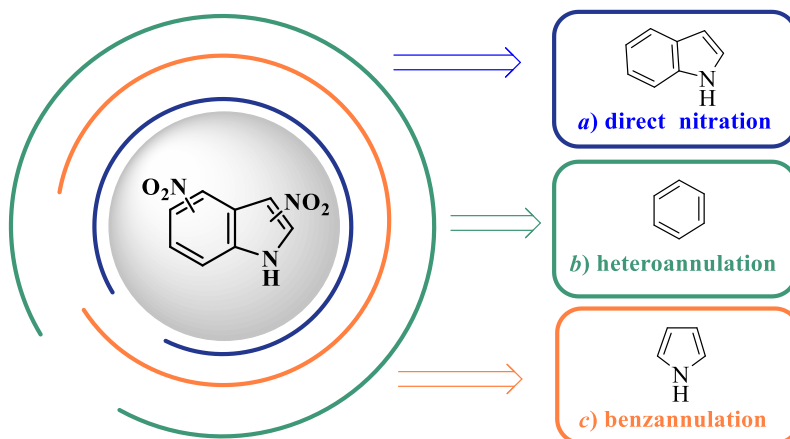


Figure 5. The three main methodologies of nitroindole synthesis.

1.4.1. Direct nitration of indoles.

Direct nitration represents the traditional procedure to get nitroindoles.^[1] Such approach, however, suffers from harsh reaction conditions due to the need for strong acids, poor regioselectivity, poor functional group compatibility, possible over nitration which leads to mixtures of regioisomers, limitation to the nitration of the more reactive pyrrole ring, while the nitration of the benzene ring is rarely achieved and limited to C2,C3-disubstituted indoles or indoles with an electron withdrawing group at C3.^[35] Indeed, while indoles nitrated on the pyrrole ring are easier to be obtained, indoles nitrated on the benzene ring, especially with an unsubstituted pyrrole ring, are a very challenging target (Scheme 1, *a*).

Direct nitration of indolines followed by a dehydrogenative step represents a possible alternative pathway to indoles nitrated on the benzene ring (Scheme 1, *b*).^[36]

In view of the advances in metal catalysis, an alternative way to get direct CH bond nitration is represented by regioselective metal-catalyzed nitration, *e.g.* Cu^[37] or Co^[38] catalysis. Buchwald, on the other hand, reported a Pd-catalyzed nitration of 6-chloroindole leading to 6-nitroindole in good yields (Scheme 1, *c*).^[39]

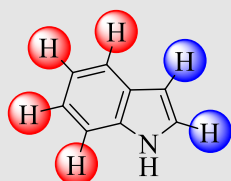
Very recently, Jian-Ping Zou reported a transition metal-free, direct and selective radical C3-nitration of indoles using NaNO₂ as NO₂ source and with the mediation of K₂S₂O₈ as oxidant (Scheme 1, *d*).^[40]

During the last years, enzymatic nitration strategies have been developed as well.^[41] Yousong Ding recently reported for the first time a whole-cell nitration system for the production of 4-NO₂-L-tryptophan analogues, by designing and expressing the biosynthetic pathway in *Escherichia coli*. Such structures are useful building blocks for synthesizing bioactive and biotechnologically relevant chemicals, materials, and proteins (Scheme 1, *e*).^[42]

1) Direct nitration of indole

a) Direct nitration with HNO_3 .^{[1],[35]}

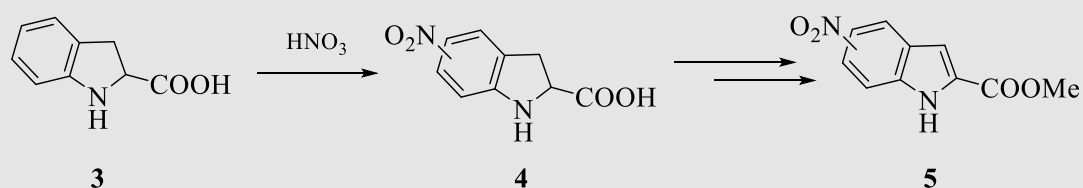
challenging
nitration



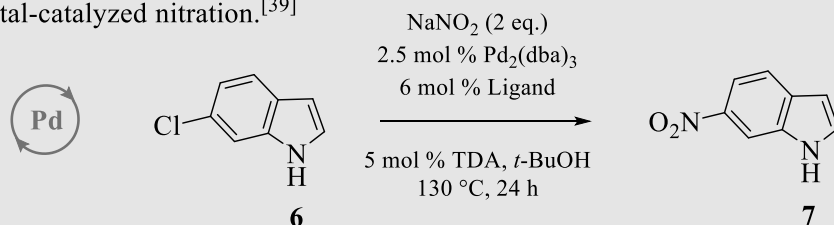
easy nitration

- ☐ harsh reaction conditions;
- ☐ poor regioselectivity;
- ☐ poor functional group tolerance;
- ☐ mixture of regioisomers.

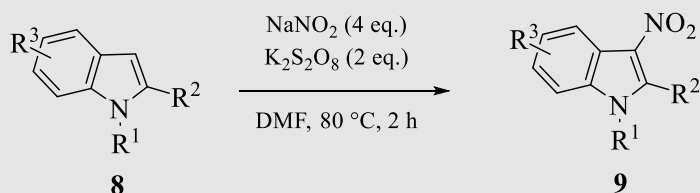
b) Direct nitration of indoline followed by oxidation.^[36]



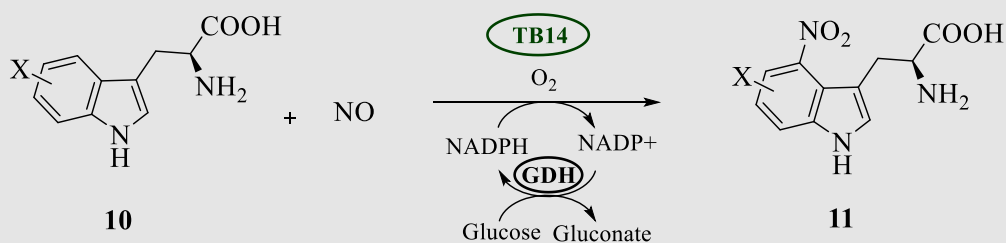
c) Metal-catalyzed nitration.^[39]



d) Metal-free direct and selective radical C3 nitration.^[42]



e) Enzymatic nitration in *Escherichia coli*.^[42]



Scheme 1. Examples of direct nitration approaches.

1.4.2. Heteroannulation approach.

Despite the recent advances in metal-catalyzed direct CH bond nitration, the *ex-novo* construction of the heterocyclic pyrrole ring onto a pre-existing benzene has been the most common synthetic approach in literature to access nitroindoles.

A comprehensive classification of such cyclization protocols, as suggested by Sundberg,^[43] could be done depending on the possible disconnections we can retrosynthetically draw on the pyrrole ring for its *ex-novo* construction (Figure 6).

The first two types of cyclizations, involving the introduction of C2 and C3 carbon atoms or C2 carbon atom respectively, are the most common ones. Formation of N-C2 bond represents usually the last cyclization step of the major part of intermediates originated from the first two kinds of cyclization: for this reason, category 3 is considered a common approach as well. For all other categories, I will report just a few examples. No example was found for category 7.

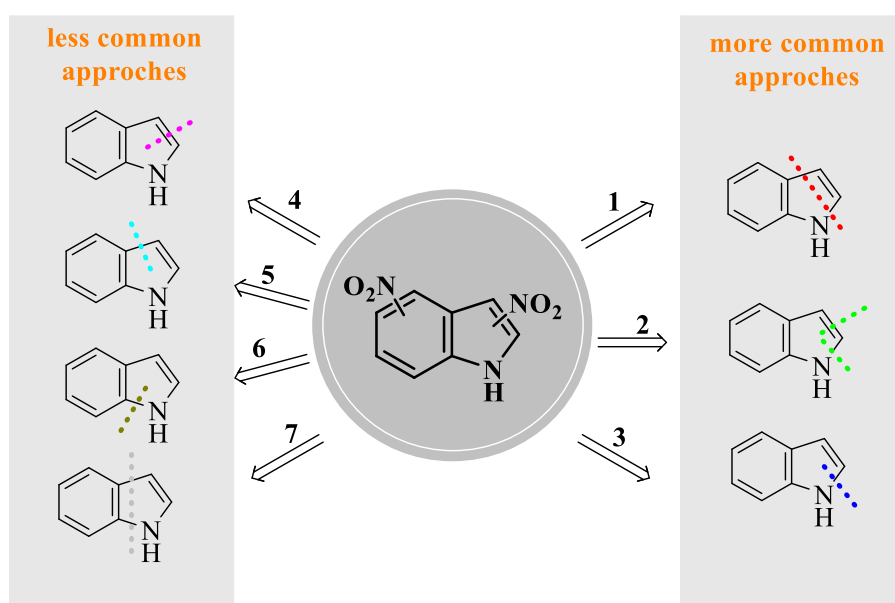


Figure 6. The possible retrosynthetic disconnections of the pyrrole ring.^[39]

Disconnection 1

The Fischer synthesis represents, from 1883, the main synthetic route to indoles;^[44] in the specific case of nitroindoles, indeed, several *o*-, *m*- and *p*-nitrophenylhydrazones derived from ketones were cyclized in hot concentrated acid to the corresponding nitroindoles.^[45] The method allows to access to indoles nitrated at any of the benzene ring positions, *i.e.* challenging positions in direct nitration reactions as mentioned above; it cannot be used, though, for the preparation of nitroindoles unsubstituted at pyrrole positions. In addition, by-products, low yields and mixtures of regioisomers, sometimes difficult to separate, are further drawbacks of the Fischer indole synthesis.^[46] Despite this, the Fischer cyclization is still a key step for the synthesis of biologically active compounds. Narayana, in 2005, reported the synthesis of some 1,3,4-oxadiazolyl nitroindoles with anti-inflammatory activity after a modified Fischer cyclization of ethyl pyruvate nitrophenyl hydrazones to ethylnitroindole-2-carboxylates,^[47] as originally reported by Singer^[46c] and Parmerter^[45] in the fifties. The same Fischer cyclization of ethyl pyruvate nitrophenyl hydrazones **13** to ethylnitroindole-2-carboxylates **14** represented a key step used by El Kihel, in 2013, for the synthesis of (3,5-dimethyl-1*H*-pyrazol-1-yl) (7-

nitro-1*H*-indol-2-yl)ketone derivatives **16**, which attract great interest due to their varied and significant pharmacological effects (Scheme 2, *a*).^[48]

Another general and versatile approach to the nitroindole ring construction appears to be vicarious nucleophilic substitution (VNS) in nitroarenes and subsequent cyclizations.^[49] By means of carbanions bearing a leaving group at the α -position, VNS introduces substituents into nitroarenes enabling replacement of hydrogen (or halogen)^[50] in the position *ortho* and/or *para* to the nitro group.^[49] The obtained *ortho*-nitrobenzyl derivatives are well suited as starting materials for the synthesis of heterocycles, particularly indoles. Thus, Mąkosza, in 1984, reported VNS in *m*-nitrobenzisonitriles with chloromethyl aryl sulfones followed by cyclization directly to give substituted 4- and/or 6-nitroindoles.^[51] In 2012, Wojciechowski reported the synthesis of 6-nitro-1-hydroxyindoles **19** after tin(II) reduction of 2,4-dinitrobenzyl ketones **18** obtained from a VNS of 1,3-dinitrobenzene **17** with α -chloroalkyl ketones (Scheme 2, *b*).^[52]

Alternatively, direct condensation of 3-nitroanilines with ketones^[53] or nitriles^[54] represents a simpler method to access to 4- and/or 6-nitroindoles. These novel indole ring constructions include the nucleophilic substitution of hydrogen (or halogen) in the nitroaromatic ring by an enolate anion or a nitrile carbanion with subsequent cyclization (Scheme 2, *c*).

The Pd-catalyzed direct coupling, of the *ortho*-iodoaniline **24** with the aldehyde **23**, has represented, in a recent work, a key step for the first total synthesis of thaxtomin A (Scheme 2, *d*).^[18]

Moreover, nitroindoles can be prepared by the Bartoli method from dinitrobenzene by reaction with a vinyl Grignard (Scheme 2, *e*).^[55]

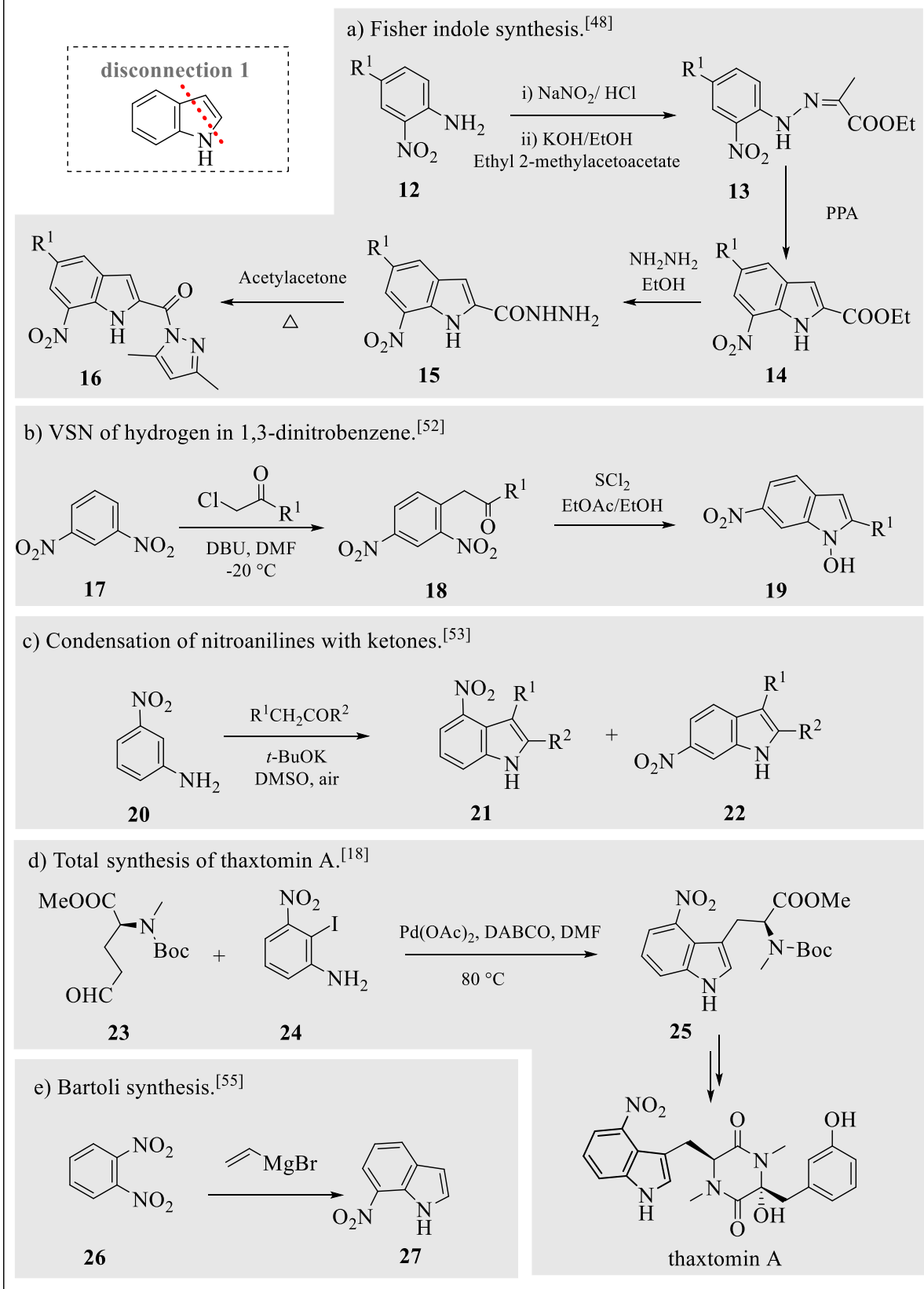
Disconnection 2

In past years, 2,4,6-trinitrotoluene (TNT) **28** has demonstrated to be a powerful starting material for the synthesis of 6-nitroindoles, and 4,6-dinitroindolezoles.^[56] Generally, these protocols require a first condensation step of TNT with an aldehyde to give the corresponding stybene. Substitution of one of the *ortho*-nitro groups with the azido group leads to the corresponding *o*-azidostyrene which after thermolysis leads to the final nitroindole (Scheme 3, *a*). However, TNT is an explosive that should be handled with great care. For this reason, the use of TNT as a start to nitroindoles is nowadays obsolete.

Given the above disadvantages, compounds similar to TNT and not explosive (so-called “TNT surrogate”) in which one nitro group is replaced with another group, *e.g.* CF₃ or SR, have been used into the Leimgruber–Batcho indole synthesis as an alternative method for the synthesis of nitroindoles starting from *o*-nitrotoluenes. The first step is the formation of an enamine using *N,N*-dimethylformamide dimethyl acetal, the nitroindole being then formed in a second step by reductive cyclization (Scheme 3, *b*).^[57]

Concerning nitration on the pyrrole ring, Gribble, in 1997, reported the synthesis of 2-nitroindoles **38** via the Sundberg Indole synthesis, which involves the thermolysis of β -substituted-*o*-azidostyrenes **37**.^[58] More recently, Driver reported the same formation of nitroindoles from β -substituted-*o*-azidostyrenes **37** in the presence of rhodium(II) carboxylate complexes,^[59] but in this case only the selective formation of 3-nitroindoles **39** has been detected due to the catalyzed migration of the NO₂ group from the original C2 carbon atom (Scheme 3, *c*).

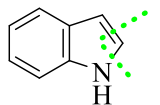
2) Heteroannulation approach



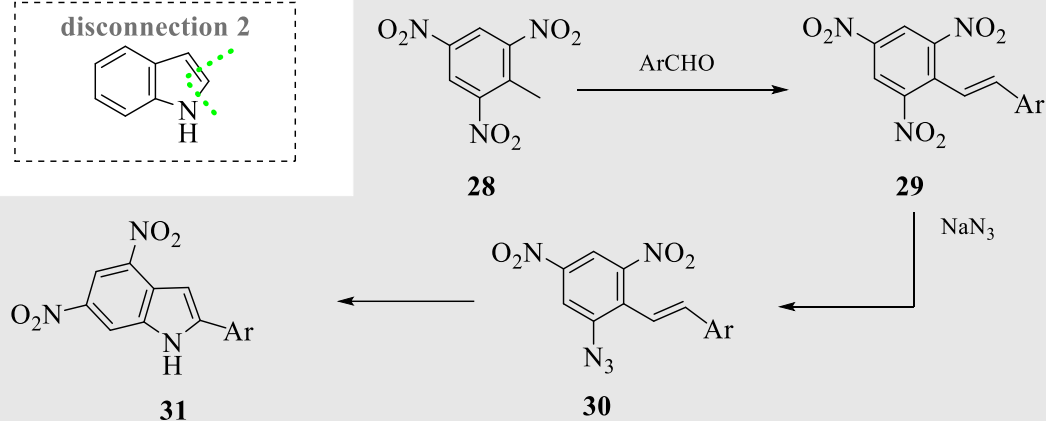
Scheme 2. Examples of heteroannulation approaches *via* disconnection 1.

2) Heteroannulation approach

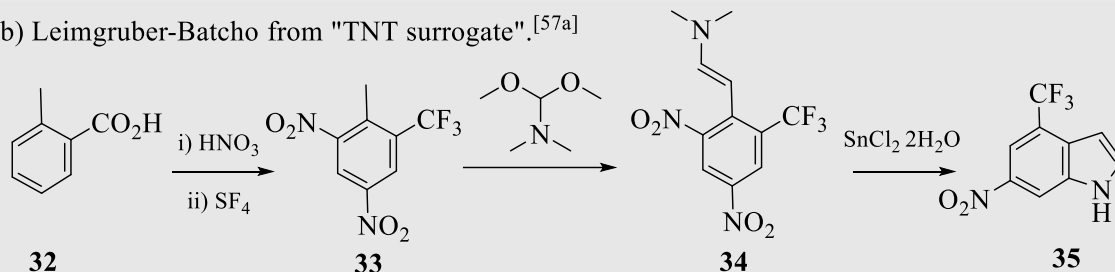
disconnection 2



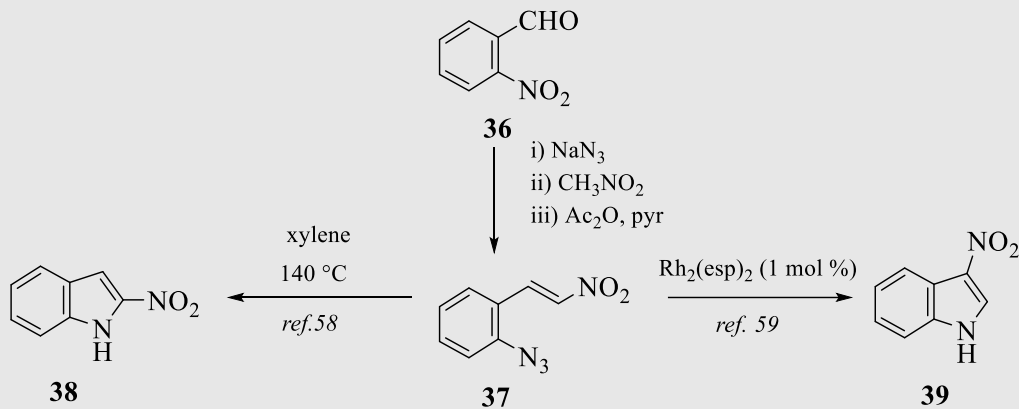
a) Synthesis from TNT. ^[56a]



b) Leimgruber-Batcho from "TNT surrogate". ^[57a]



c) Selective synthesis of 2- or 3-nitroindole from nitrostyrylazides.



Scheme 3. Examples of heteroannulation approaches *via* disconnection 2.

Disconnection 3

Actually, the major part of intermediates originated from the synthetic methods reported before (*e.g.* Fisher, Bergman, Reissert, Sundberg intermediates) performs disconnection 3 as the last step for the *ex-novo* construction of the pyrrole ring.

Interestingly, this kind of disconnection is shown in a very recent work of Shu-Jiang Tu and Bo-Jiang in which they reported a silver-catalyzed nitration-annulations of 2-arylalkynylanilines **40** with tert-butyl nitrite (TBN) as a mild, easy-to-handle nitrating reagent for the tunable selective synthesis of 5- or 7-nitroindoles (Scheme 4, *a*).^[60]

Disconnection 4

The Madelung synthesis, a base-catalyzed thermal cyclization of *N*-phenylamides, is one of the few reactions that produce indoles by closure of C2- C3 bond.^[61]

Special cases of such Madelung reaction are the ring closure reactions used by Bergman for the synthesis of a variety of 4- or 6-nitroindoles prepared, respectively, from imide, amidine, and *sec*-anilide derivatives of 2-alkyl-3- or 5-nitroanilines by a base-induced cyclization promoted by dialkyl oxalates at room temperature (neither 5- nor 7- nitroindoles could be synthesized using this method) (Scheme 4, *b*).^[62]

Disconnection 5

Oxidative cyclizations of *N*-aryl enamines and *N*-aryl imines are the common approach belonging this disconnection class.^[63] Pd-catalyzed oxidative cyclization of *N*-aryl enamines have recently developed for the efficient synthesis of 2-nitroindoles.^[64]

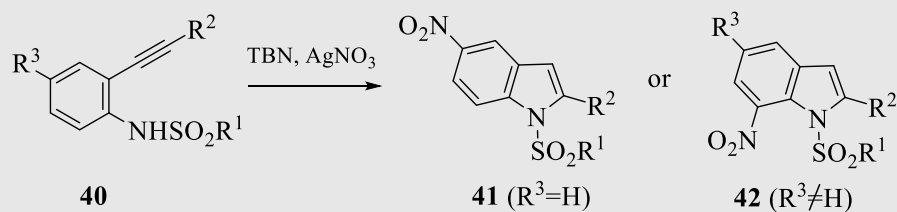
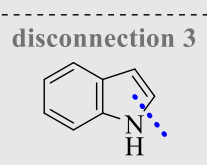
Although these approaches possess an operationally simple, highly atom-economical and broad substrate scope, they are limited to the requirement of expensive Pd catalysts and additives. Thus, a new metal-free nitrate oxidative cyclization of *N*-aryl imines **45** with tert-butyl nitrite have been reported as an alternative method (Scheme 4, *c*).^[65]

Disconnection 6

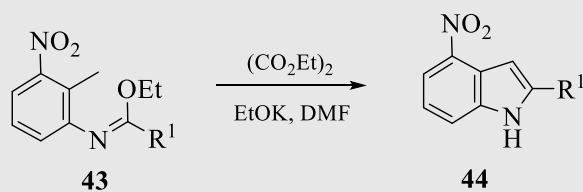
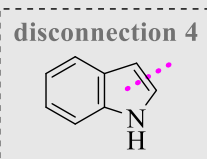
The Cadogan-Sundberg reaction, *i.e.* deoxygenation of *o*-nitrostyrenes or *o*-nitrostilbenes with trialkyl phosphite or trialkylphosphine and subsequent cyclization of the resulting intermediate nitrene to form indoles, is a possible synthetic method forming connection 6.^[66] Although Cadogan reaction is nowadays a good way to build up a new *N*-containing ring into a system, it has not been a common route to access nitroindoles. As an old example, Russell, in 1991, reported the cyclization of 1,1-dinitro-2,2-diphenylethylene **47** to 2-nitro-3-phenylindole **48** with diethyl phosphite at 150 °C (Scheme 4, *d*).^[67]

2) Heteroannulation approach

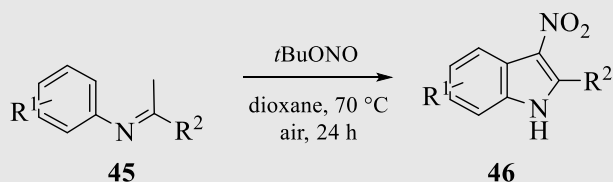
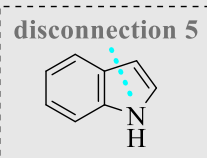
a) Ag-catalyzed nitration of 2-arylalkynylanilines with TNT.^[60]



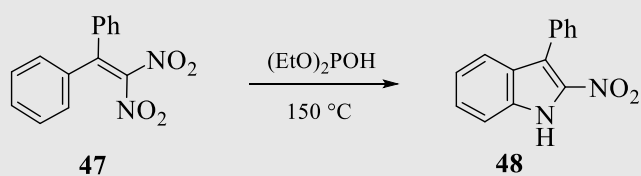
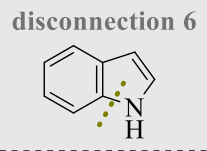
b) Bergman indole synthesis.^[62]



c) Metal-free nitrate oxidative cyclization of N-aryl imines.^[65]



d) The Cadogan-Sundberg reaction.^[67]

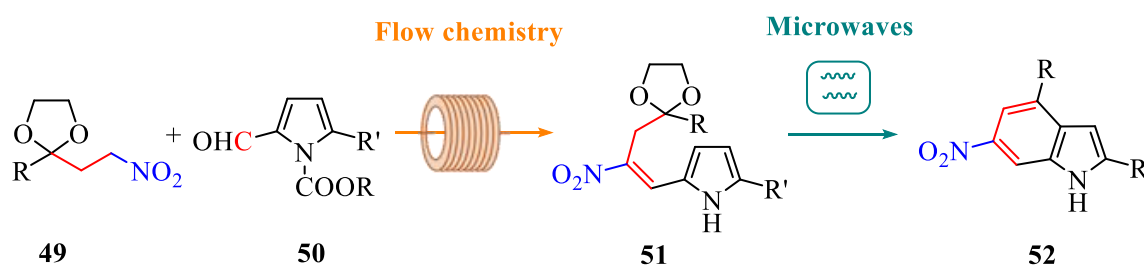


Scheme 4. Examples of heteroannulation approaches *via* disconnection 3, 4, 5 and 6.

1.4.3. Benzannulation approach.

A more recent approach to indoles is the *ex-novo* construction of the benzene ring onto a pyrrole derivative (*i.e.* benzannulation): such procedure has started to be successfully applied to diverse 4-, 5-, 6- or 7-substituted indoles by means of different building blocks and reaction typologies, often exploiting metal catalysis.^[68]

In this scenario, though, nitro indoles are practically absent, except for a very recent report on a two-step procedure to 6-nitroindoles **52** where a β -nitro ketone **49** with a protected carbonyl provides a nitrated C₃ building-block for an overall annulation occurring through an initial condensation with a suitable 2-pyrrolecarbaldehyde **50** followed by a second, intramolecular condensation (Scheme 5).^[69] The method is based on the peculiarity of the flow chemistry and microwave technology.

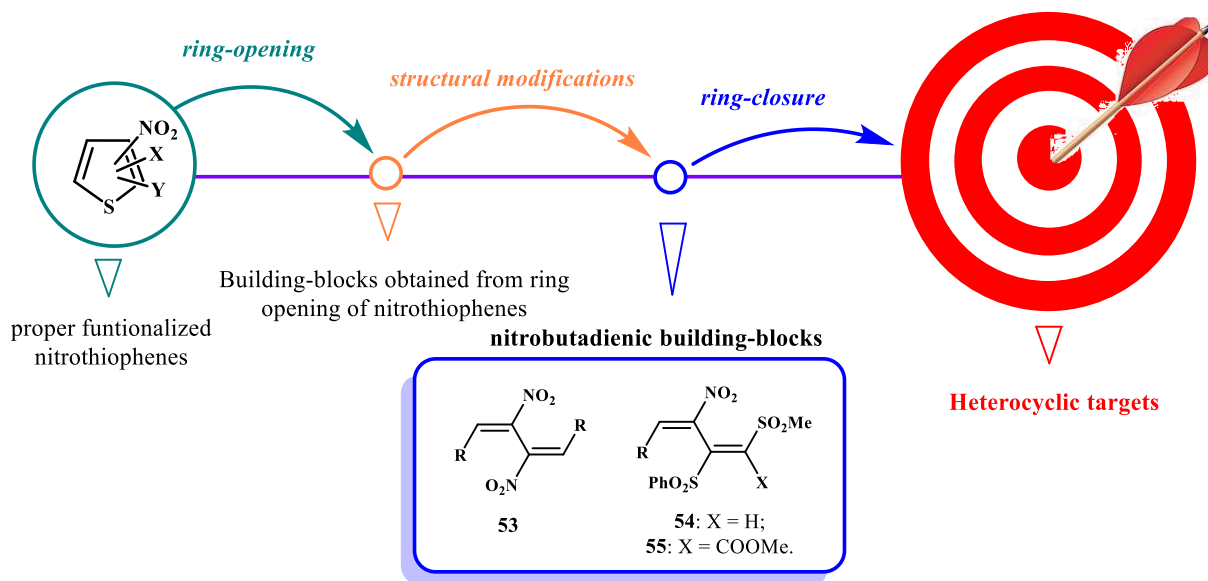


Scheme 5. 6-Nitroindoles *via* annulation onto pyrrole by means of a C₃ building block.

In this unexplored context of benzannulation methodologies for the synthesis of nitroindoles my Ph.D. work, in part, has found its place.

2. SCOPE

The present Ph.D. project is part of a long-standing project carried out at Genoa University by the ORSA research group, whose focus is on the study of the reactivity of nitro and dinitro-1,3-butadienes, obtained from the initial ring opening of nitro- and dinitrothiophenes, respectively. Previous papers in the series have demonstrated the synthetic potential of such nitrobutadienes to develop a preparative method for diversely functionalized and versatile heterocyclic targets (Scheme 6).^[70]



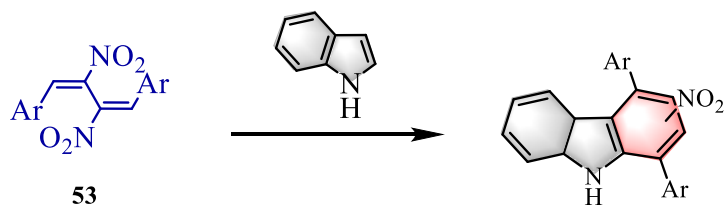
Scheme 6.

In a precedent work, such nitrobutadienes have already demonstrated to be valuable nitrated C₄ building-blocks for a benzannulation onto indole leading to nitrocarbazoles (Scheme 7, a).^[71]

Proud of the results achieved, the aim of the present work has been a study of reactivity of mono and dinitro-1,3-butadienes towards pyrrole, in order to build up a new protocol into the unexplored context of benzannulation methodologies for the synthesis of nitroindoles. The targets, never reported so far, appear of sure interest because of their pattern of substitution not easy to be obtained otherwise. Due to the possible further elaborations the nitro group is promising for, the aim of the work has been also the application of the designed nitroindoles as valuable precursor *e.g* of fused nitrogenated polycycles (Scheme 7, b).

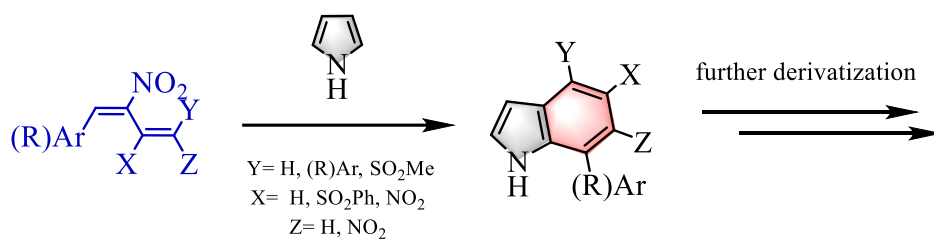
In addition, during my Ph.D. I have had an Erasmus internship of six months at York University. Aim of the Erasmus project has been the development of a precedently-unreported visible-light promoted dearomatizing spirocyclization of indole-tethered ynones for the preparation of novel spiroindoles and/or spiroindolines (Scheme 7, c). Although they look like different projects, they find a point common in the use of the reactivity of indole derivatives in order to build up new polycyclic structures.

a) Previous work: "nitration" at C2 and/or C3 of carbazoles.^[71]

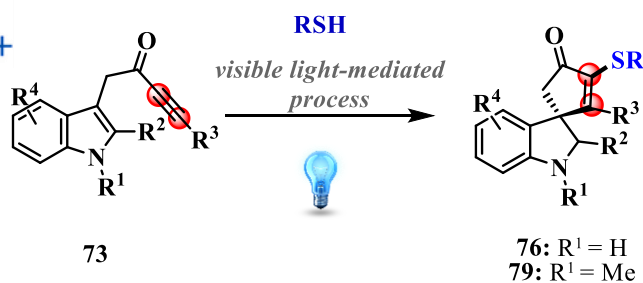


*C₄ nitrated
benzannulating agents*

b) Present work: "nitration" at C5 and/or C6 of indoles.^{[2],[3],[4]}



c) Light Promoted Dearomatizing Spirocyclizations of Ynone-Tethered Indoles.^[5]

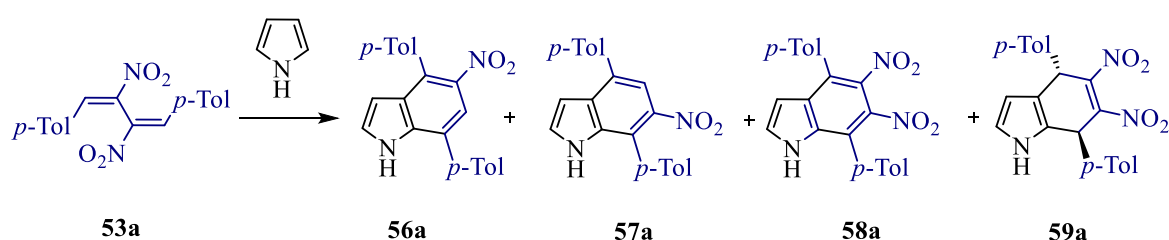


Scheme 7.

3. RESULTS AND DISCUSSION

3.1. An unprecedented easy access to rare nitroindoles.

Our study began carrying out an optimization of experimental condition on the model reaction between the bis(*p*-tolyl)dinitrobutadiene **53a** and pyrrole, the main results from such preliminary screening being collected in Table 1. Under the reaction conditions previously employed for the benzannulation of indole [2,2,2-trifluoroethanol (TFE) at 50 °C: entry 1]^[71] an overall substrate conversion has been obtained. As in the case of carbazoles, a nitrosubstituted benzene ring is actually constructed, leading to a final mixture of three different nitroindoles (**56a**, **57a**, and **58a**),



Scheme 8.

Table 1. Results of reaction of **53a** with pyrrole (2 equiv.) in different experimental conditions.^a

Entry	Solvent ^b	T	t	53a	56a + 57a	58a	59a	Balance
1	TFE	50° C	24 h	-	20	40	-	60
2	TFE ^c	50° C	24 h	-	24	43	-	67
3	TFE	50° C	1,5 h	-	41	27	13	81
4	TFE	50° C	45 min	6	6	7	49	68
5	TFE	30° C	4 h	4	4	8	77	93
6	TFE	r.t.	48 h	-	14	8	62	84
7	HFIP	r.t.	48 h	-	23	28	-	51
8	Toluene	50 °C then reflux.	24 + 48 h	^d	-	-	-	-

^aYields refer to chromatographically isolated compounds (or mixtures). ^bTFE = 2,2,2-trifluoroethanol; HFIP = 1,1,1,3,3,3-hexafluoro-2-propanol. ^cUnder argon atmosphere. ^dOnly substrate evidenced on TLC, with at most traces of possible products.

As oxidative steps are needed for the formation of the isolated products, the same reaction conditions have been performed under argon atmosphere (entry 2), demonstrating that the oxidant cannot be atmospheric oxygen: thus, as already observed in previous recent papers of ours,^[70b, 71-72] the nitrite ion, deriving from elimination, must be responsible for the observed “endogenous” oxidation (see later in the text).

Unfortunately, the low selectivity among the three nitroindoles and the complicated chromatographic isolation due to structural similarities represent practical drawbacks. Anyway, interestingly enough, lowering the reaction temperature has brought to evidence (TLC) the

formation of the intermediate **59a**, which could be isolated (entry 5) in rather satisfactory yields at 30 °C. Such an outcome was actually rather unexpected, as no intermediate had been ever detected in the analogous benzannulation reactions of indole.^[71] Further temperature decrease (entry 6) revealed to be unfavorable to the “interception” of **59a**, while much poorer results were provided by the use of another fluorinated solvent such as 1,1,1,3,3,3-hexafluoro-2-propanol (HFIP; entry 7).

X-ray analysis of **59a** testified for the 4,7 dihydro-indole reported in Figure 7, with an exclusive relative anti configuration at C4 and C7.

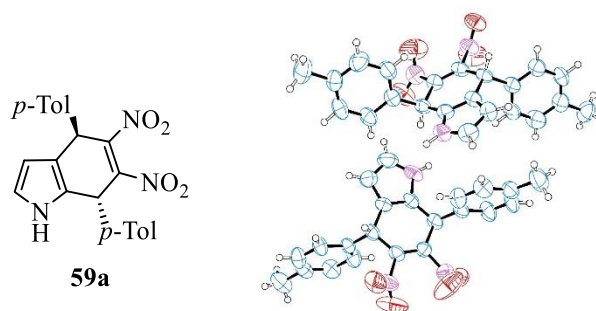
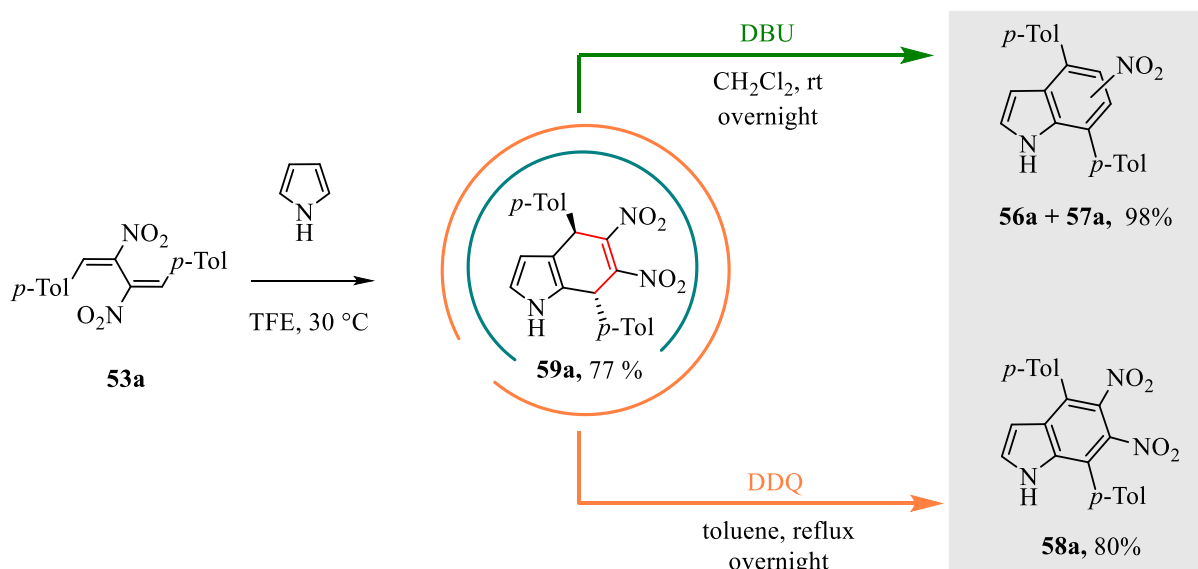


Figure 7. Structure and ORTEP of **59a**; ellipsoids enclose 50% probability.

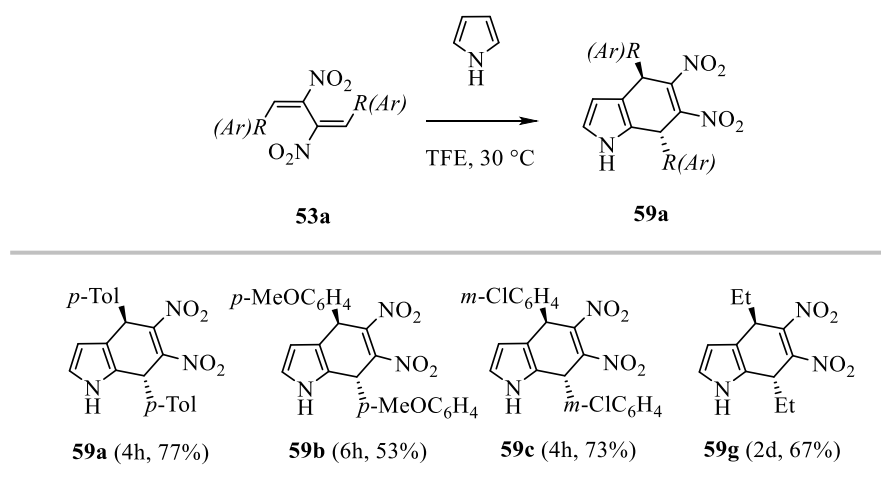
Dihydroindole **59a** has demonstrated to be a common precursor of the three different nitroindoles and its isolation allows us to optimize their final yields by means of separate follow-up procedures. Thus, overnight treatment of **59a** with the strong base DBU (1,8-diazabicyclo[5.4.0]undec-7-ene) in dichloromethane at room temperature very efficiently leads to the mixture of the two mononitroindoles (**56a** + **57a**). On the other hand, overnight treatment of the same dihydrodinitroindole with the oxidant 2,3-dichloro-5,6-dicyano-1,4-benzoquinone (DDQ) in toluene at reflux leads to the dinitroindole **58a** in excellent yield (Scheme 9).



Scheme 9. Selective formation of mono- or dinitroindoles *via* interception of the common dihydro intermediate **59a**.

This protocol can be followed, with similar success, for dinitrodienes with different aryl and alkyl substituents, by suitably changing temperature and reaction time.

The dihydro intermediate could be isolated in acceptable or satisfactory yields (Scheme 10) also from the 1,4-diaryl-2,3-dinitro-1,3-butadienes **53b**, **53c** and 4,5-dinitro-3,5-octadiene **53g**, although it normally suffers from more or less extensive decomposition during chromatographic purification: thus it was found in general more convenient to simply remove the solvent by rotoevaporation after disappearance (TLC) of **53**, and then submit the residue to DBU-elimination or DDQ-oxidation (Table 2).



Scheme 10. Isolation of **59** from the reaction of pyrrole (2 mol equiv.) with **53**. Yields refer to chromatographically isolated compounds. Reported times refer to the maximal formation of **59**, as judged by TLC.

Table 2. Results from the reaction of pyrrole (2 mol equiv.) with **53** in TFE at 30 °C, followed by one-pot DBU or DDQ treatment of the mixture rotoevaporated after the time reported in column 3, without the isolation of the dihydro intermediate **59**.^a

Entry	53 : Ar(R)	<i>t</i> ^{b,c}	Follow-up with DBU ^d		Follow-up with DDQ ^e	
			56 + 57	58	56 + 57	58
1	53a : <i>p</i> -Tolyl	4 h	78		7	70
2	53b : <i>p</i> -MeOC ₆ H ₄	6 h	58			57
3	53c : <i>m</i> -ClC ₆ H ₄	4 h	86		8	50
4	53d : 1-Naphthyl ^{f,g}	3 d	51	16	14	63
5	53e : 2-Thienyl ^f	2 d	58	16	17	68
6	53f : Methyl	9 h	38	13		41
7	53g : Ethyl	2 d	39	4		44

^aYields refer to chromatographically isolated compounds (or mixtures). ^bTime for the maximal formation of **59**, as judged by TLC. ^cAfter the time in column 3, TFE was removed before treatment for the alternative follow-up reactions, without further purification. ^dTreatment with DBU (1.1 mol equiv.)/CH₂Cl₂, rt for 24 h; yields refer to **53**; in some case minor quantities of **58** were also isolated. ^eTreatment of **59** with DDQ (2 mol equiv.)/toluene at reflux for 24 h; yields refer to **53**; in some case minor quantities of the **56**+**57** mixture was also isolated. ^fMol equiv. of pyrrole = 4. ^gThe synthesis of **58d** has been already described.^[4]

Steric hindrance most likely contributes to slow down the annulation leading to **59d** (Table 2, entry 4, Ar = 1-naphthyl), while electronic effects possibly play a significant role in the case of **59e**. As far as the possibility to extend the synthesis to 4,7-dialkyl (di)nitroindoles is concerned, both the dimethyl derivative **53f** (Table 2, entry 6) and the diethyl derivative **53g** (Table 2, entry 7) furnish nitroindoles **56+57** or **58** in significantly lower yields, possibly also due to some loss during the TFE rotoevaporation prior to follow-up, as a consequence of a somewhat higher volatility of the relevant dihydro intermediates.

The mixtures of regioisomeric mono-nitroindoles **56** and **57** for the diaryl derivatives a-e were separated by HPLC. Anyway, the direct assignment by X-Ray crystallography was feasible only for the 2 thienyl derivatives **56e** and **57e**: actually, good crystals were obtained for the minor regioisomer **56e**, which was found to have the nitro group at C5 (Figure 8), thus assigning a 6 nitroindole structure to the major regioisomer **57e**.

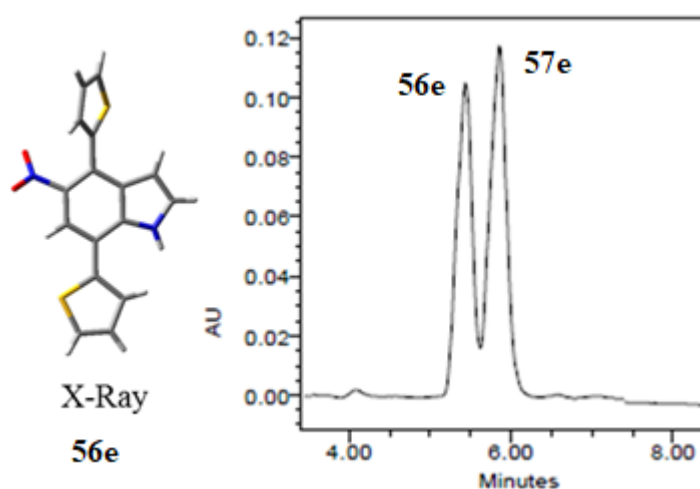


Figure 8. X-Ray structure of the first eluted bis(2-thienyl) regioisomer from **53e** (HPLC: Luna 5 μ C18(2) 100 Å, acetonitrile/H₂O 90/10, 5 mL/min).

For all the other compounds, NOESY experiments confirm that the 5-nitroindole **56** is, in any case, the minor component, **56:57** ratios most often falling within the 1:1 – 0.7:1 range. The HPLC and NOESY analyses reported in Figure 9 refer to the *p*-tolyl compound **56a**. The NOESY traces 1) and 2) were obtained irradiating the NH and H-3 protons, respectively, to assign the H-15 and H-11 protons. Then, H-6 and H-5 protons of compounds **56a** and **57a**, respectively, were saturated. In this way, H-6 showed NOESY effect on H-15, and H-5 showed NOESY effect on H-11.

Pleasingly, a simple silica-gel column chromatography allowed a satisfactory separation of the **56f/57f** and **56g/57g** couples.

Mechanistic aspects of the benzannulation process: a proposed rationalization

Any rationalization of the annulation mechanism should obviously justify the dihydroindole **59** as a common intermediate.

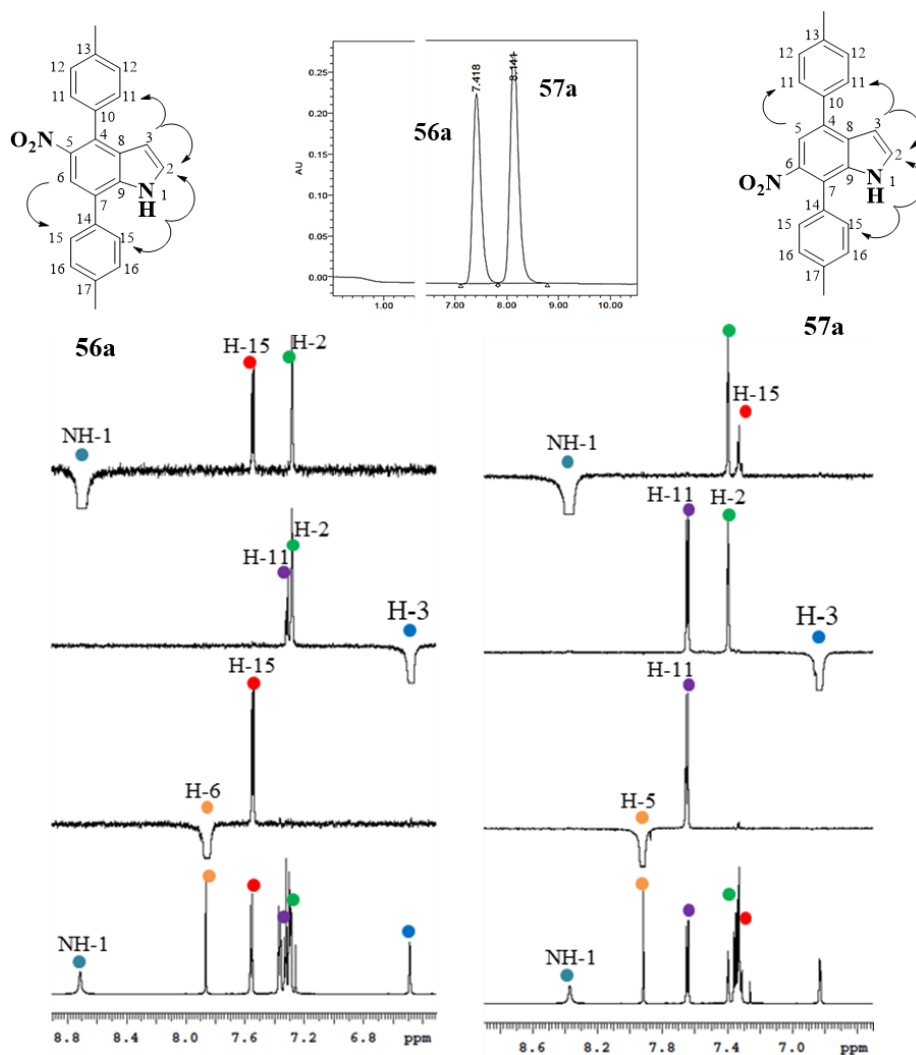
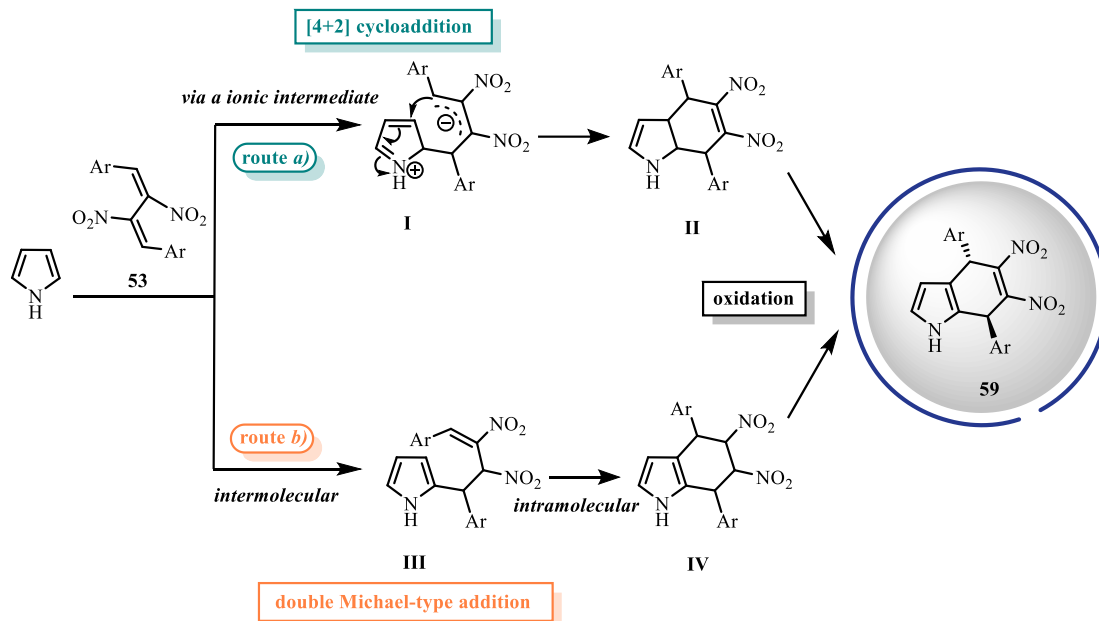


Figure 9. HPLC and NOESY analyses of mononitroindoles **56a** and **57a**. Trace 4) is relevant to the ^1H NMR spectra in CDCl_3 . Traces 1), 2), 3) are the NOESY experiments irradiating NH, H-3, and H-6 or H-5 proton, respectively.

A fully-concerted [4+2] cycloaddition can be reasonably excluded because, as a consequence of the expected diastereospecific process onto the *E,E*-1,3-diene, it would end up with the substituents at C4 and C7 *syn* to each other unlike the *anti*-configuration of **59a**. Indeed, pyrroles are known to behave mostly as dienes,^[73] and only a limited number of them act as dienophiles.^[74] On the other hand, within a long-standing research based on the use of nitro- and dinitrobutadienes as building-blocks, we have never observed a behaviour of the four-carbon skeleton of **53** as a diene: rather the single nitrovinyl fragment ($\text{C}=\text{C}-\text{N}=\text{O}$) can be involved in hetero-DA processes. Furthermore, no reaction occurring in an apolar solvent such as toluene (entry 8 of Table 1) is a further evidence that a fully-concerted mechanism, with no charge separation, is not involved.^[75]

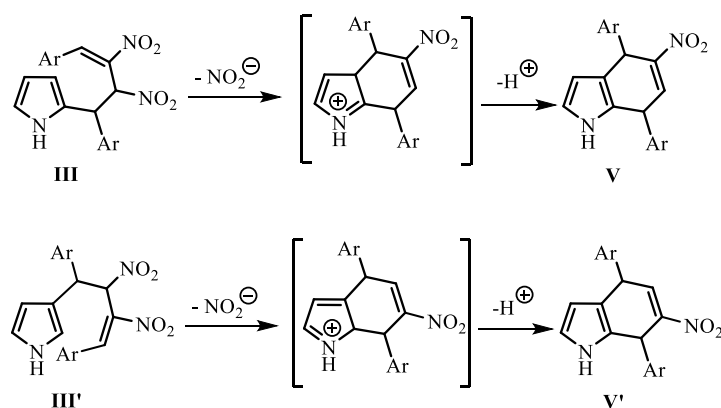
On these grounds, a [4+2] not fully-concerted cycloaddition through the zwitterionic intermediate **I** possessing an inverted polarity^[76] (Scheme 11, *route a*) and a two-step ionic mechanism involving consecutive (inter- and intramolecular) Michael-type additions (*route b*) can be hypothesized. In either case, a dehydrogenative step is required to complete the formation of **59** from **II** or **IV**, respectively. Whichever the actual pathway, the surprising

complete diastereoselectivity for the formation of **59** can be justified by the presumably higher stability of the *anti* configuration.



Scheme 11. Mechanistic hypotheses for the formation of dihydroindoles **59**.

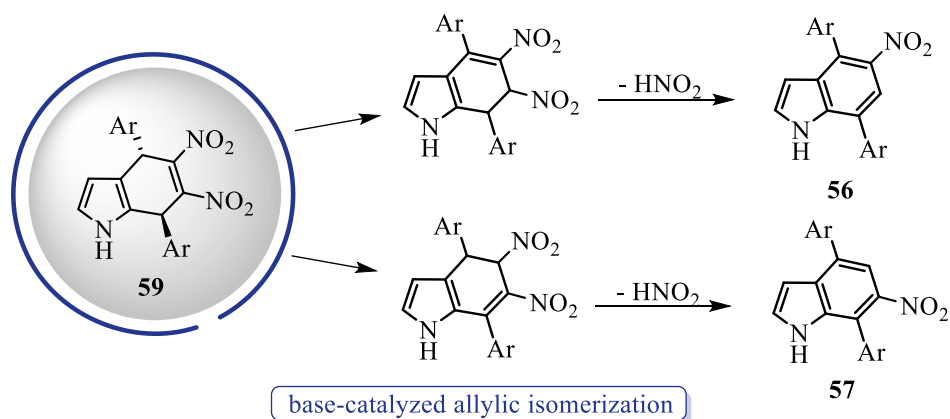
While route *a*) better justifies the double bond position found in the isolated dihydroindole **59** due to the re-aromatization of the pyrrole ring, route *b*) better justifies the oxidation steps of **II** or **IV** performed by endogenous nitrite ion: indeed, on intermediate **III** the intramolecular addition leading to **IV** (Scheme 11) could compete with elimination of nitrite and rearomatization of the pyrrole ring (Scheme 12). The effectiveness of nitrite as a leaving-group could be favored by the acidity of TFE. A less efficient initial formation of **III'** by concurrent electrophilic substitution at C3 of pyrrole would lead, in a similar way, to **V'** (Scheme 12).



Scheme 12. Rationalization of formation of the endogenous oxidant (HNO_2) in TFE, in the absence of an added base.

While Scheme 12 rationalizes the possibility to eventually obtain mononitroindoles in the normal conditions (TFE) within reaction pathways not having **59** as an intermediate, a further effort must be done in order to justify the formation of **56** and/or **57** from **59**. In the experiment where the intercepted **59** is treated with DBU, most likely a base-catalyzed allylic isomerization

(driven by the attainment of an extended conjugation within a push-pull system) would precede HNO_2 elimination (Scheme 13). On the other hand, in the normal reaction conditions (TFE, excess pyrrole) the amphoteric solvent itself should be the most effective base, although bifunctional catalysis cannot be excluded (possibly within a solvent cage). The properties of polyfluorinated solvents have been recently investigated^[77] (oxidations and isomerizations, in particular, being favored processes), but a deeper mechanistic investigation would go beyond the practical significance of the results herein.



Scheme 13. Rationalization of formation of **56** and **57** from **59**.

3.1.1. Atropisomerism.

A very interesting side project originated from the observation that, much as it happens in the more classical case of *ortho*-substituted biphenyls, the steric hindrance cooperatively played, in the bis(1-naphthyl)dinitroindole **58d**, by the two nitro groups and by the N(1)H and C(3)H moieties of the pyrrole ring forces the naphthyl groups out of the indole plane, thus generating two stereogenic axes; furthermore the asymmetry of the indole “spacer” makes both the *syn* and *anti* diastereoisomers entail an atropisomeric pair (Figure 10), while in other cases, such as the biphenyl system, where the two phenyl rings are directly linked to each other, the *syn* diastereoisomer is a *meso* form and the *anti* is racemic.

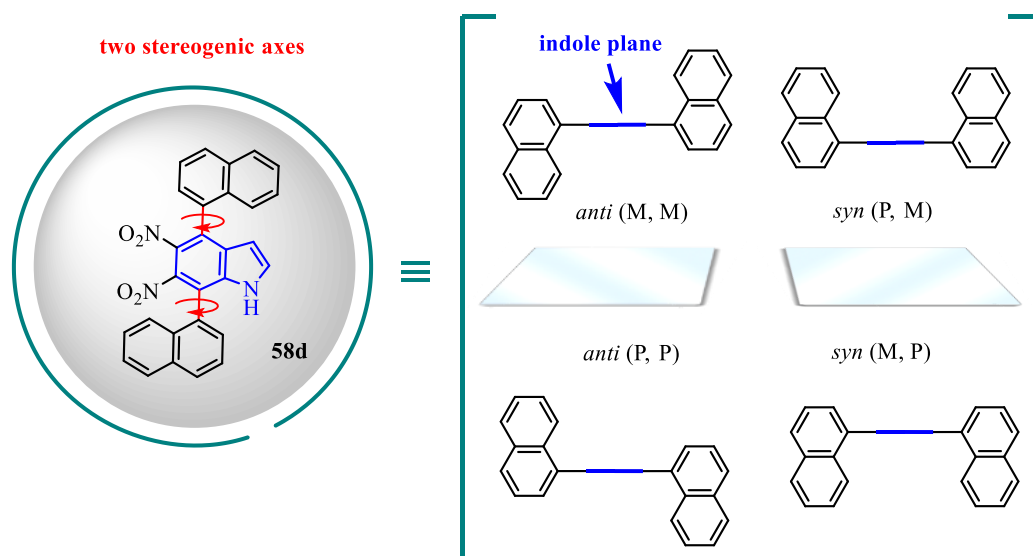


Figure 10. The four atropisomers generated by the two stereogenic axes in **58d**.

Atropisomerism, *i.e.* the optical activity generated by a chiral axis, was first recognized by Christie and Kenner in 1922^[78] and later its definition was refined by Oki.^[79] This phenomenon has been largely overlooked as an alternative source of stereoisomerism for many decades. However, the situation changed with the preparation of atropisomeric catalysts^[80] and with the discovery of many bioactive natural compounds containing stereogenic axes.^[81] More recently, Clayden and LaPlante underlined the pharmaceutical implications of atropisomerism in drug discovery.^[82] On the other hand, enantiopure 1,2-diamines are found in biologically active molecules and are largely employed as ligands for organometallic enantioselective catalyst.^[83]

A stereodynamic study of compound **58d** was carried out in collaboration with the research group of Professor Mazzanti of Bologna University.^[4]

In order to optimize the ground state geometry, DFT calculations [B3LYP/6-31g(d) level of theory]^[84] showed the 1-naphthyl rings not perpendicular to the plane of the indole; hence, for each atropisomer, four different conformations have to be considered corresponding to the four combinations of the two dihedral angles that can be smaller or larger than 90° .^[85] However, in the case of the *syn* diastereoisomer, the two conformations where both angles are larger or smaller than 90° do not correspond to energy minima. This occurrence is due to the presence of the two nitro groups in positions 5 and 6. In the optimized structures, the two

naphthyl rings and the two nitro groups are linked in a geared system,^[86] which means that the movement of one naphthyl ring causes the movement of the two nitro groups and eventually the rotation of the second naphthyl ring. In the *anti* diastereoisomer, for the same reason, only the conformations with the two angles smaller or larger than $|90|^\circ$ are energy minima (Figure 11). DFT calculations suggested that the *syn* and *anti* diastereoisomers have very close energies and they should be both populated.

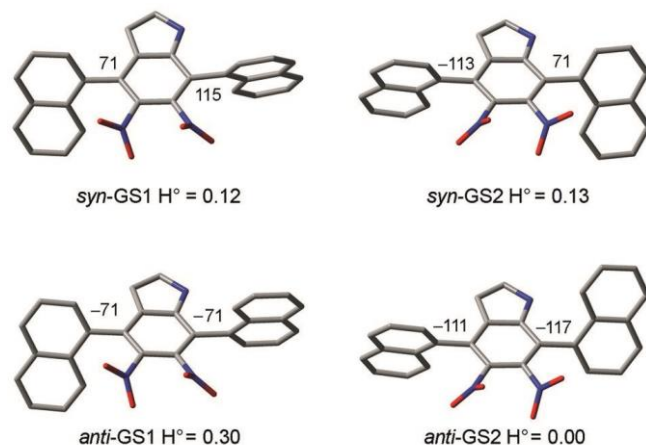


Figure 11. The four ground states of compound **58d**. Only one atropisomer is shown for each conformation. The numbers are the values of the dihedral angle defined by the quaternary carbon bearing the nitro group on the indole and the quaternary carbon of the 1-naphthyl ring. Energies are given in kcal mol⁻¹ as ZPE-corrected enthalpies.

Calculations were also run to evaluate the two rotational barriers of the 1-naphthyl rings. For both barriers the calculated value exceeds 29 kcal mol⁻¹ (29.78 and 29.76 for C4-naphthyl rotation and C7-naphthyl rotation, respectively); hence, both stereogenic axes should be configurationally stable at room temperature.

Experimental rotational barriers can be evaluated by kinetic experiments run on the enantiopure diastereoisomers of **58d**. However, a good separation of them on a chiral stationary phase (CSP) HPLC was not obtained, despite many efforts with different HPLC columns and conditions. Fortunately, such separation has been possible after Boc protection (**58d** → **61**, reaction II in Scheme 14) of the NH (Figure 12).

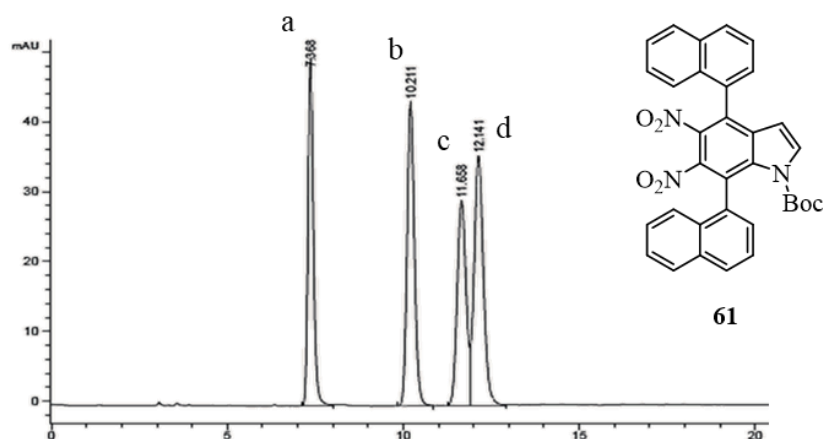
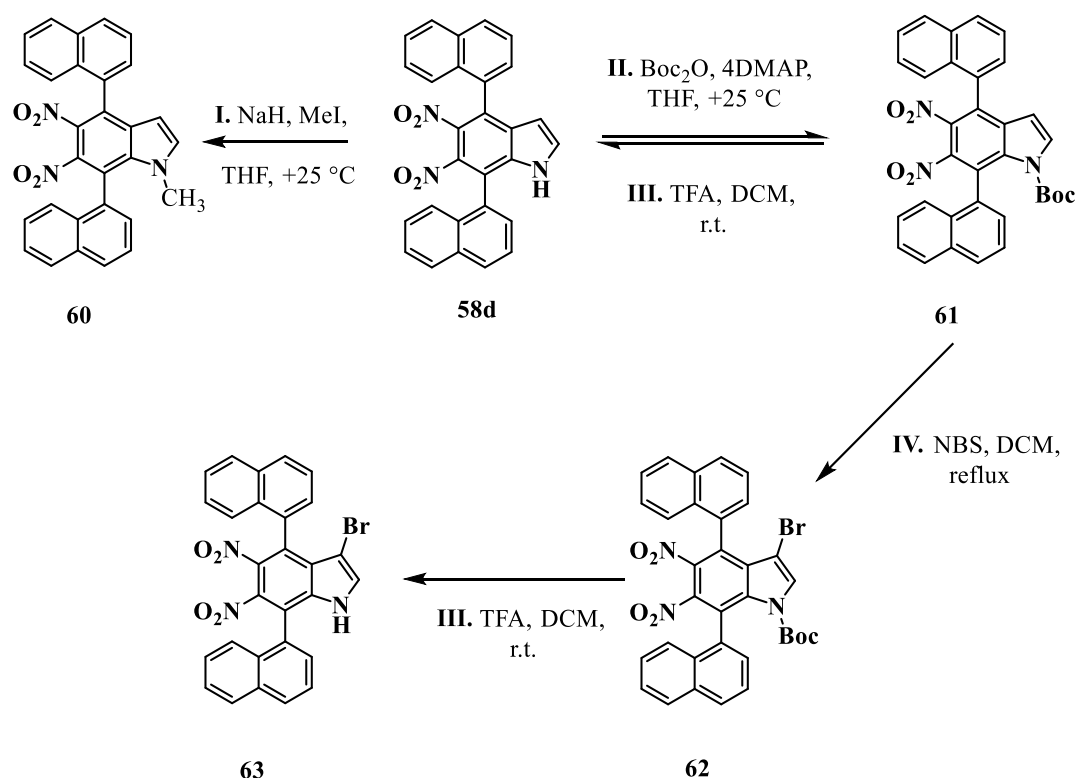


Figure 12. HPLC chromatogram of **61** on Chiralpak AD-H, 250x4.6 mm, *n*-hexane/*i*-PrOH 90:10, 1 mL/min. The peaks are named in the order of elution a, b, c, d.

After preparative chromatography, by NMR the first two eluted peaks have demonstrated to be diastereoisomers. The two enantiopure diastereoisomers of **58d** have been, then, obtained after Boc removal (**61** → **58d**, reaction III in Scheme 14).

The rotational barriers can be evaluated by kinetic experiments followed by HPLC and NMR. For this analysis it should be pointed out that the two rotational barriers have different stereochemical effects: the lower energy barrier converts one diastereoisomer into the other (a process which can be followed by NMR), while the higher energy barrier exchanges the atropisomers due to the presence of the second stereogenic axis (a process which can be followed by CSP-HPLC). However, in the case of compound **58d**, the suggested calculated barriers are very similar and a mixed situation is conceivable. While the diastereomerization was actually performed following the process by NMR (32.6 kcal/mol, Figure S10 in Experimental Section), the impossibility to obtain a good HPLC separation did not allow to perform a simple kinetic experiment to obtain the racemization barrier.

To overcome this additional problem, we figured the preparation of two compounds (Scheme 14) where one of the two barriers was raised by replacing N(1)H with N-Me (compound **60**) and the C(3)H with a C-Br (compound **63**). The presence of additional steric hindrance on the indole core should make the two rotational barriers for the naphthyl groups much more different, so the enantiomerization barrier should be easily distinguishable from the diastereomerization one.



Scheme 14. Synthetic plan to overcome problems related to the separation of the four atropisomers of **58d** and to the distinguishable determination of enantiomerization and diastereomerization barriers.

For **60** the diastereomerization barrier was followed by NMR starting from a sample of the last eluted stereoisomer **60(d)** (letter refers to the elution order of the HPLC reported in Figure S11 of Experimental Section) that was heated at +130 °C and +140 °C and checked at

fixed times, following the growth of the second diastereoisomer (Figure S12 in Experimental Section). By applying a first-order reversible kinetic equation, a rate constant of $1.44 \times 10^{-5} \text{ s}^{-1}$ was derived at +130 °C (and $3.16 \times 10^{-5} \text{ s}^{-1}$ at +140 °C), yielding a rotational barrier of $32.8 \pm 0.15 \text{ kcal/mol}$ by means of the Eyring equation. After 18 hours at +140 °C the diastereomerization was complete, and the sample was checked by CSP-HPLC, showing the presence of two main diastereomeric peaks [**60(a)** + **60(d)**], and two tiny peaks of the remaining stereoisomers **60(b)** and **60(c)** (0.7% and 0.8%, respectively, Figure 13). The enantiomerization barrier was estimated by considering 0.75% of conversion, yielding a value of about 37.5 kcal/mol , in agreement with the difference suggested by DFT calculation (Table 3).

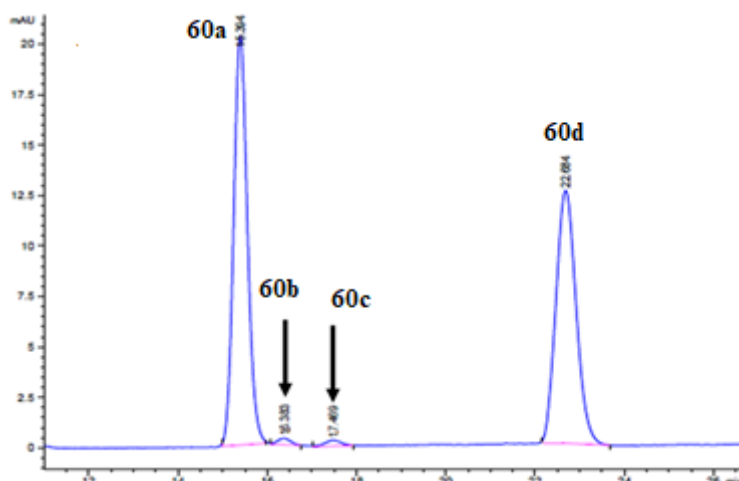


Figure 13. CSP-HPLC of compound **60d** after thermal equilibration at +140 °C for 18 h. (Chiralpak AD-H column, eluent *n*-hexane/*i*-PrOH (9:1), 1 mL/min).

The same approach was used to analyze compound **63**, where the diastereomerization barrier was found to be $33.1 \pm 0.15 \text{ kcal/mol}$ and the enantiomerization was found to be above 38 kcal/mol .^[87]

Experimental and calculated enantio- and diastereomerization barriers are summarized in Table 3.

Table 3. Experimental and calculated Interconversion Barriers.^a

	Experimental		Calculated ^b	
	enant.	diast.	enant.	diast.
58d	≈ 32.6	32.6	29.79 ^c (C7)	29.76 ^c (C4)
60	≈ 37.5	32.8	33.8 ^c (C7)	30.2 ^c (C4)
63	>38	33.1	33.4 ^d (C4)	30.7 ^d (C7)

^aThe calculated energies are reported in kcal/mol. ^bIn parenthesis the stereogenic axis involved. ^cAt the B3LYP/6-31g(d) level of theory. ^dAt the B3LYP/6-311g(d,p) level of theory.

To compare the diastereoisomerization barriers, the kinetic experiments were run by keeping the samples of **58d**, **60**, and **63** in the same oil bath, in order to avoid any temperature difference between the experiments. Within this framework, the error due to the temperature is ruled out and any difference in the rate constants is meaningful. Looking at the calculated results reported in Table 3, the rotational barrier of the 7-naphthyl ring in **58d** is higher than that of the 4-naphthyl. This implies that the NH exerts a slightly larger steric hindrance with respect to the

CH in position 3 of indole. It should be noted that the experimental diastereoisomerization barrier of **58d** is lower than the diastereoisomerization barrier of **60** and **63**. This apparent discrepancy confirms, as a matter of fact, that the two energy barriers in **58d** are very similar. Indeed, if the barriers were identical, the probability for diastereoisomerization by the rotation of one naphthyl group would be double; hence, the corresponding barrier would be lowered by a factor of $RT\ln 2$.^[88]

Absolute configurations were assigned by the combination of X-ray crystallography, ECD spectra, and TD-DFT calculations.^[4] (Table 4).

Table 4. Summary of the Absolute Configurations.^a

	a	b	c	d
58d	4M,7M	4P,7M	4P,7P	4M,7P
60	4M,7M	4P,7P	4M,7P	4P,7M
61	4M,7M	4P,7M	4P,7P	4M,7P
62	4M,7M	4P,7M	4P,7P	4M,7P
63	4M,7M	4P,7M	4P,7P	4M,7P

^aLetters refer to HPLC elution order.

Instead, in the cases of 1-naphthyl derivatives **56d** and **57d**, there is just one stereogenic axis, due to the large steric hindrance between the naphthyl moiety and the NO₂ group, generating two atropisomers for each regioisomer. The atropisomers were separated by means of CSP-HPLC (Figure 14, left). The absolute configurations were determined by chiroptical Electron Circular Dichroism (ECD), simulating the ECD spectrum with TD-DFT calculations (see Experimental Section): for both **56d** and **57d** the calculated spectrum for the M absolute configuration is in agreement with the experimental spectrum of the first eluted (Figure 14, right).

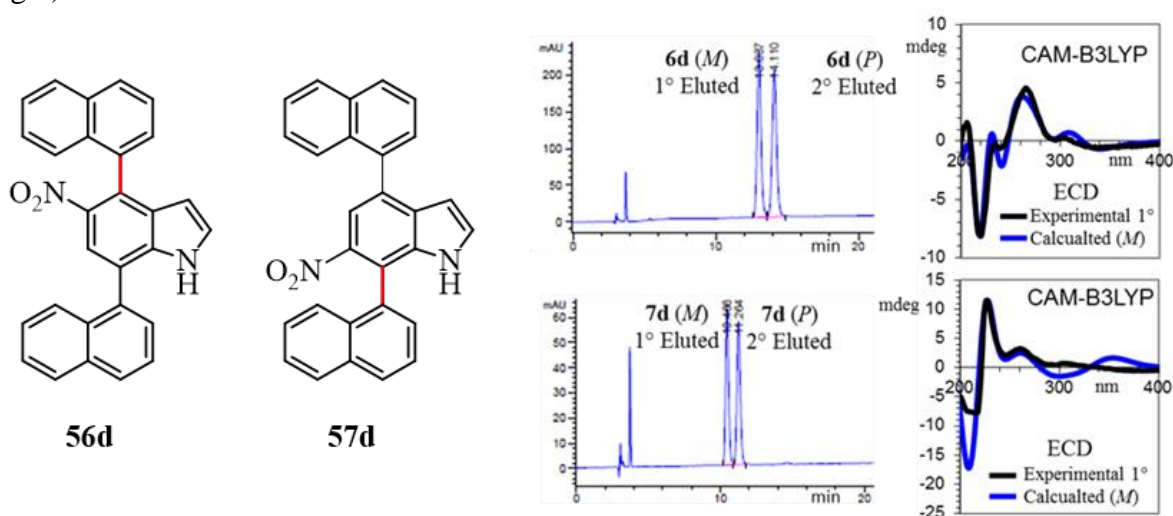
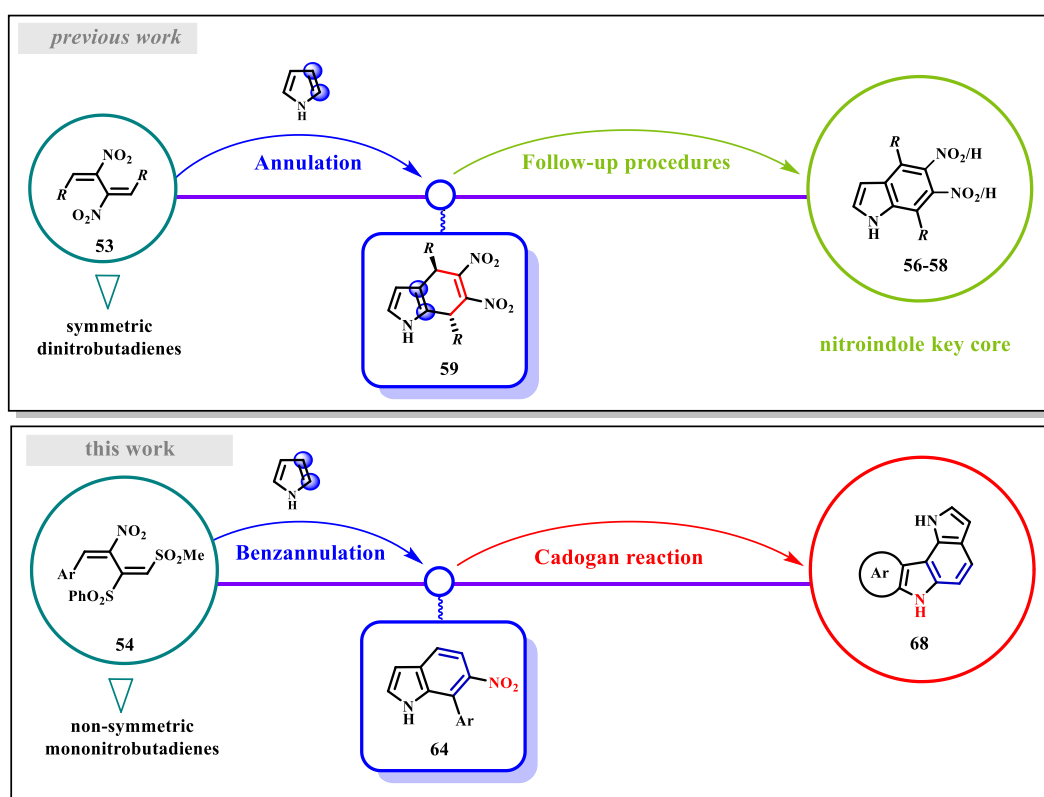


Figure 14. Left: CSP-HPLC chromatograms of compounds **56d** and **57d**; right: experimental and calculated ECD spectra, for the first eluted and M absolute configuration, respectively.

3.2. Sequential annulations to novel pyrrolo[3,2-*c*]carbazoles.

In the previous section, I have reported the use of symmetric 2,3-dinitro-1,3-butadienes in a mild, metal-free, and original benzannulation onto pyrrole to form 4,7-disubstituted indoles mono or dinitrated on the otherwise not-easily-accessible benzene ring. The possibility to intercept an intermediate common precursor for either mono- (**56** and **57**) or dinitroindoles (**58**) allowed a definitely better selectivity to the whole process (Scheme 15, previous work).^[2]

Such interesting results have encouraged us to proceed in this research by studying the non-symmetric 2-nitro-1,3-butadienes as annulation agents of pyrrole (Scheme 15, this work). As I will show, new access to precedently-unreported 7-aryl-6-nitroindoles **64** has figured out, which have proven to be valuable precursors of pyrrolo[3,2-*c*]carbazoles **68**, with an unusual type of fusion. Unlike the previous work, no intermediate has been ever detected.^[3]

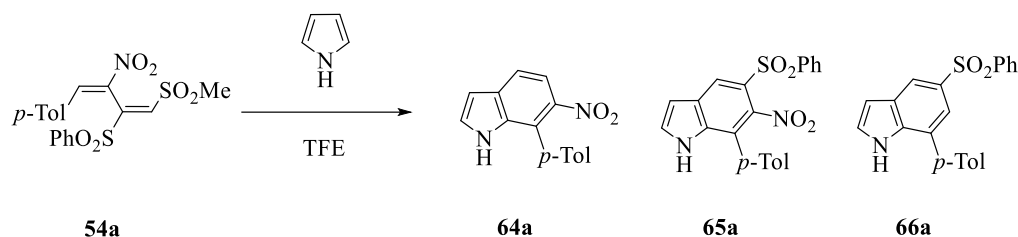


Scheme 15.

An optimization study of the experimental conditions on the model reaction between nitrobutadiene **54a**^[70] (Ar = *p*-Tol) and pyrrole started using 2 mol equiv. of pyrrole in TFE at 50 °C. The complete disappearance of **54a** was observed by TLC after 24 h; the analysis of the chromatographed final reaction mixture highlighted the formation of three different indole derivatives (**64a-66a**, Scheme 16), **64a** being by far the prevalent one (Table 5, entry 1). Despite the satisfying balance, we continued the optimization study hoping to get more selective reaction conditions.

Increasing the equivalents of pyrrole, even if the reaction was faster (Table 5, entry 2), results were almost unchanged, in particular as far as the main product is concerned. We, then, decreased the temperature with the hope to intercept an unsaturated intermediate analogous to

the dihydroindole **59** of Figure 7. Anyway, while a progressive slowdown (entries 3 and 4) was obtained, absolute and relative yields were again almost unchanged without a possibility to observe any kind of intermediate. At the end of this screening, we judged those of entry 3 as the conditions of choice, as they allow a reasonable reaction time and a better yield of **64a**.



Scheme 16. Results from the reaction between the 2-nitrodiene **54a** and pyrrole.

Table 5. Search for conditions of choice in the reactions of nitrobutadiene **4a** with pyrrole.^a

Entry	T (°C)	Pyrrole equiv.	t (h)	64a	65a	66a	Overall balance
1	50	2	24	52 %	16 %	14 %	82%
2	50	4	2.5	53 %	21 %	17 %	91%
3	40	4	5	57 %	17 %	12 %	86%
4	30	4	24	57 %	16 %	19 %	92%
5	0	4	48	-	-	-	^b

^aYields reported are for chromatographically isolated compounds; ^bThe unreacted substrate was quantitatively recovered.

We proceeded then to verify the scope of the reaction, applying the same conditions to a series of 2-nitro-1,3-butadienes substituted at position 1 with different Ar groups, Table 7 showing the results obtained. It can be observed that the good selectivity and the satisfying balance evidenced for **64a** were not exhibited by the whole series, being maintained only for **64b**, **64d**, and, somewhat less so, for **64c** and **64e**. Particularly negative was the result for **64f**, while for **64g** a fourth product (**67g**) originates in a yield comparable to **64g**. Longer reaction times were required by **64i**, and after 7 hours the control TLC still showed traces of substrate. The data obtained until now reveal a not negligible effect exerted both by EWG and EDG substituents on Ar, so the best conditions for the model substrate do not have general validity. Further attempts will be necessary in order to broaden the efficiency and applicability of the process.

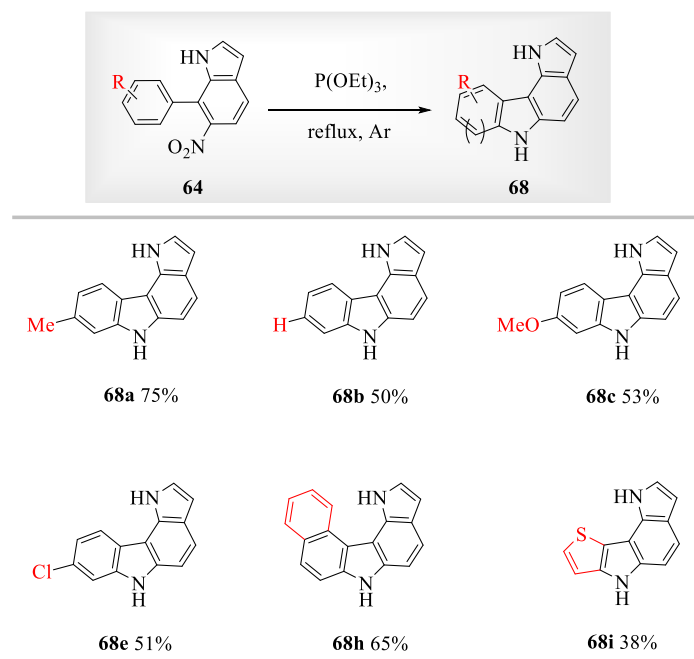
Table 6. Diene scope^a

Entry	Ar	64	65	66	67
1	54a: <i>p</i> -Tol	57	17	12	
2	54b: Ph:	60	10	10	
3	54c: <i>p</i> -MeOC ₆ H ₄	44	17	13	
4	54d: <i>m</i> -ClC ₆ H ₄	53	11	18	
5	54e: <i>p</i> -ClC ₆ H ₄	42	8	15	18
6	54f: <i>p</i> -MeSO ₂ C ₆ H ₄	19	nq ^b	nq ^b	nq ^b
7	54g: 3,5-(CF ₃) ₂ C ₆ H ₃	22	10	11	25
8	54h: 1-Naphthyl	40	14	13	13
9	54i: 2-Thienyl ^c	33	7	11	14

^aYields reported are for chromatographically isolated compounds, unless otherwise specified;

^bObserved by TLC and hypothesized on the grounds of ¹H NMR signals, but not quantified. ^cReaction time: 7h.

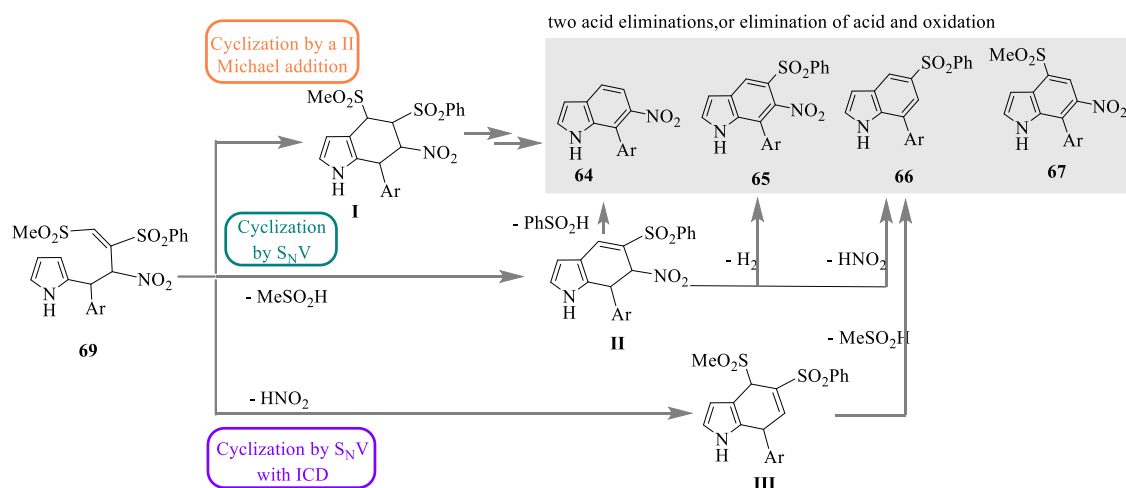
The principal products 7-aryl-6-nitroindoles **64** have been never reported so far and appeared of sure interest because of a pattern of substitution not easy to be obtained otherwise. The nitro group at C-6 of the indole ring system is promising e.g. for further elaborations: for instance, the application of the classic Cadogan reaction conditions^[89] could hopefully build up unusual pyrrolo[3,2-*c*]carbazoles (Scheme 17), very rarely reported before in the literature^[90] notwithstanding, many other similar scaffolds, different from the kind of fusion between pyrrole and carbazole, have been described. For instance, some pyrrolo[2,3-*a*]carbazoles have been recently synthesized and tested for their pharmacological properties (Pim kinase inhibitory potencies),^[87] while the pyrrolo[2,3-*c*]carbazole scaffold characterizes the biologically active natural compounds dictyodendrines.^[91] Encouraged by the wide diffusion of fused carbazole scaffolds among natural or synthetic biologically-active compounds, we submitted compound **64a** to reflux in triethyl phosphite. The reaction went on smoothly to give the expected compound **68a**, in a 75% yield (Scheme 17). For the extension of the Cadogan reaction to other derivatives, we excluded those items for which, because of the poorer results of the benzannulation, the two-step procedure would be inconvenient. The compounds obtained and relative yields are reported in Scheme 17.



Scheme 17. Results obtained in the Cadogan reaction (triethyl phosphite at reflux, 5 h, under Ar) applied on 7-aryl-6-nitroindoles **64**; yields are for chromatographically isolated compounds.

In order to rationalize the formation of the observed products, the absence of any isolable intermediate does not let the discussion to have more than just a speculative significance.

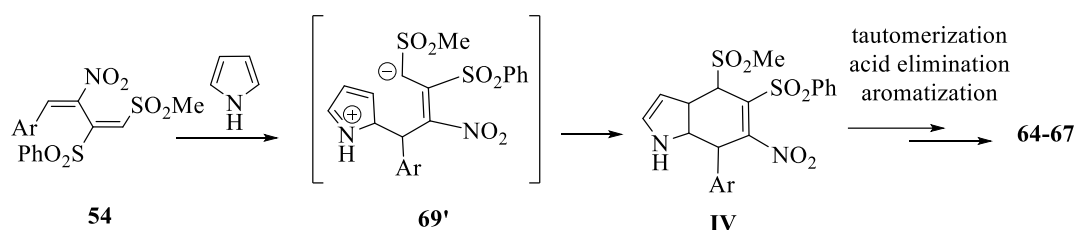
As already ascertained in other processes studied before,^[70a] the nitrovinyl moiety is the more reactive electrophilic site within butadienes **54**: thus, the nucleophilic attack of pyrrole gives presumably origin to the Michael adduct **6**, whose most reasonable evolutions is reported in Scheme 18. The cyclization step could in principle generate the tetrahydroindole **I** (through a *6-endo-trig* Michael addition) or the dihydroindole **II** (through a $\text{S}_{\text{N}}\text{V}$ *6-exo-trig* process). A third possible way ($\text{S}_{\text{N}}\text{V}$ with ICD)^[92] to give **III** could be labeled again as a *6-endo-trig* process. The main products (**64-66**) actually observed can find in **II** an obvious common precursor, while **I** could be the precursor of all the four possible products. As far as **III** is concerned, it could at most be a competitive precursor only of **66**.



Scheme 18. Conceivable evolutions of **69** according to the observed products.

As a matter of fact, experimental results in previously studied systems, as well as Baldwin's rules^[93] encourage to consider the intermediate **II** as the most likely one, although it is only through **I** that **67** can originate. Thus, the observed distribution could be the result of a competition between these two alternative cyclization ways, rather than the consequence of different evolutions of **I**, with **II** anyway playing a significant role.

Actually, as considered also in the analogous reactions of dinitrobutadienes **52** (Scheme 11, *route a*) we cannot exclude an alternative cyclization mechanism where the initially formed zwitterionic form of **69** (**69'**) could evolve through an ionic cycloaddition in which the hexa-atomic ring closes with an inversion of polarity, generating **IV**, not yet aromatic in the penta-atomic ring (Scheme 19). From this tetrahydroindole, processes involving tautomerizations, elimination(s) of acid, oxidative aromatizations (not necessarily in this sequence) would generate all the observed products.



Scheme 19. Alternative ionic cycloaddition to tetrahydroindole **IV**.

While in the cited case of dinitrobutadienes **52** this occurrence would better fit with the isolation of intermediate **59** (Scheme 11), it should be recalled that no intermediates were ever isolated herein, although a zwitterion would be perhaps more justified than in the previous system. Actually, the presence of the electron-withdrawing SO_2Me group on C4 would increase the stabilization of the negative charge delocalized by the nitrovinyl moiety, making intermediate **69'** a better nucleophile and a weaker base. This last hypothesis seems more intriguing, but only the interception of **IV**, possibly by trapping with a suitable diene, could furnish adequate evidence.

4. ERASMUS PROJECT

Within the Erasmus+ program, I had an internship of six months at the “Department of Chemistry” of York University under the supervision of Dr. William Unsworth. The project was focused on the development of a precedent-unreported visible-light promoted dearomatizing spirocyclization of indole-tethered ynones for the preparation of novel spiroindoles and spiroindolines.

4.1. Spiroindoles and spiroindolines.

A spirocompound is a chemical compound presenting a polycyclic structure in which at least two rings are linked together by one common atom. Spirocyclic compounds are unique because of their rigidity and three-dimensional geometries: spiroindolines and spiro-3H-indoles (also referred to as spiroindolenines) are important classes of spirocyclic compounds, present in a wide range of pharmaceuticals and biologically important natural alkaloids (Figure 14).^[94]

Spiroindolines and spiroindoles possess versatile reactivity which enables them to act as precursors for other privileged heterocyclic scaffolds,^[95] including 1H-indoles, carbazoles, oxindoles, and polycyclic frameworks.

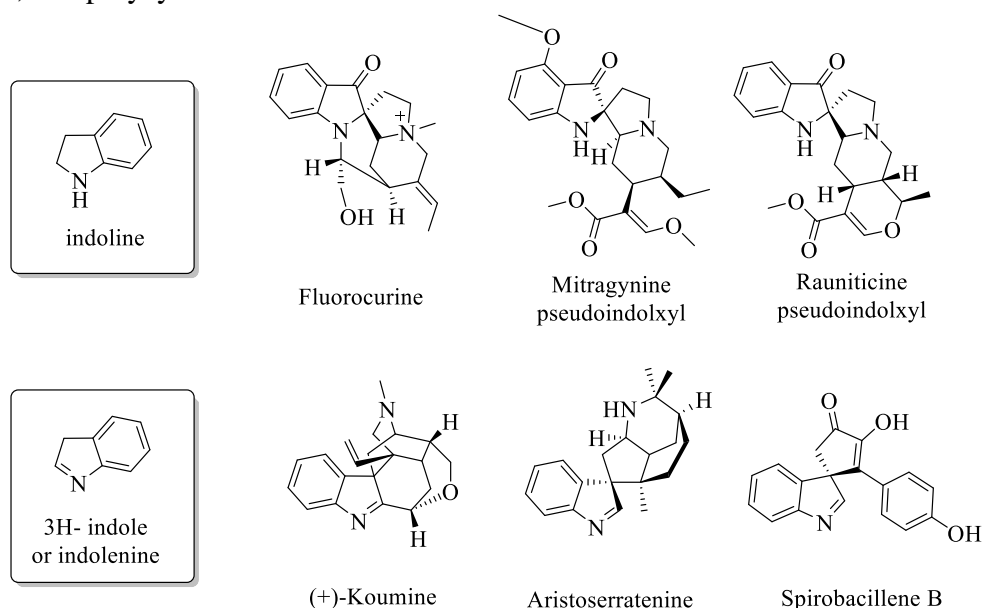


Figure 15. Natural alkaloids containing the C2 or C3-spirocyclic indoline/indolenine core.

Indoles can be spirocyclized at their 2- or 3- position to give C2-spiroindolines and C3-spiroindoles/indolines. In both classes, the ring size and the number and nature of spiroendocyclic heteroatoms could change, rising the number of the possible spirocompounds (Figure 16).^[94]

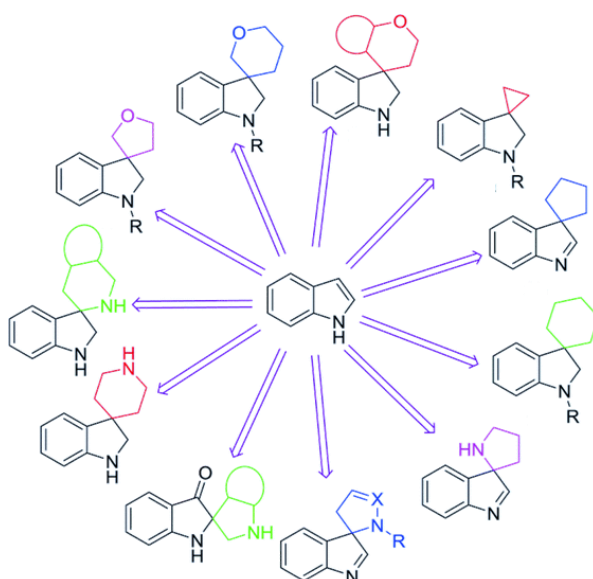


Figure 16. Different categories of spiroindolines and spiroindoles.

The spirocyclic core structure in the field of indoles was first reported by A. Pictet and T. Spengler in 1911 as an intermediate, which rapidly underwent 1,2-migration to restore aromaticity.^[96] The first successful isolation of a spiroindoline was achieved in 2010 by the research group of S.-L. You utilizing an Ir catalyst.^[97] Since then, many synthetic strategies have been successfully applied for the synthesis of spiroindolines and spiroindoles.^[94] In particular, Unsworth *et al.*^[98] grouped the various synthetic strategies for the synthesis of spirocyclic indolenines into three main categories: (1) interrupted Fischer indolisations, (2) dearomatization reactions of indoles, and (3) condensation reactions.

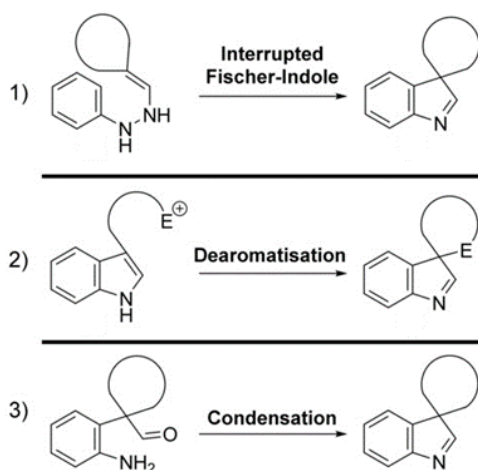
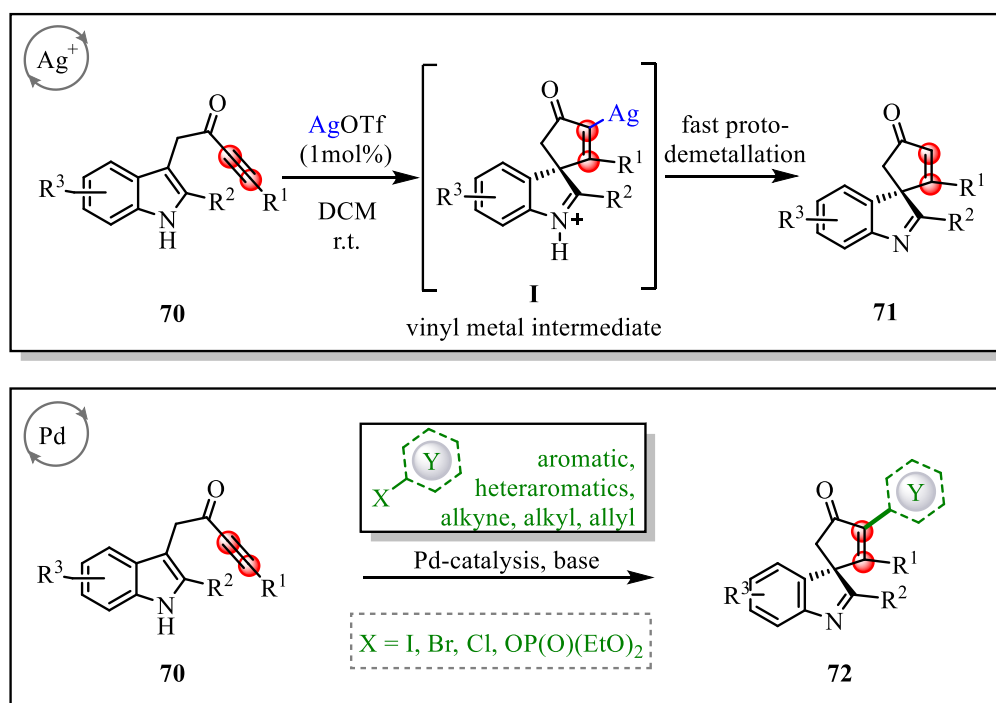


Figure 17. Spirocyclic indolenine synthetic strategies.

The dearomatization of an indole precursor is, today, the most popular method to access spiroindoles: one possible strategy is based on the addition to alkynes. These cyclizations typically proceed by activation of the alkyne by a π -acidic catalyst, followed by a nucleophilic attack of the indole through its C-3 position.

In this scenario, one of the research lines of Unsworth's group is grounded. They have recently published the dearomatizing spirocyclizations of indole-tethered ynones **70** (Scheme 20: Ag⁺) into spirocycles **71** promoted by alkyne activation with a Ag- π -acidic catalyst *via* nucleophilic attack from the tethered indoles to form a vinyl metal intermediate **I**, followed by fast protodemetalation.^[99] However, the interception of these intermediates with any external electrophile other than a proton was prevented by the ease with which such vinyl metal species undergo protodemetalation when π -acidic catalysts are used, meaning that tetrasubstituted alkenes are inaccessible with these methods.

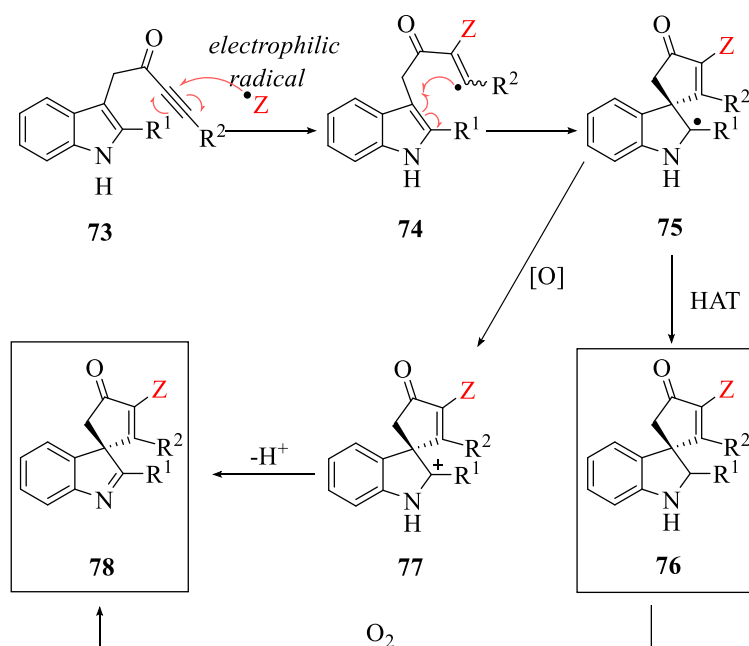
For this reason, the research group developed a one-pot protocol for dearomatizing spirocyclization/cross-coupling of alkyne-tethered indoles **70** (Scheme 2: Pd) in which palladium complexes generated *in situ* act as both π -acid and cross-coupling catalysts.^[100] In this way, an efficient cascade process enables the simultaneous preparation of synthetically challenging quaternary spirocyclic carbons and tetrasubstituted alkenes in a single operation.



Scheme 20. Dearomatizing spirocyclization of alkyne-tethered indoles.

4.2. Radical Spirocyclisation of Indole-Tethered Ynones.¹⁰

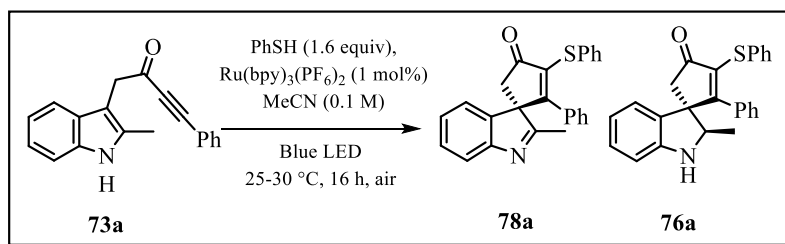
Due to the enormous growth of photochemistry in recent years,^[101] the aim of my Erasmus project at York University was to develop a visible-light-mediated spirocyclisation protocol of indole-tethered ynones **73** in which a radical generation was required instead of an alkyne activation. We postulated that such ynones **73** would react with electrophilic radicals *via* regioselective addition to the alkyne group (**73** → **74**) before cyclizing onto the indole at its 3-position to form a spirocyclic radical intermediate (**74** → **75**). Radical **75** could then go on to form either spirocyclic indoline **76** via hydrogen atom transfer (HAT), or spirocyclic indolenine **78** via single-electron oxidation followed by proton loss (Scheme 21).



Scheme 21. Planned reaction pathways.

Confidence in this general idea was raised by reports of radical-based dearomative processes involving phenol- and anisole-tethered alkynes.^[102] These studies confirm that electrophilic radicals can react with ynones with the desired regioselectivity, and that the so-formed radical species can go on to react with tethered aromatics; however, to the best of our knowledge, such a strategy had not been applied to indole-tethered alkynes prior to this report.^[5]

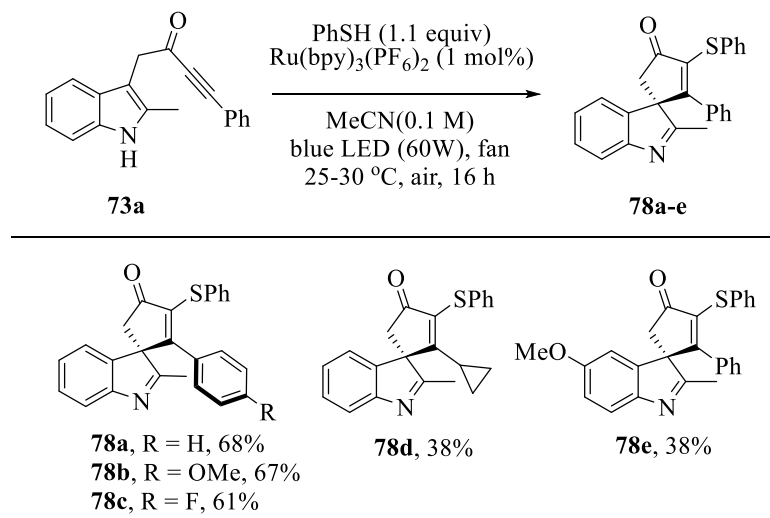
At the start, we examined the reaction of ynone **73a** with a thiyl radical generated in situ from thiophenol: we reasoned that the ensuing sulfur-containing products could be relevant in drug discovery, in view of the presence of vinyl sulfides in bioactive compounds.^[103] We originally chose a photoredox catalysis approach to generate the thiyl radical (Scheme 22). Thus, the combination of thiophenol, catalytic Ru(bpy)₃(PF₆)₂ and irradiation with a blue LED lamp ($\lambda_{\text{max}} = 455 \text{ nm}$, 60 W) at r.t. under air, enabled the conversion of indole-tethered ynone **73a** into spirocyclic indolenine **78a** in reasonable yield *via* an overall oxidative dearomative process (Scheme 22, entry 1) with indoline **76a** as minor side-product. The latter demonstrated to be an intermediate on the route to indolenine: control experiments revealed that oxygen is required for the efficient formation of **78a** (indoline **76a** is the major product in the absence of oxygen: Scheme 22, entry 4) and more intriguingly, a mixture of both products **78a** and **76a** is formed even in the absence of any photocatalyst (Scheme 22, entry 5). In the absence of light, no reaction occurs (Scheme 22, entry 6).



Variation from <i>above conditions</i>	78a	76a
1. none	68% ^a	8% ^a
2. in the dark	0%	0%
3. CFL bulb (23 W)	42%	4%
4. under argon	17%	63%
5. no Ru(bpy) ₃ (PF ₆) ₂	54%	9%
6. no Ru(bpy) ₃ (PF ₆) ₂ and dark	0%	0%

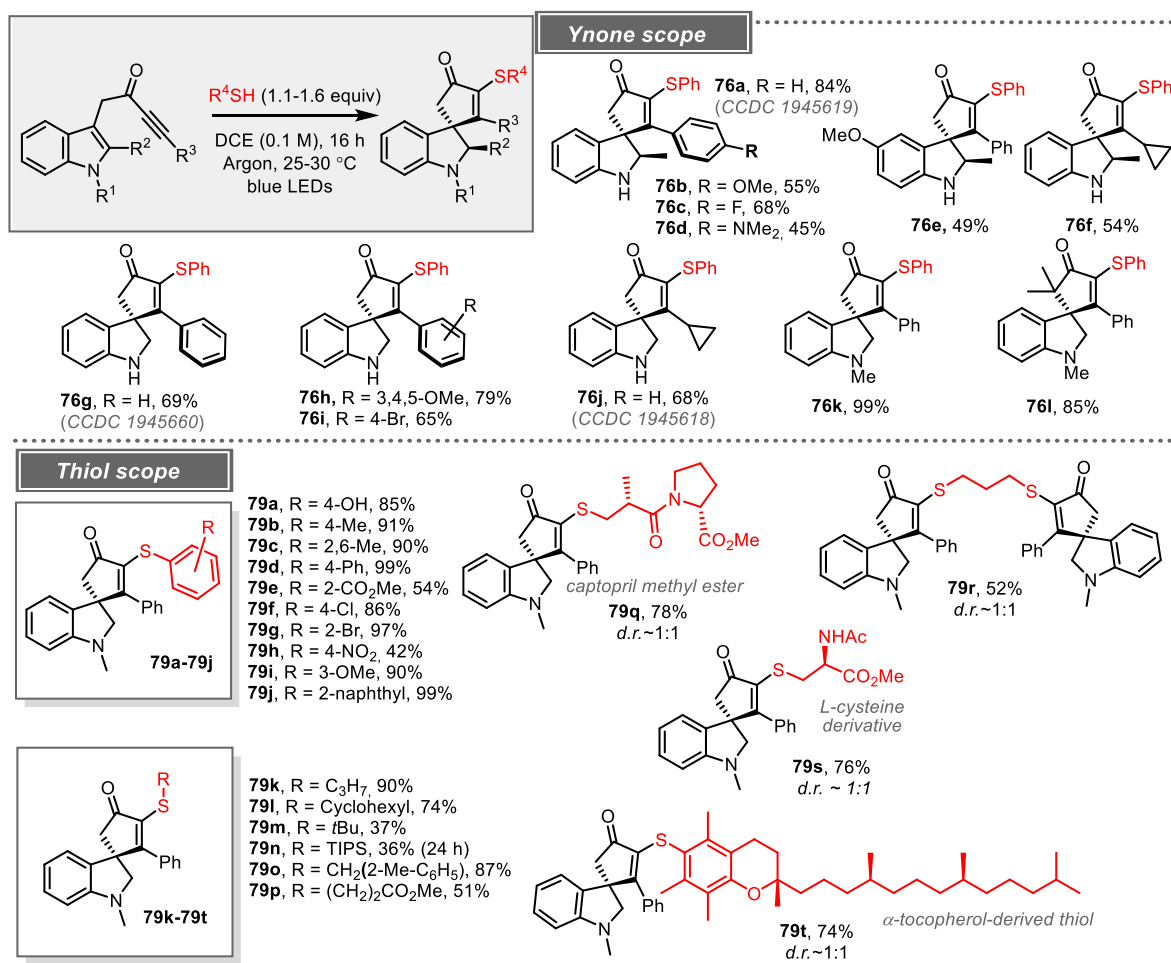
Scheme 22. Photocatalytic synthesis of spirocyclic indolenines and control reactions; all yields are based on comparison to an internal standard in the ¹H NMR spectrum of the unpurified reaction mixture except for ‘a’ which is an isolated yield. CFL = compact fluorescent lamp.

In Scheme 23 a restricted substrate scope of this photoredox-catalyzed radical spirocyclisation is reported because, instead of focusing our attention on the evaluation of substrate scope, we considered the unexpected discovery that spirocyclisation can be achieved without photocatalysis more intriguing, both from a mechanistic standpoint, and in view of the practical and environmental benefits of avoiding metal-based photocatalysts.



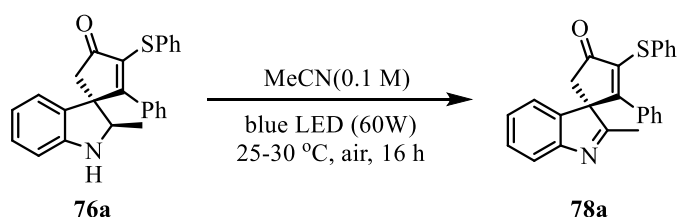
Scheme 23. Substrate scope of photoredox-catalysed radical spirocyclisation.

An additional photocatalyst-free optimization was performed with the main results summarized in Table S3 in the Experimental Section. An important change is that the reactions were performed under argon rather than air favouring the synthesis of indoline products **76/79** rather than of indolenines **78**. The optimized conditions were then tested across a range of indole-tethered ynones and thiols confirming that the reaction is broad in scope (Scheme 24).



Scheme 24. Light-induced charge-transfer radical spirocyclisation. Isolated yields following column chromatography are given.

Interestingly, spiroindoline **76a** underwent oxidation to spiroindolenine **78a** when exposed under light in the presence of oxygen, disclosing a new light-mediated process to access spiroindoles. Anyway, instead of investigating in such direction, attention turned to understand how the reactions operate in the absence of photocatalysis.



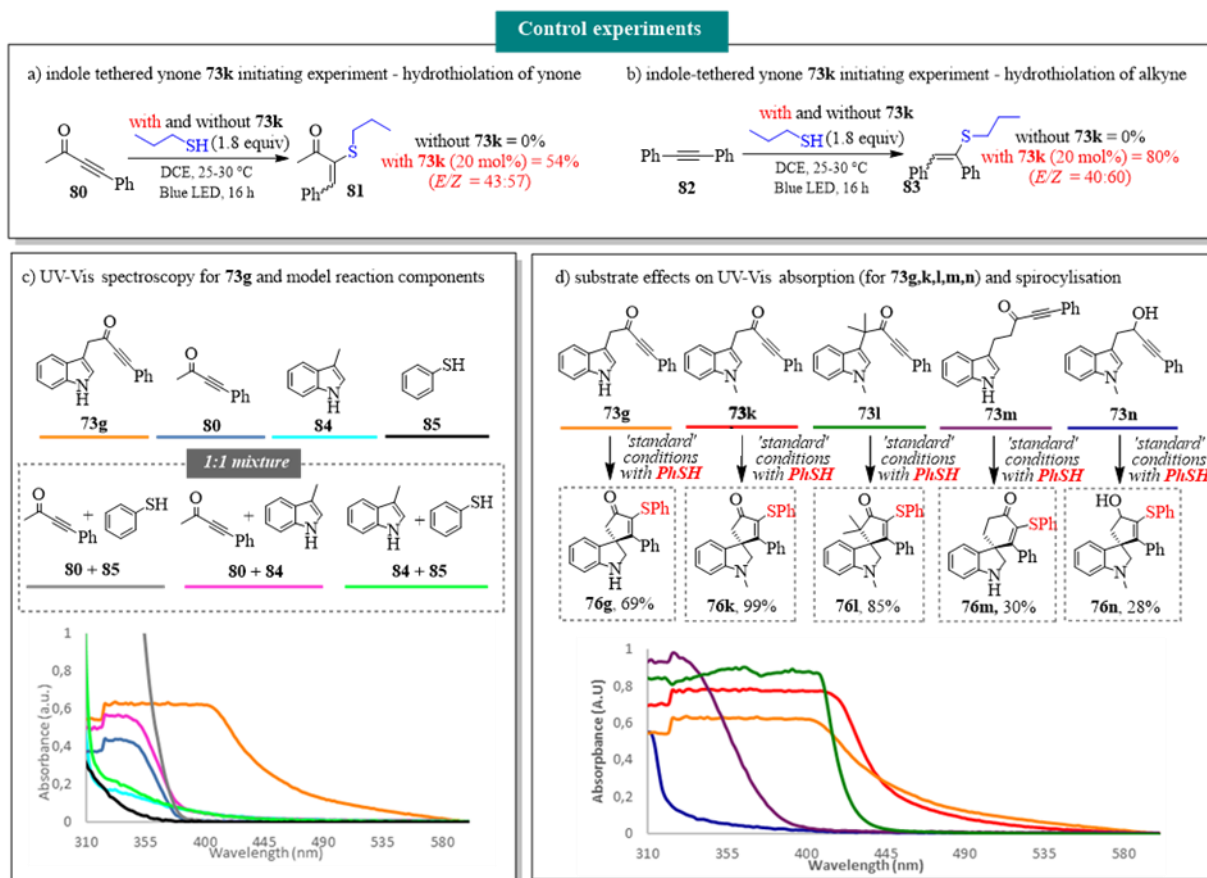
entry	variation from above condition	yield of 18a (%)
1	-	(92)
2	reaction in dark	0
3	reaction under Argon	10

¹H NMR yield determined by using CH₂Br₂ as internal standard. Isolated yield shown in parenthesis

Scheme 25 Visible light-mediated oxidation of **76a** to **78a** under air.

4.3. Mechanistic investigations.

We reasoned that visible-light activation of one of the starting materials must play a key role. Control experiments were designed based on the hydrothiolation of simple alkynes **80** and **82** reacting with *n*-propanethiol under blue LED irradiation at r.t., but no conversion into vinyl sulfides **81** and **83** was observed (Schemes 26a and 26b). The lack of hydrothiolation in these experiments supports the view that the indole-tethered ynone moiety **73** itself is critical to the observed reactivity. Indeed, when alkynes **80** and **82** were again reacted with *n*-propanethiol, but this time with the addition of catalytic (20 mol%) ynone **73k**, hydrothiolation products **81** and **83** were obtained in 54% and 80% yields, respectively, supporting the involvement of the ynone in initiating thiyl radical chemistry.



Scheme 26. (a) Hydrothiolation of ynone **80**; (b) Hydrothiolation of alkyne **82**; (c) UV-Vis spectroscopy studies of indole-tethered ynone **73g** compared with model reaction components; (d) UV-Vis spectroscopy of indole-tethered ynone (**73g**, **73k-m**) and propargylic alcohol **73n**.

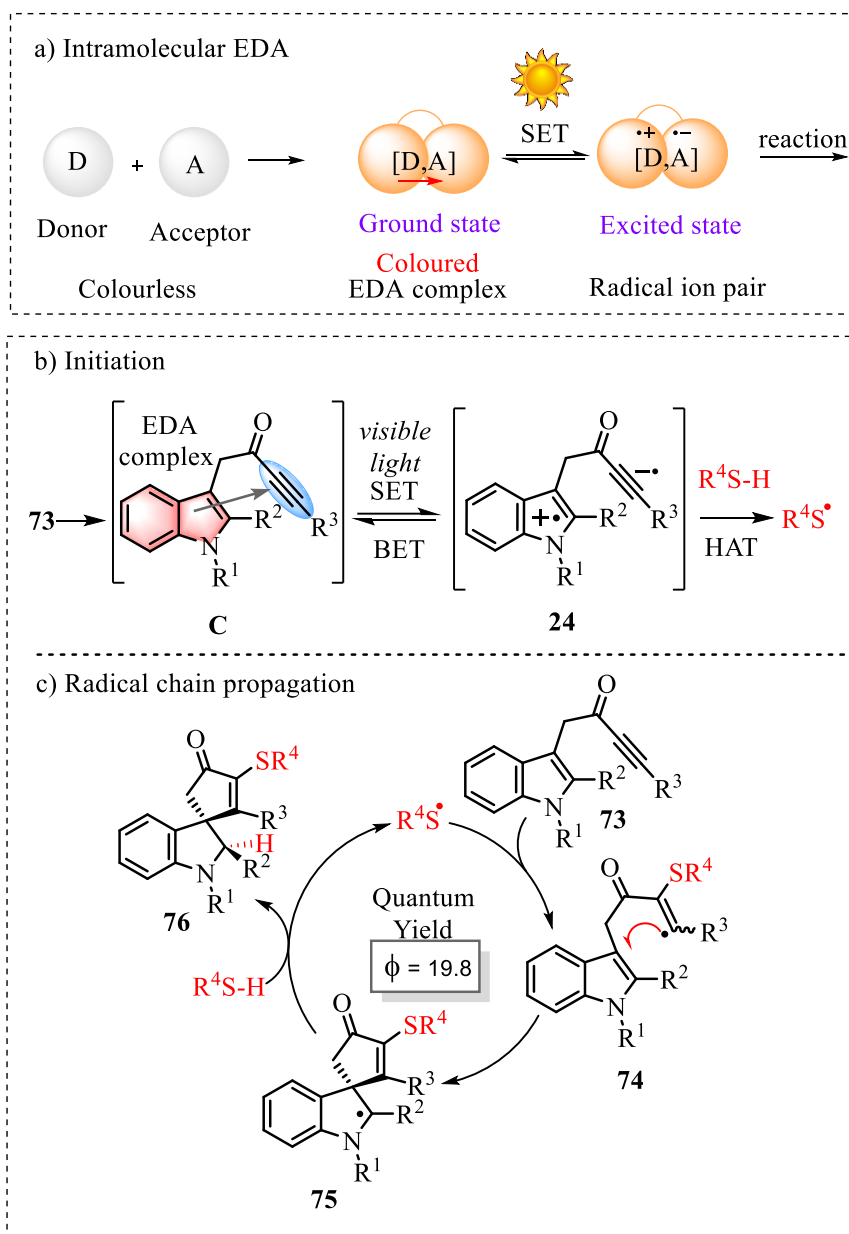
Normally, neither ynone nor 3-substituted indoles would be expected to absorb photons from visible light. However, the ynone **73** used in this study tend to be yellow in colour, and indeed, ynone **73g** was found to absorb relatively strongly around 455 nm (the λ_{max} of the light source) when analyzed using UV-Vis spectroscopy (orange line, Scheme 26c). In contrast, model ynone **80** (light blue line), 3-substituted indole **84** (cyan line), thiophenol **85** (black line) and equimolar mixtures of these compounds (**80+85** in grey, **80+84** in pink and **84+85** in green) displayed little/no absorption in the same region. The ability of the starting material to absorb

visible light around 455 nm appears to correlate well with the success of the radical cascade processes, as illustrated by the data presented in Scheme 26d. For example, alkynes **73m** and **73n**, showed low absorption at 455 nm (purple and blue lines respectively) and both the conversion and yields for these reactions were much lower than those for the standard substrates. In contrast, ynones **73g**, **73k**, and **73l**, which all reacted efficiently to form **76g**, **76k** and **76l** with full conversion and in good yields, show a clear red-shift into the visible region (orange, red and green lines respectively).

We postulate an intramolecular charge transfer interaction to explain the enhanced visible light absorption of the reactive ynone systems, *via* the formation of an intramolecular electron donor-acceptor (EDA) complex C (Scheme 27, *b*). The charge-transfer theory was formulated in 1952 by Robert Mulliken to rationalize the appearance of strong colours on bringing together two colourless organic compounds.^[104] This theory explains how the association of an electronrich molecule (a donor D) and an electron-accepting molecule (an acceptor A) can induce the formation of a molecular aggregation in the ground state. This complex (Scheme 27, *a*)^[105] has physical properties that differ from those of the separated substrates, *e.g.* the appearance of a new absorption band, the charge-transfer band (hvCT), which is associated with a transfer of a single electron (SET) from the donor to the acceptor. Often, the energy of this transition lies in the visible frequency range. The photo-physics of EDA complexes have been extensively studied since the 1950s,^[106] while their use in chemical synthesis was exploited in a more intensive way only 20 years later.^[107] Recently, the resurgence of visible-light-driven processes has motivated chemists to reinvestigate the potential of EDA complex activation for promoting photochemical processes.^[108] Here, we expand the synthetic potential of this activation strategy demonstrating the possibility to form an intramolecular EDA complex and using its photochemical activity to initiate a radical reaction.

Thus, a mechanism is proposed in which the formation of an EDA complex C is followed by visible light absorption to a photoexcited state, loosely represented as the charge transfer complex **24**. This species may simply relax to reform the EDA complex C via back electron transfer, or alternatively, the open shell excited state **24** could abstract a hydrogen atom from the thiol, thus generating the thiyl radical needed to start a radical cascade (Scheme 27, *b*). At this point, a more typical radical chain process can operate (Scheme 27, *c*), which likely proceeds *via* the addition of thiyl radical to the ynone, spirocyclisation and hydrogen atom abstraction from thiol, thus enabling chain propagation. Quantum yield measurements ($\phi = 19.8$) support a chain process.

In general, all the synthetic methods reported so far relied on the excitation of intermolecular EDA complexes. To our knowledge, this study offers the second demonstration of the potential of photon-absorbing intramolecular EDA complexes in synthetic applications after a 2018 report by Melchiorre and co-workers.^[109] This rare radical activation mode was uncovered entirely by serendipity.



Scheme 27. Proposed mechanism.

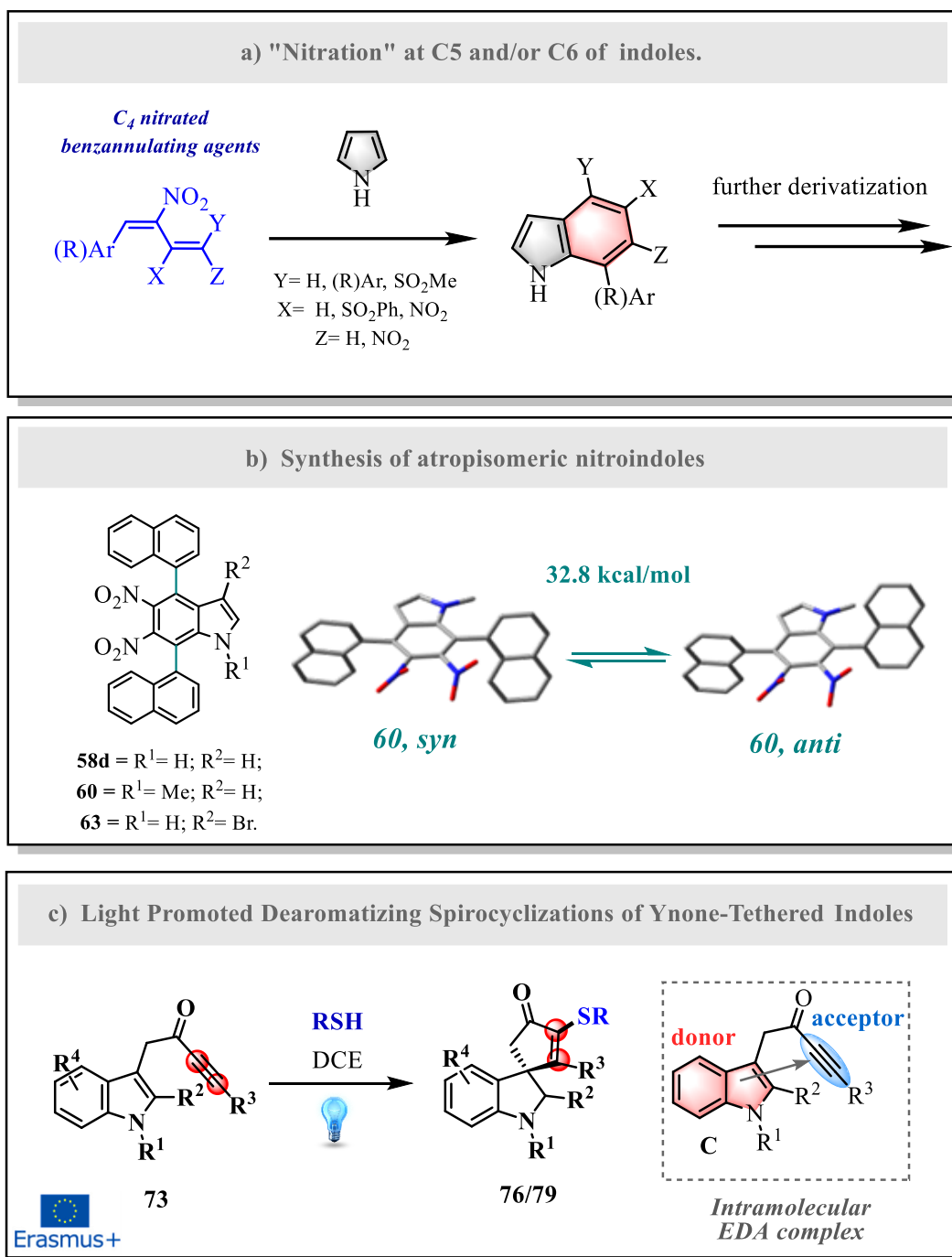
5. CONCLUSIONS

In summary, we reported a novel original approach for the benzannulation onto pyrrole to form 4,7-dialkyl- or diaryl-substituted mononitro- or dinitroindoles from conjugated 2,3-dinitro-1,3-butadiene precursors with the possibility to capture in high yields a reaction intermediate which can independently be brought to the final expected nitroindoles much efficiently in different, selected experimental conditions. Very interestingly, the so assembled indole scaffolds bear one or two nitro groups on the benzene ring (the C5, C6 dinitro pattern being so far unreported in literature, indeed) while maintaining C2 and C3 free and ready for further manipulations: it is worth recalling that electrophilic nitration of the benzene ring of indoles requires, besides rather harsh conditions, that at least the most reactive C3 position be engaged in substitution.^[2]

In this scenario, a stereodynamic study of atropisomeric **58d** has been performed, in view of a possible use in asymmetric catalysis: namely, the presence of hindering naphthyl moieties at C4 and C7 coupled with the two nitro groups at C5 and C6 provide the molecule with two chiral axes which generate different atropisomers due to the asymmetry of the separating indole moiety. To overcome some issues, the synthesis of other two atropisomeric nitroindoles (**60**, **61**) has been necessary for this study. All atropisomers have been separated by chiral HPLC determining absolute configuration and rotational barriers. The high interconversion barriers make them very stable at room temperature.^[4]

The nitrobenzannulation protocol has been then extended to 2-nitro-1,3-butadienes for the synthesis of unusual 7-aryl-6-nitroindoles which, encouraged by the wide diffusion of fused carbazole scaffolds among natural or synthetic biologically active compounds, have been proven to be valuable precursors of unusual pyrrolo[3,2-*c*]carbazoles **30**, never reported before.^[3]

Finally, a new dearomative method for the synthesis of sulfur-containing spirocyclic indolines is described, based on the reaction of indole-tethered ynones with thiyl radicals generated *in situ* from thiols. The reactions are promoted by visible light, operate at room temperature under mild reaction conditions and need neither a transition metal catalyst nor added photocatalyst to proceed efficiently across a wide range of substrates. The reaction is thought to be self-initiated, with visible-light-mediated photoexcitation of an intramolecular EDA complex formed between the indole and ynone moieties in the starting material leading to the formation an open shell excited charge-transfer complex, capable of abstracting a hydrogen atom from the thiol and initiating radical chain propagation. To the best of our knowledge, this is only the second report that details the use of intramolecular EDA complexes in synthesis. This rare radical activation mode was uncovered entirely by serendipity.^[5]



Scheme 28.

6. EXPERIMENTAL SECTION

Table of Contents

1. GENERAL INFORMATION.....	49
2. EXPERIMENTAL UV AND ECD SPECTRA OF 56D AND 57D.	50
3. CONFORMATIONAL ANALYSIS OF COMPOUND 56D AND 57D.	51
4. ABSOLUTE CONFIGURATION OF COMPOUND 56D-57D BY MEANS OF ECD METHOD.....	52
5. CONFORMATIONAL ANALYSIS OF 58D, 60 AND 63.....	54
6. KINETIC EXPERIMENTS	55
7. QUANTUM YIELD MEASUREMENTS.....	58
8. X-RAY CRYSTALLOGRAPHY	59
9. OPTIMIZATION DETAILS	60
10. GENERAL PROCEDURES.....	61
11. IMAGES OF PHOTOCHEMISTRY EXPERIMENTAL SET UP	64
12. SPECTROSCOPIC DATA	65

1. General information

Except where stated, all reagents were purchased from commercial sources and used without further purification. Compounds **53**,^[110] **54**^[70b] and **73**^[100] were prepared as previously reported. Except where stated, anhydrous solvents were obtained from commercial sources. 1,2-Dichloroethane (DCE) and acetonitrile (MeCN) were degassed using argon balloon and stored over activated 3 Å molecular sieves before use. ¹H NMR and ¹³C NMR spectra were recorded with a Varian Inova spectrometer (600 MHz for ¹H, 150.8 MHz for ¹³C), a Varian Mercury 300 Plus spectrometer (300 MHz for ¹H, 75 MHz for ¹³C), a JEOL ECX400 or JEOL ECS400 (400 MHz for ¹H, 100 MHz for ¹³C, and 376 MHz for ¹⁹F). All spectral data was acquired at 295 K, unless otherwise stated; Chemical shifts are given as δ values (ppm) relative to the internal standard relative to the residual peak of the solvents. Coupling constants (*J*) are reported in Hertz (Hz). The multiplicity abbreviations used are: s singlet, d doublet, t triplet, q quartet, td triple doublet, tt triple triplet, dd double doublet, dq double quartet, m multiplet. Signal assignment was achieved by analysis of DEPT, COSY, NOESY, and HMQC experiments where required. ECD spectra were recorded on a Jasco 810 spectropolarimeter at +25 °C in far-UV HPLC grade acetonitrile solutions. The concentrations of the samples (about 10⁻⁴ M) were tuned by dilution of a mother solution (1·10⁻³ M) to obtain a maximum absorbance of about 0.8 ÷ 0.9 in the UV spectrum when using a 0.2 cm path length. Infrared (IR) spectra were recorded on a PerkinElmer UATR 2 spectrometer, either as a compressed solid or neat oil. HRMS mass spectra were recorded with an Agilent ESI-QTOF 6520A mass spectrometer, an Agilent MSD TOF mass spectrometer, and a Bruker Daltonics Micro-Tof spectrometer, using electrospray ionization (ESI). Melting points were determined with a Büchi 535 and Gallenkamp apparatus and are uncorrected. UV-Vis spectroscopy was recorded using Shimadzu UV-Vis Spectrophotometer UV-2600 system. Flash column chromatography was carried out using slurry packed Fluka silica gel (SiO₂), 35–70 μ m, 60 Å or Fuji Silysia Chromatorex Silica gel (SiO₂), neutral MB100, 75–200 μ m, 100 Å under a light positive pressure, eluting with the specified solvent system.

2. Experimental UV and ECD spectra of 56d and 57d.

ECD spectra were recorded on a Jasco 810 spectropolarimeter at +25 °C in far-UV HPLC grade acetonitrile solutions. The concentrations of the samples (about 10^{-4} M) were tuned by dilution of a mother solution ($1 \cdot 10^{-3}$ M) to obtain a maximum absorbance of about $0.9 \div 1$ in the UV spectrum, when using a 0.2 cm path length. The acquisition windows were from 400 to 190 nm by step of 1 nm for 32 seconds acquisition time, with high sensitivity mode.

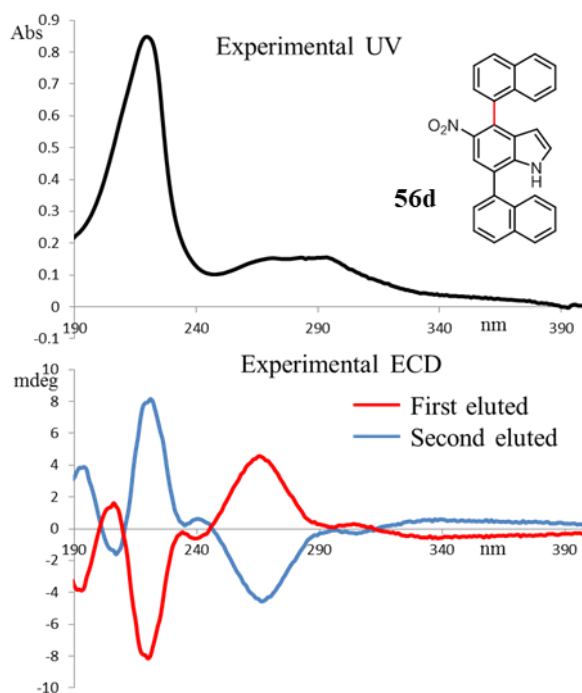


Figure S1. Experimental UV and ECD spectra of compound **56d**.

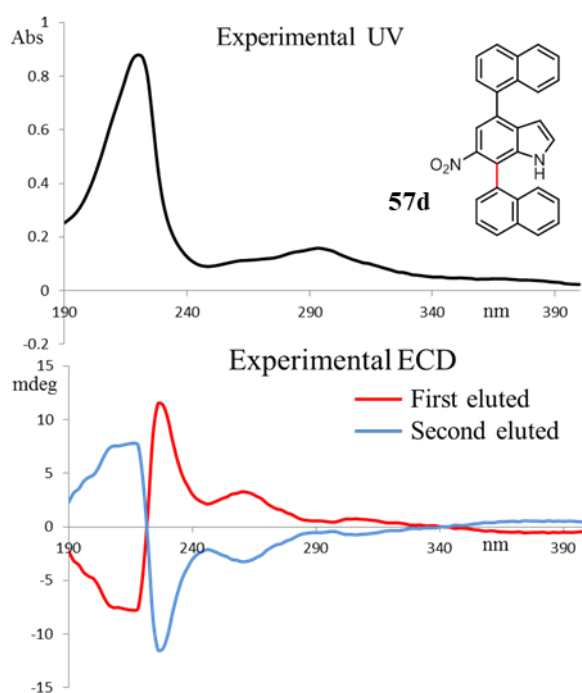


Figure S2. Experimental UV and ECD spectra of compound **57d**.

Absolute configuration^[111]

3. Conformational analysis of compound **56d** and **57d**.

As the first step for AC assignment, we performed a conformational search on compound **56d** and **57d**, assuming *M* absolute configuration. The 1-naphthyl moieties can be positioned in the *syn* or *anti* dispositions, and the rings are not perfectly orthogonal to the indole. This situation yields four conformations, that have been optimized using DFT at the B3LYP/6-31+G(d) level.

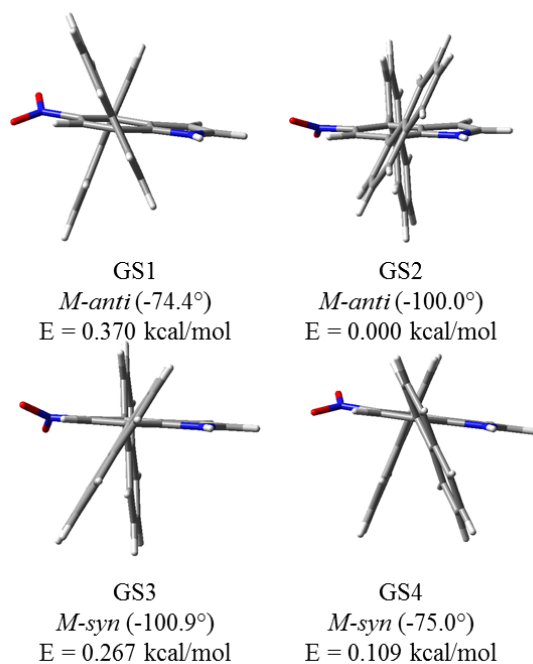


Figure S3. Optimized geometries of **56d** at the B3LYP/6-31+G(d) with *M* absolute configuration.

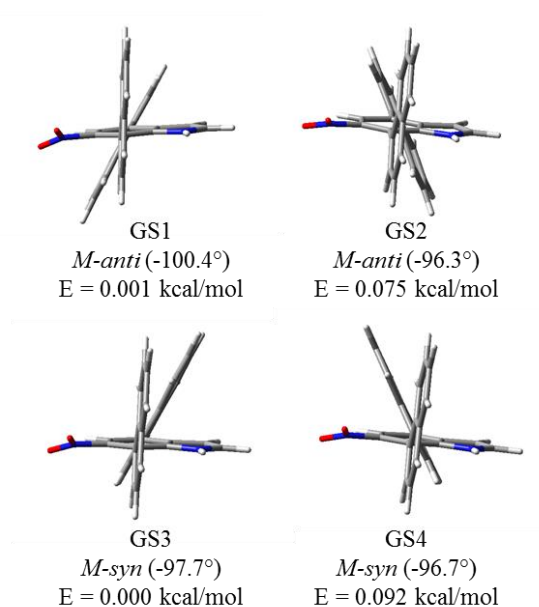


Figure S4. Optimized geometries of **57d** at the B3LYP/6-31+G(d) with *M* absolute configuration.

4. Absolute configuration of compounds **56d** and **57d** by means of ECD method.

The ECD spectra have been calculated for the isolated molecule in the gas phase for the four conformations of **56d** and **57d** using TD-DFT with four different functionals, to ascertain if different computational approaches provide different shapes of the simulated spectra (Figure S5 and S6).^[112] Simulations were performed with the hybrid functionals BH&HLYP^[113] and M06-2X,^[114] with ω B97X-D that includes empirical dispersion,^[115] and CAM-B3LYP that includes long-range correction using the Coulomb Attenuating Method.^[116] The calculations employed the 6-311++G(2d,p) basis set that has proven many times to provide good accuracy at a moderate computational cost.^[117]

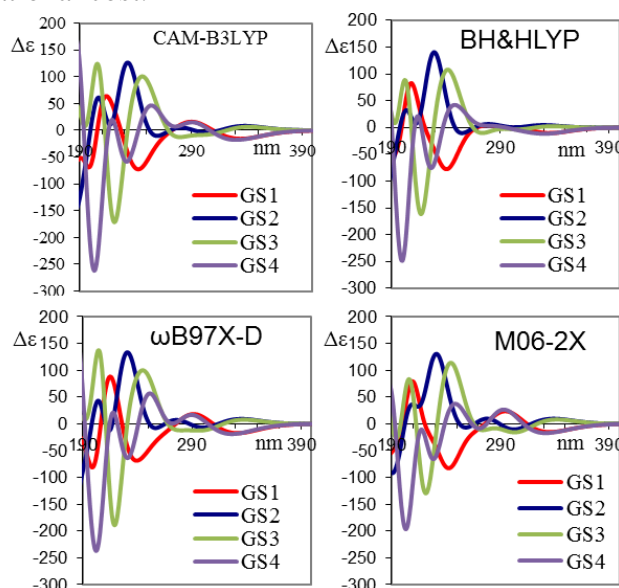


Figure S5. TD-DFT spectra calculated for the four conformations of **56d** (*M*) using four different functionals (CAM-B3LYP, BH&HLYP, M06-2X, ω B97X-D) and the same 6-311++G(2d,p) basis set. For each conformation the first 70 excited states were calculated, and the spectrum was obtained using a 0.25 eV line width at half height.

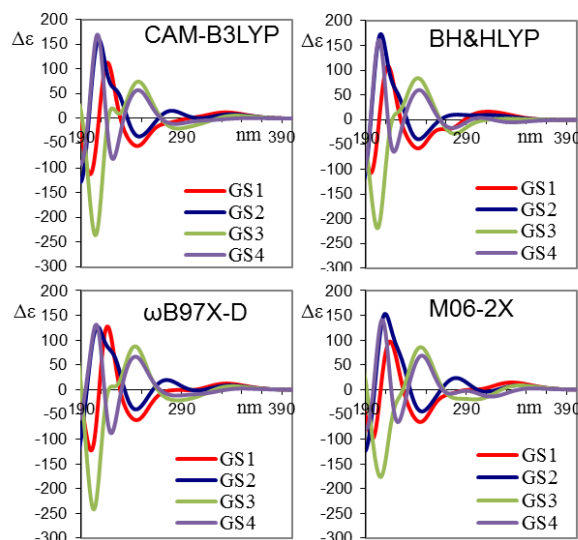


Figure S6. TD-DFT spectra calculated for the four conformations of **57d** (*M*) using four different functionals (CAM-B3LYP, BH&HLYP, M06-2X, ω B97X-D) and the same 6-311++G(2d,p) basis set. For each conformation the first 70 excited states were calculated, and the spectrum was obtained using a 0.25 eV line width at half height.

The four calculated ECD spectra have different shapes, therefore the simulated spectra to be compared with the experimental were obtained using Boltzmann weighting with the total energies calculated using B3LYP (Figures S7-S8). In both cases, the ECD simulation agrees very well with the ECD spectrum of the first eluted atropisomer, to which the *M* absolute configuration can be assigned.

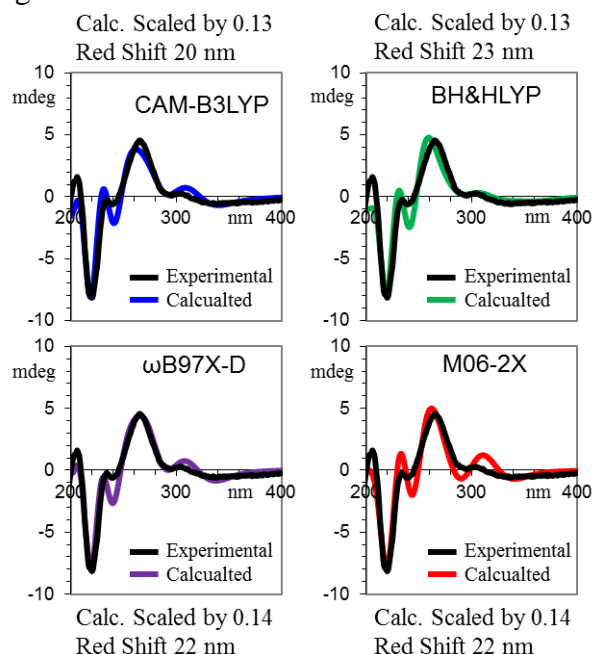


Figure S7. Simulations of the experimental ECD spectrum of first eluted **56d**. The calculated spectra for the four conformations have been mixed using the energies from B3LYP/6-31+G(d) level. For each quarter, the black line corresponds to the experimental spectrum and the colored line to the TD-DFT simulations (6-311++G(2d,p) basis set). The simulated spectra were vertically scaled and red-shifted to get the best match with the experimental spectrum.

All the simulations are for the *M* absolute configuration.

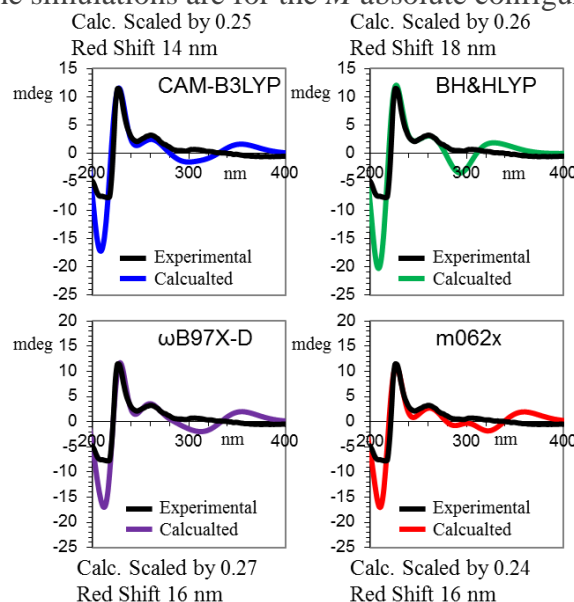


Figure S8. Simulations of the experimental ECD spectrum of first eluted **57d**. The calculated spectra for the four conformations have been mixed using the energies from B3LYP/6-31+G(d) level. For each quarter, the black line corresponds to the experimental spectrum and the colored line to the TD-DFT simulations (6-311++G(2d,p) basis set). The simulated spectra were vertically scaled and red-shifted to get the best match with the experimental spectrum.

All the simulations are for the *M* absolute configuration.

5. Conformational analysis of 58d, 60 and 63

Table S1. Dihedral angles, relative energies and calculated population for compounds **58d**, **60**, **63** at the B3LYP/6-31G(d) level (energies in kcal/mol). The ϕ_{C4} is relative to the C5-C4-C α -C γ dihedral angle, the ϕ_{C7} is relative to the C6-C7-C α -C γ dihedral angle.

Compd.	GS1			GS2			%GS1	%GS2
	ϕ_{C4}	ϕ_{C7}	H°	ϕ_{C4}	ϕ_{C7}	H°		
63a	-86	-76	0.42	-99	-107	0.00	33	67
63d	-85	108	0.00	-99	76	0.00	50	50
60b	71	86	0.48	108	99	0.00	31	69
60d	71	-100	0.00	109	-85	0.26	61	39
58d(a)	-71	-71	0.30	-112	-117	0.00	38	62
58d(b)	71	-116	0.00	113	-71	0.01	51	49

Table S2 Dihedral angles, relative energies and calculated population for compounds **58d**, **60**, **63** at the PCM-B3LYP/6-311G(d,p) level (energies in kcal/mol). The ϕ_{C4} is relative to the C5-C4-C α -C γ dihedral angle, the ϕ_{C7} is relative to the C6-C7-C α -C γ dihedral angle.

Compd.	GS1			GS2			%GS1	%GS2
	ϕ_{C4}	ϕ_{C7}	H°	ϕ_{C4}	ϕ_{C7}	H°		
63a	-84	-75	0.52	-99	-102	0.00	29	71
63d	-85	101	0.20	-99	75	0.00	42	58
60b	75	83	0.61	104	99	0.00	26	74
60d	75	-99	0.00	104	-84	0.11	55	45
58d(a)	-78	-77	0.85	-106	-104	0.00	19	81
58d(b)	78	-104	0.08	105	-78	0.00	47	53

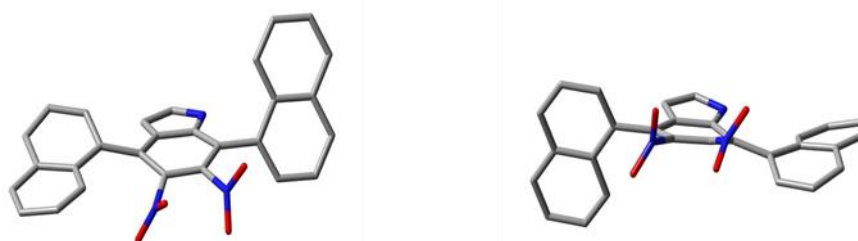


Figure S9 The two calculated transition states for naphthyl rotation of compound **58d**. Left: TS-1 (C4-naphthyl rotation) 29.78 kcal/mol. Right: TS-2 (C7-naphthyl rotation) 29.76 kcal/mol

6. Kinetic experiments

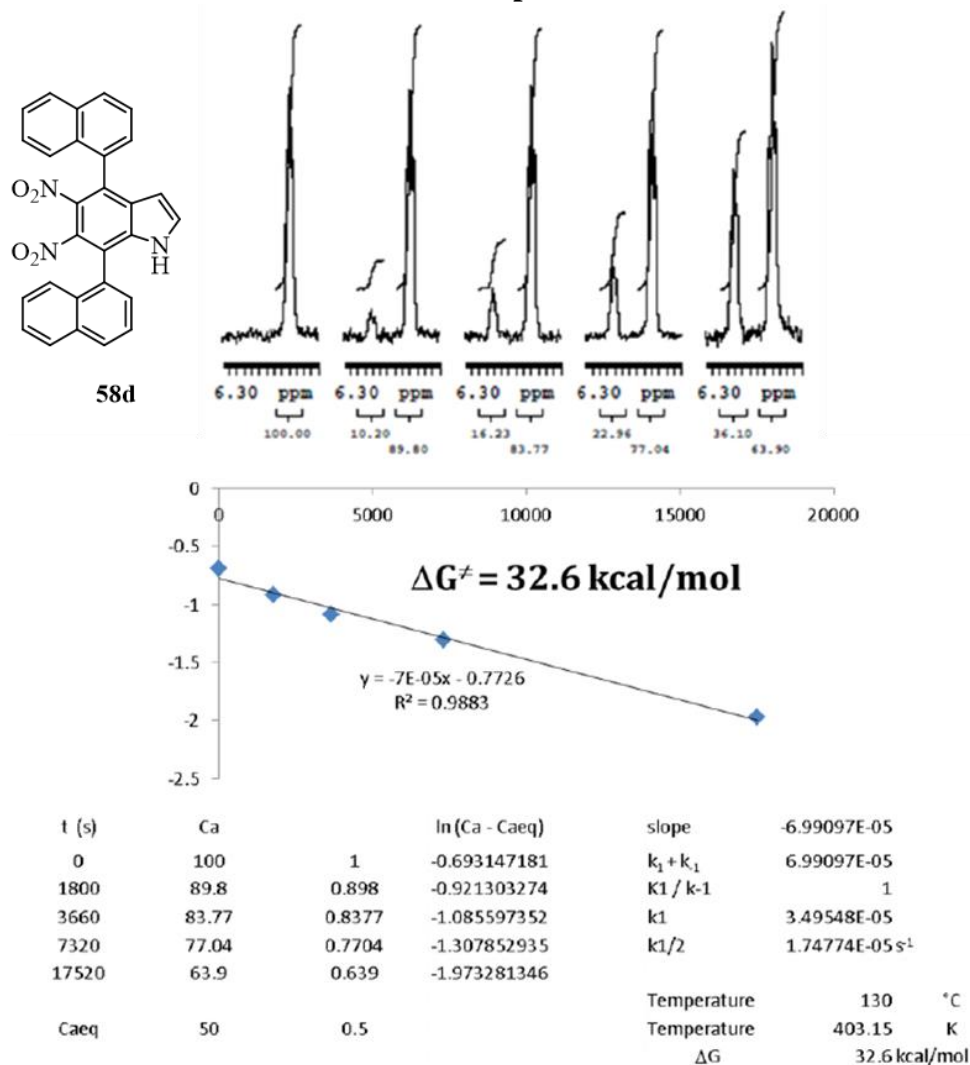


Figure S10. Top: kinetic experiment for the diastereomerization of **58d** (letter refers to the substituent on position 4 and 7 of indole). The enantiopure sample of **58d** was kept at +130 °C in C₂D₂Cl₄, and the NMR spectra were recorded at +25 °C after a fast cooling of the sample. Bottom: kinetic analysis.

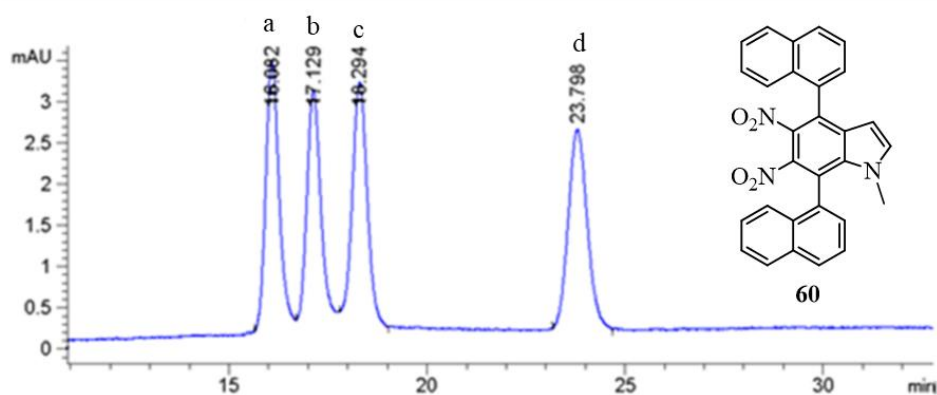


Figure S11. HPLC of **60** after thermal equilibration at +147 °C for 24 h. Chiralpak AD-H 250x4.6 mm, eluent *n*-hexane/*i*-PrOH (9:1), 1 mL/min).

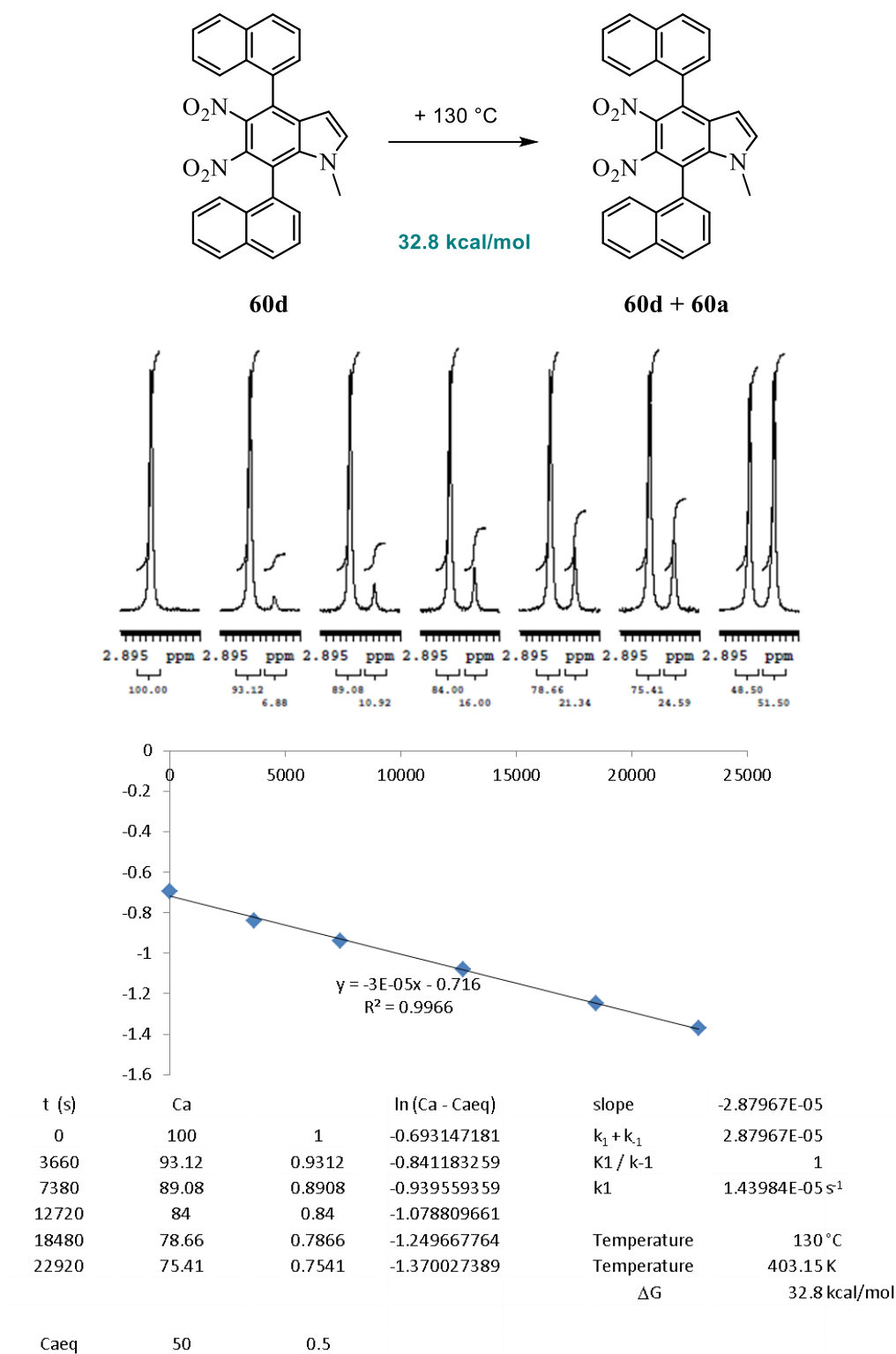


Figure S12. Kinetic experiment for the conversion of **60d** into **60a** (letter refers order of elution in HPLC reported in Figure S11). The enantiopure sample of **60d** was kept at +130 °C in C₂D₂Cl₄, and the NMR spectra were recorded at +25 °C after a fast cooling of the sample.

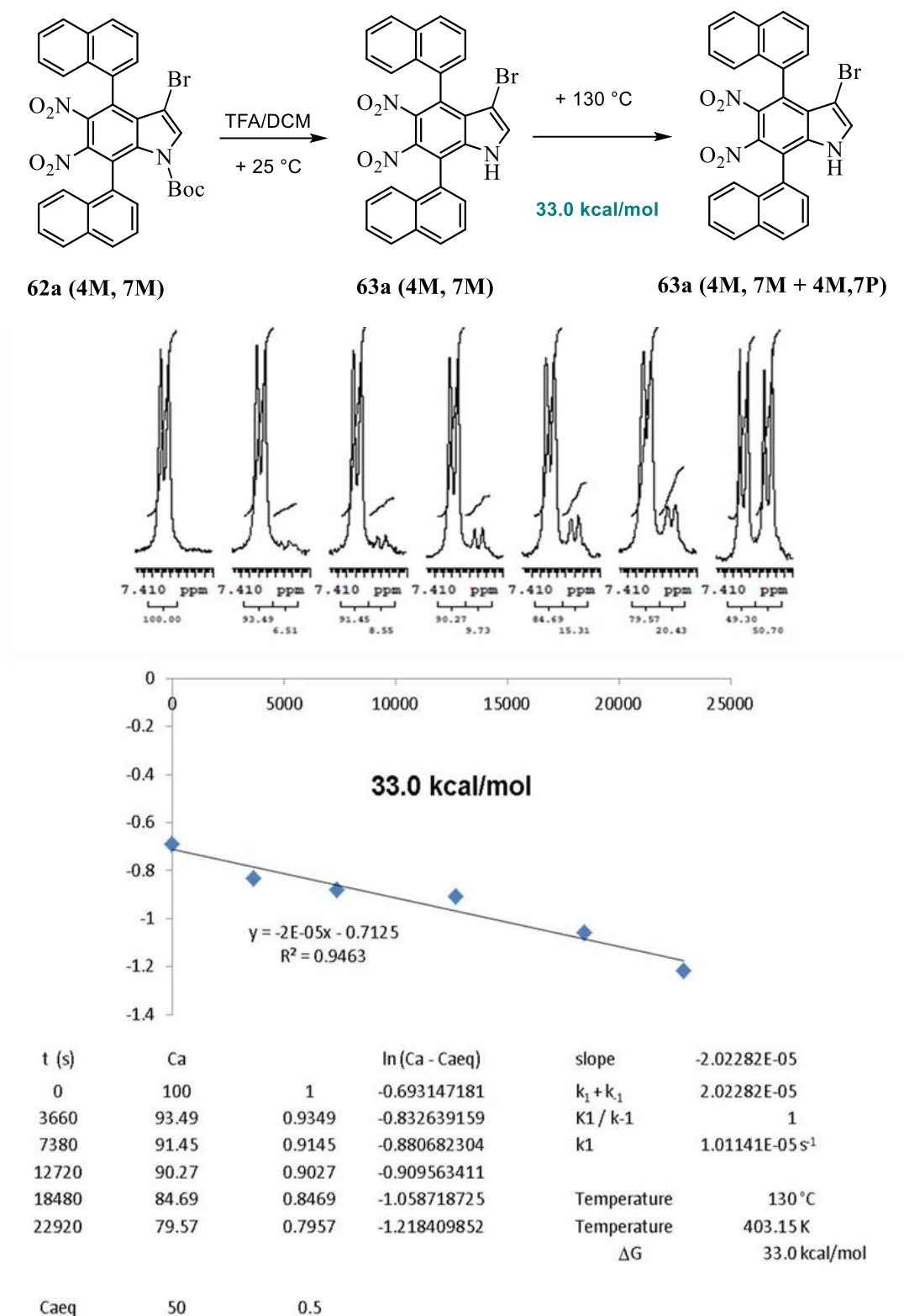


Figure S13. Kinetic experiment for the conversion of **63a** into the *syn/anti* mixture. The enantiopure sample of **63a** was kept at +130 °C in C₂D₂Cl₄, and the NMR spectra were recorded at +25 °C after a fast cooling of the sample.

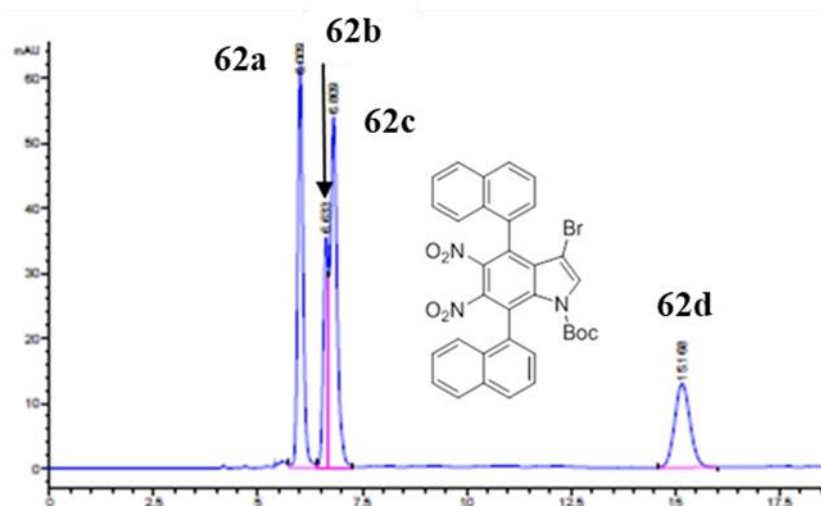


Figure S14. CSP-HPLC chromatogram of compd **62** (ChiralPak AD-H 250x4.6 mm, eluent *n*-hexane/*i*-PrOH 90:10, 1 mL/min).

7. Quantum Yield Measurements

Quantum yield of the reaction was measured based on reported methods by Yoon *et al*.^[118] and the calculations at $\lambda = 455$ nm ($\Phi = 0.85$) by Xia *et al*.^[119]

The photon flux of the LED set up was measured by standard ferrioxalate actinometry.^[120] Cuvettes were placed 1 cm from the LED light source.

Sample calculations:

$$\text{Mol of Fe}^{2+} = \frac{v \cdot \Delta A}{l \cdot \epsilon} = \frac{0.025 \cdot 0.99463}{1 \cdot 11100} = 2.24 \times 10^{-7} \text{ mol}$$

$$\text{Photon flux, } = \frac{\text{mol Fe}^{2+}}{\Phi \cdot t \cdot f} = \frac{2.24 \times 10^{-7}}{0.85 \cdot 30 \cdot 0.99463} = 8.83 \times 10^{-9} \text{ einstein s}^{-1}$$

Average photon flux from three experiments = 8.58×10^{-9} einstein s^{-1} .

Thiophenol **85** (35 μL , 0.32 mmol), **73k** (54.6 mg, 0.2 mmol) and DCE (2.0 mL) were charged into a glass cuvette equipped with a PTFE septum and a magnetic stirrer bar. The mixture was further sparged with argon while stirring for 5 mins. After sparging was complete, additional parafilm was sealed on top of the cuvette and the reaction was irradiated with a 60 W blue LED (1 cm away) for 15 min with stirring and cooling from a small fan to maintain ambient temperature.

^1H NMR yield = 64%

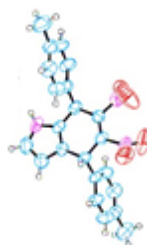
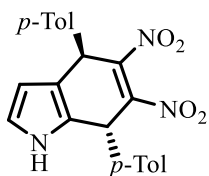
Sample calculation:

$$\text{Quantum yield, } \Phi = \frac{\text{mol of product}}{\text{photon flux} \cdot t \cdot f} = \frac{1.28 \times 10^{-4}}{8.83 \times 10^{-9} \cdot 900 \cdot 0.8408} = 19.2 \text{ einstein s}^{-1}$$

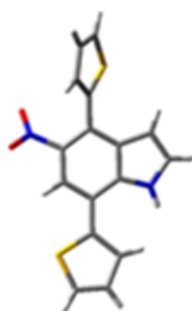
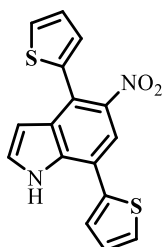
Average quantum yield from three experiments: 19.8 einstein s^{-1}

8. X-Ray Crystallography

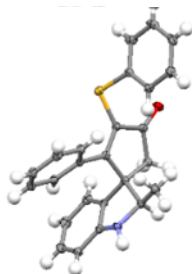
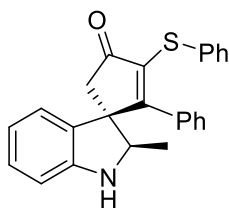
Compounds **59a** (CCDC 1898200), **56e** (CCDC 1968434), **76a** (CCDC 1945619), **76g** (CCDC 1945660), and **76j** (CCDC 1945618), were confirmed by X-ray crystallography. Supplementary crystallography data can be downloaded free of charge via www.ccdc.cam.ac.uk/conts/retrieving.html.



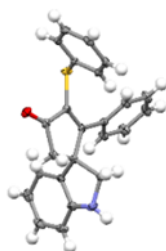
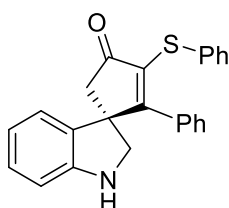
59a (CCDC 1898200)



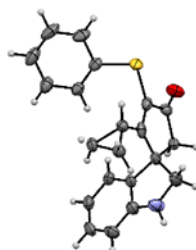
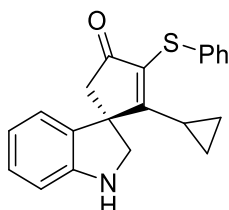
56e(CCDC 1968434)



76a, (CCDC 1945619)



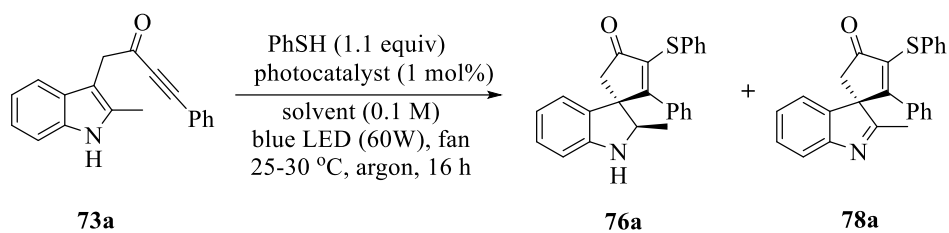
76g, (CCDC 1945660)



76j, (CCDC 1945618)

9. Optimization details

Table S3. Optimisation with thiophenol (PhSH).



entry	photocatalyst (1 mol%)	solvent (0.1M)	yield of 76a (%) ^a	yield of 78a (%) ^a
1	Ru(bpy) ₃ (PF ₆) ₂	MeCN	(63)	(17)
2 ^b	Ru(bpy) ₃ (PF ₆) ₂	MeCN	(8)	(68)
3 ^{b, c}	Ru(bpy) ₃ (PF ₆) ₂	MeCN	4	42
4 ^d	Ru(bpy) ₃ (PF ₆) ₂	MeCN	0	0
5	-	MeCN	(60)	(9)
6	-	MeOH	48	52
7	-	DMF	0	0
8	-	DMSO	0	0
9	-	DCE	(66)	(10)
10 ^d	-	DCE	0	0
11 ^e	-	DCE	10	55
12 ^{b, f}	-	DCE	6	54
13 ^g	-	DCE	(84)	Trace
14 ^g	-	DCE (0.01M)	48	42

Reaction conditions: **73a** (0.10 mmol), PhSH (0.11 mmol), photocatalyst (1.0 mol%), degassed solvent (0.1 M), stirred under argon atmosphere with irradiation of blue LED light for 16 h. ^a ¹H NMR yield determined by using CH₂Br₂ or 1,3,5-trimethoxybenzene as internal standard. Isolated yields are shown in parentheses. ^b Sealed in air condition. ^c Reaction under CFL bulb (23W). ^d Reaction in the dark. ^e Reaction sealed under oxygen atmosphere. ^f with additional 5 mol% of PhSSPh. ^g Reaction with 1.6 equivalent of PhSH.

10. General procedures

General procedure for the synthesis of compounds **56a-g** and **57a-g**.

To a solution of the 4,7-disubstituted-5,6-dinitro-4,7-dihydro-1*H*-indole **59** (0.25 mmol) in toluene (0.05 M), DBU (1.1 mol equiv.) was added and the reaction mixture stirred at r.t. for 24 h. The solvent was removed under reduced pressure and the residue purified by flash chromatography over a silica gel column (petroleum Ether/EtOAc 8:2) to afford the mixture of the two mononitroindoles **56** and **57**. In the cases of **56d-f** and **57d-f**, being the corresponding dihydroindole difficult to isolate, the treatment with DBU was made immediately after removing the TFE solvent under reduced pressure.

General procedure for the synthesis of compounds **58a-g**.

To a solution of the 4,7-disubstituted-5,6-dinitro-4,7-dihydro-1*H*-indole **59** (0.25 mmol) in toluene (0.05 M), DDQ (2 mol equiv.) was added and the reaction mixture stirred at reflux for 24 h. The solvent was removed under reduced pressure and then the residue was purified by flash chromatography over a silica gel column (petroleum Ether/EtOAc 7:3) to afford compounds **58**. In the cases of **58d-f**, being the corresponding dihydroindole difficult to isolate, the treatment with DDQ was made immediately after removing the TFE solvent under reduced pressure.

General procedure for the synthesis of compounds **59a-g**.

To a stirred suspension of the dinitrobutadiene **53** (0.25 mmol) in TFE (0.05 M), pyrrole (2 mol equiv.) was added. Temperature and time are reported in table 2. In the cases of **59d-e**, after 24 h, a second addition of pyrrole (2 equiv.) was done. After the needed time, the solvent was removed under reduced pressure and then the residue purified by flash chromatography over a silica gel column (petroleum Ether/EtOAc 85:15). Compounds **59a-c** and **59g** could be effectively isolated, while **59d-f** during silica gel chromatography convert into the mixture of the two mononitroindoles. They must be submitted to the following treatments with DBU or DDQ without chromatographic purification.

Synthesis of compound **60**.

To a solution of 4,7-di(naphthalen-1-yl)-5,6-dinitro-1*H*-indole **58d** (97 mg, 0.21 mmol) in THF (0.07 M) at 0 °C NaH (13 mg, 60% dispersion in mineral oil, 0.31 mmol) was added. The heterogeneous mixture was stirred at 0 °C for 1 h, then iodomethane (17 μ L, 0.27 mmol) and the mixture was added and warmed to room temperature. After 30 min, the reaction mixture was quenched with saturated NH₄Cl (10 mL) and extracted with ether (3x5 mL). The organic layers were combined, washed with brine, dried over anhydrous Na₂SO₄ and concentrated under reduced pressure to afford compound **60** (99 mg, 0.21 mmol, quantitative) as a white solid. The atropisomers of compound **60** were purified with semipreparative HPLC using a ChiralPak AD-H column (2 cm ϕ x 25 cm, eluent n-hexane/*i*-PrOH 90:10, 20 mL/min), yielding the four stereoisomers.

Synthesis of compound **61**.

A solution of 4,7-di(naphthalen-1-yl)-5,6-dinitro-1*H*-indole **58d** (40 mg, 0.087 mmol), 4-DMAP (16 mg, 0.13 mmol) and Boc₂O (38 mg, 0.174 mmol) in THF (0.1 M), was stirred at room temperature until the disappearance of the starting indole monitoring the evolution of the

reaction by TLC (petroleum ether/ EtOAc 1:1). Then, water was added and the organic layer was extracted with EtOAc (3 x 5 mL), dried over Na₂SO₄, filtered and the solvent removed under reduced pressure. The crude was purified by flash chromatography (petroleum ether/EtOAc 7:3) obtaining a white solid (45 mg, 0.08 mmol). The diastereomeric ratio of compound 3a vs 3b was 3:7. This mixture was purified with semipreparative HPLC using a ChiralPak AD-H column (2 cmφ x 25 cm, eluent *n*-hexane/*i*-PrOH 90:10, 20 mL/min), obtaining the enantiopure **61a-61d**.

Synthesis of compound 62.

A solution of N-tert-butoxycarbonylindole **61** (90 mg, 0.16 mmol) and NBS (0.57 mg, 0.32 mmol) in CH₂Cl₂ (0.08 M) was refluxed. After 24 h, despite the constant presence of the starting indole (as judged by TLC), the cooled reaction mixture was diluted with H₂O (2 mL). The layers were separated, and the organic phase was washed (10% KOH, H₂O), dried (Na₂SO₄), and concentrated. The residue was purified by flash chromatography over a silica gel column (petroleum ether/EtOAc 7:3), affording compound **62** (37 mg, 0.06 mmol, 36%) as a white solid. The atropisomers of compound **62** were purified with semipreparative HPLC using a ChiralPak AD-H column (2 cmφ x 25 cm, eluent *n*-hexane/*i*-PrOH 90:10, 20 mL/min), obtaining the enantiopure **62a** and **62d**, and a mixture of **62b** and **62c**. Single crystals were obtained from the latter mixture by slow evaporation of an *n*-hexane/CH₂Cl₂ solution.

Boc deprotection of 61a, 61b and 62a.

To a stirred solution of **61a**, **61b** or **62a** (0.02 mmol), in CH₂Cl₂ (0.06 M), TFA was added (TFA/CH₂Cl₂ 1:1). The reaction mixture was stirred at room temperature until the disappearance of starting material as determined by TLC (typically 1-2 h). The mixture was diluted with CH₂Cl₂ and KOH 2M was added. The organic layer was extracted, washed with brine, dried over anhydrous Na₂SO₄ and concentrated under reduced pressure to afford compound **58d(a)**, **58d(b)** or **63a**, with 92, 95 and 99% yield, respectively.

General procedure for the synthesis of 7-arylsubstituted indoles (64-66 a-i)

To a stirred suspension of the suitable nitrobutadiene **54** (0.245 mmol) in TFE (5 mL, 0.05 M), pyrrole (4 mol equiv.) was added. Temperature and time are reported in Table 2. After the time necessary for the disappearance of **54** (5-7 h), the solvent was removed under reduced pressure and the residue purified by flash chromatography over a silica gel column (petroleum ether/ethyl acetate gradients).

General procedure for the Cadogan reaction: synthesis of pyrrolo[3,2-*c*]carbazoles 68

A 5 mL flame-dried round-bottomed flask, equipped with a condenser, was charged with 0.11 mmol of the relevant **54** and 2.2 mL of triethylphosphite (d = 0.969 g/mL, 2.13 g, 12.8 mmol). The resulting mixture was heated at reflux under nitrogen for 5 h, and then the excess of triethylphosphite was partly removed under reduced pressure (bath temperature 80 °C). The residue was dissolved in ethyl acetate and washed with HCl 5% solution, and water, then dried. The crude was purified by column chromatography (ethyl acetate/petroleum ether 4:1) to isolate compound **68**.

General procedure for the synthesis of compounds 78a-e.

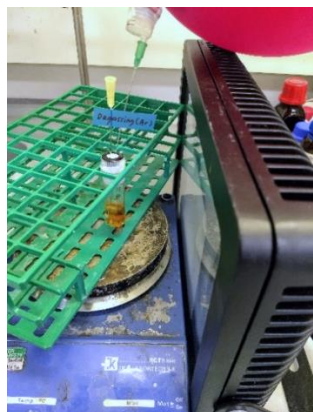
Thiophenol (0.32 mmol, 1.6 equiv) was added to the solution of the indolyl-ynone **73** (0.2 mmol) and Ru(bpy)₃(PF)₂ (1mol%) in MeCN (0.1 M). The reaction mixture was sealed under air and stirred for 16 h under the irradiation of 60W blue LED flood light (1–2 cm away) with a cooling fan. After completion of the reaction, the solution was concentrated in vacuo and purified by flash column chromatography. See next for photographs illustrating the reaction set-up.

General procedure for the synthesis of compounds 76a-n and 79a-t.

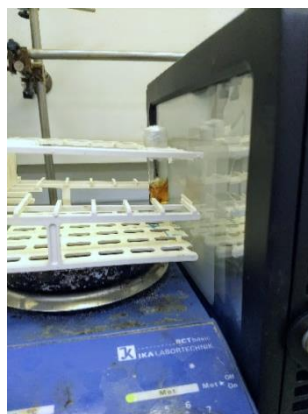
To a 8.0 mL screw-neck-vial (17 x 60 mm) equipped with a septa seal screw cap and stirrer bar was loaded thiol (0.20–0.32 mmol, 1.0–1.6 equiv) and ynone (0.2 mmol) in degassed DCE (2 mL, 0.1 M). The mixture was sparged with argon while stirring for 5 mins. After completion of sparging, the vial was additionally sealed with paraffin film and stirred for 16 h under irradiation of a 60 W blue LED flood light (1–2 cm away). A cooling fan was mounted on top of the photoreactor box to maintain ambient reaction temperature (25–30 °C). After completion of the reaction, the solution was concentrated in vacuo and purified by flash column chromatography. See next for photographs illustrating the argon sparge and reaction set-up.

11. Images of photochemistry experimental set-up

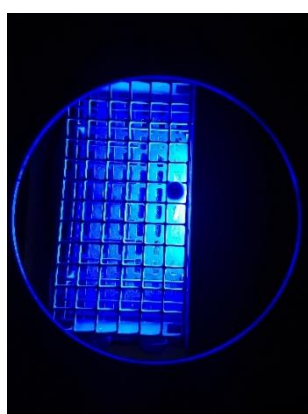
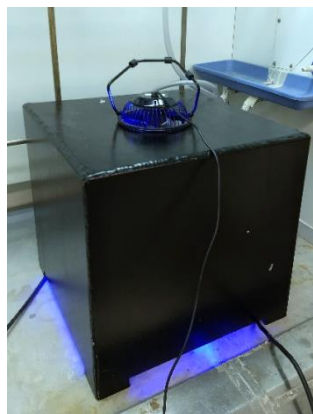
1. Sparging of the reaction mixture with argon balloon



2. Sealed reaction vial ready to run

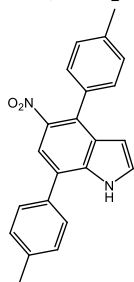


3. The reaction in progress covered in a black box with a cooling fan.



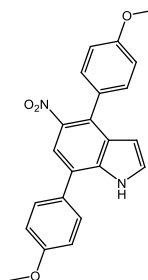
12. Spectroscopic data

5-nitro-4,7-di-*p*-tolyl-1*H*-indole 56a



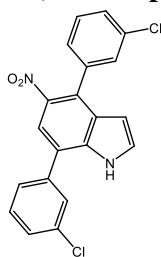
Yellow solid, mp 199–200 °C (ethanol). ¹H NMR (CDCl₃, 600 MHz): δ (ppm) 2.45 (s, 3H), 2.46 (3H, s), 6.49 (t, *J* = 2.6 Hz, 1H), 7.29–7.38 (m, 3H), 7.33 (d, *J* = 7.9 Hz, 2H), 7.37 (d, *J* = 7.8 Hz, 2H), 7.56 (d, *J* = 7.9 Hz, 2H), 7.87 (s, 1H), 8.71 (br s, 1H). ¹³C NMR (CDCl₃, 151 MHz): δ (ppm) 21.42, 21.51, 105.39, 118.38, 125.08, 126.96, 128.16, 128.62, 128.90, 129.38, 129.76, 130.33, 133.61, 134.06, 135.25, 137.68, 138.59, 142.60. HRMS (ESI) *m/z* calcd. for C₂₂H₁₉N₂O₂ [M + H]⁺: 343.1447, found 343.1449

4,7-bis(4-methoxyphenyl)-5-nitro-1*H*-indole 56b



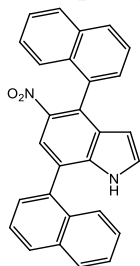
Yellow solid, mp 228–229 °C (ethanol). ¹H NMR (CDCl₃, 600 MHz): δ (ppm) 3.89 (s, 3H), 3.90 (3H, s), 6.50 (dd, *J* = 3.2, 2.2 Hz, 1H), 7.03 (d, *J* = 8.7 Hz, 2H), 7.09 (d, *J* = 8.7 Hz, 2H), 7.31 (t, *J* = 2.8, 1H), 7.37 (d, *J* = 8.7 Hz, 2H), 7.60 (d, *J* = 8.7 Hz, 2H), 7.83 (s, 1H), 8.68 (br s, 1H). ¹³C NMR (CDCl₃, 151 MHz): δ (ppm) 55.44, 55.62, 105.42, 114.16, 115.10, 118.32, 124.77, 126.91, 128.74, 128.98, 129.19, 129.32, 129.48, 130.01, 135.28, 142.73, 159.41, 159.95. HRMS (ESI) *m/z* calcd. for C₂₂H₁₉N₂O₄ [M + H]⁺: 375.1345, found 375.1343.

4,7-bis(3-chlorophenyl)-5-nitro-1*H*-indole 56c



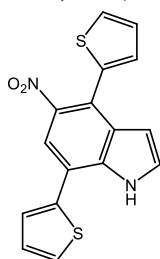
Yellow solid, mp 213–214 °C (ethanol). ¹H NMR (CDCl₃, 600 MHz): δ (ppm) 6.45 (dd, *J* = 3.2, 2.1 Hz, 1H), 7.28–7.30 (m, 1H), 7.36 (dd, *J* = 3.3, 2.4 Hz, 1H), 7.41–7.44 (m, 3H), 7.48 (dt, *J* = 7.5, 1.4 Hz, 1H), 7.52 (t, *J* = 7.7 Hz, 1H), 7.56 (dt, *J* = 7.5, 1.4 Hz, 1H), 7.67 (t, *J* = 1.6 Hz, 1H), 7.94 (s, 1H), 8.75 (br s, 1H). ¹³C NMR (CDCl₃, 75 MHz): δ (ppm) 105.39, 118.66, 124.16, 126.54, 126.94, 127.67, 128.24, 128.36, 128.74, 128.95, 129.09, 129.93, 131.05, 134.46, 135.07, 135.63, 138.35, 138.55, 141.99 (two carbons are accidentally isochronous). HRMS (ESI) *m/z* calcd. for C₂₀H₁₃Cl₂N₂O₂ [M + H]⁺: 383.0354, found 383.0356.

4,7-di(1-naphthyl)-5-nitro-1*H*-indole 56d



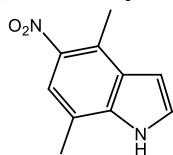
Yellow solid, mp 267–268 °C (ethanol). ¹H NMR (CDCl₃, 600 MHz): δ (ppm) 6.16 (td, *J* = 3.4, 2.2 Hz, 1H), 7.14 (t, *J* = 2.7 Hz, 1H), 7.35–7.78 (m, 10H), 7.92–7.98 (m, 2H), 7.98–8.05 (m, 2H), 8.19 (s, 1H), 8.23 (br s, 1H) (two atropisomers are present). ¹³C NMR (CDCl₃, 151 MHz): δ (ppm) 105.51, 120.21, 124.13, 125.46, 125.55, 125.57, 125.94, 126.09, 126.31, 126.38, 126.46, 126.63, 127.10, 128.07, 128.40, 128.59, 128.90, 129.08, 129.39, 129.45, 131.40, 131.91, 133.75, 134.11, 134.81, 136.53, 136.56, 142.82. HRMS (ESI) *m/z* calcd. for C₂₈H₁₉N₂O₂ [M + H]⁺: 415.1447, found 415.1445.

5-nitro-4,7-di(2-thienyl)-1*H*-indole 56e



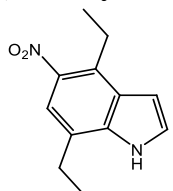
Yellow solid, mp 170–171 °C (ethanol). ¹H NMR (CDCl₃, 400 MHz): δ (ppm) 6.70 (dd, *J* = 3.3, 2.2 Hz, 1H), 7.11–7.19 (m, 2H), 7.24 (dd, *J* = 5.1, 3.6 Hz, 1H), 7.39 (t, *J* = 2.7 Hz, 1H), 7.45 (dd, *J* = 3.6, 1.1 Hz, 1H), 7.46–7.50 (m, 2H), 7.94 (s, 1H), 8.98 (br s, 1H). ¹³C NMR (CDCl₃, 101 MHz): δ (ppm) 105.57, 117.85, 118.65, 122.01, 126.03, 126.38, 126.87, 127.24, 127.45, 127.72, 128.36, 129.68, 134.10, 135.68, 138.17, 143.27. HRMS (ESI) *m/z* calcd. for C₁₆H₁₁N₂O₂S₂ [M + H]⁺: 327.0262, found 327.0266.

4,7-dimethyl-5-nitro-1H-indole 56f



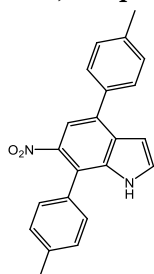
Yellow solid, mp 245–246 °C (ethanol). ¹H NMR (Acetone-d₆, 300 MHz): δ (ppm) 2.55 (s, 3H), 2.76 (s, 3H), 6.82 (dd, *J* = 3.2, 2.0 Hz, 1H), 7.52 (t, *J* = 2.9 Hz, 1H), 7.67 (s, 1H), 10.83 (br s, 1H). ¹³C NMR (Acetone-d₆, 75 MHz): δ (ppm) 15.58, 15.72, 103.30, 115.66, 118.33, 119.40, 125.22, 126.97, 128.39, 137.14. HRMS (ESI) *m/z* calcd. for C₁₀H₁₁N₂O₂ [M + H]⁺: 191.0821, found 191.0823.

4,7-diethyl-5-nitro-1H-indole 56g



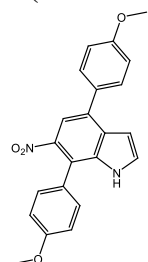
Yellow solid, mp 129–130 °C (ethanol). ¹H NMR (300 MHz): δ (ppm) 1.40 (t, *J* = 7.6 and 7.4 Hz, 6H, two part. overlapped), 2.89 (qd, *J* = 7.6, 0.7 Hz, 2H), 3.21 (q, *J* = 7.4 Hz, 2H), 6.78 (dd, *J* = 3.3, 2.1 Hz, 1H), 7.35 (dd, *J* = 3.1, 2.7 Hz, 1H), 7.74 (s, 1H), 8.50 (br s, 1H). ¹³C NMR (CDCl₃, 75 MHz): δ (ppm) 13.34, 14.75, 23.50, 23.67, 103.95, 117.67, 124.80, 125.72, 127.60, 132.14, 136.34, 141.97. HRMS (ESI) *m/z* calcd. for C₁₂H₁₅N₂O₂ [M + H]⁺: 219.1134, found 219.1133.

6-nitro-4,7-di-*p*-tolyl-1H-indole 57a



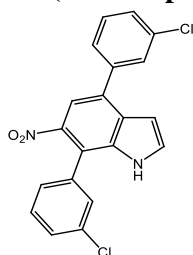
Yellow solid, mp 226–227 °C (ethanol). ¹H NMR (CDCl₃, 600 MHz): δ (ppm) 2.45 (s, 3H), 2.47 (s, 3H), 6.83 (dd, *J* = 3.0, 2.2 Hz, 1H), 7.28–7.35 (m, 6H), 7.39 (t, *J* = 2.8 Hz, 1H), 7.65 (d, *J* = 8.0 Hz, 2H), 7.92 (s, 1H), 8.37 (br s, 1H). ¹³C NMR (CDCl₃, 151 MHz): δ (ppm) 21.39, 21.48, 103.49, 116.04, 120.80, 128.55, 128.65, 129.31, 129.34, 129.67, 130.05, 131.27, 133.84, 135.22, 136.33, 137.95, 138.41, 143.13. ¹HRMS (ESI) *m/z* calcd. for C₂₂H₁₉N₂O₂ [M + H]⁺: 343.1447, found 343.1446.

4,7-bis(4-methoxyphenyl)-6-nitro-1H-indole 57b



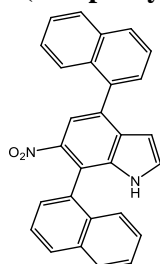
Yellow solid, mp 183–184 °C (ethanol). ¹H NMR (CDCl₃, 600 MHz): δ (ppm) 3.88 (s, 3H), 3.90 (s, 3H), 6.82 (dd, *J* = 3.1, 2.2 Hz, 1H), 7.02–7.10 (m, 4H), 7.36 (d, *J* = 8.6 Hz, 2H), 7.40 (t, *J* = 2.8 Hz, 1H), 7.68 (d, *J* = 8.7 Hz, 2H), 7.87 (s, 1H), 8.38 (br s, 1H). ¹³C NMR (CDCl₃, 151 MHz): δ (ppm) 55.50, 55.54, 103.51, 114.41, 114.84, 115.86, 120.23, 126.22, 129.20, 129.23, 129.90, 130.00, 131.71, 133.53, 135.40, 143.32, 159.64, 159.80. HRMS (ESI) *m/z* calcd. for C₂₂H₁₉N₂O₄ [M + H]⁺: 375.1345, found 375.1347.

4,7-bis(3-chlorophenyl)-6-nitro-1H-indole 57c

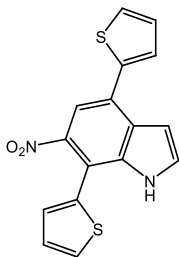


Yellow solid, mp 139–140 °C (ethanol). ¹H NMR (CDCl₃, 600 MHz): δ (ppm) 6.82 (dd, *J* = 3.2, 2.1 Hz, 1H), 7.29–7.32 (m, 1H), 7.43–7.44 (m, 2H), 7.46–7.49 (m, 4H), 7.61 (dt, *J* = 7.5, 1.5 Hz, 1H), 7.72 (t, *J* = 1.8 Hz, 1H), 7.96 (s, 1H), 8.40 (br s, 1H). ¹³C NMR (CDCl₃, 151 MHz): δ (ppm) 103.37, 116.37, 120.08, 126.97, 127.02, 128.33, 128.75, 128.81, 128.91, 129.58, 130.27, 130.30, 130.66, 132.91, 134.91, 135.01, 135.23, 136.08, 140.76, 142.60. HRMS (ESI) *m/z* calcd. for C₂₀H₁₃Cl₂N₂O₂ [M + H]⁺: 383.0354, found 383.0355.

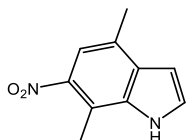
4,7-di(1-naphthyl)-6-nitro-1H-indole 57d



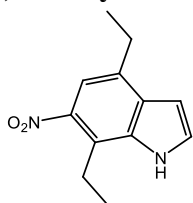
Yellow solid, mp 263–264 °C (ethanol). ¹H NMR (CDCl₃, 600 MHz): δ (ppm) 6.34 (s, 1H), 7.24 (t, *J* = 2.8 Hz, 1H), 7.35–8.05 (m, 14H), 8.09 (s, 1H), 8.16 (br s, 1H) (two atropisomers are present). ¹³C NMR (CDCl₃, 151 MHz): δ (ppm) 103.74, 118.02, 119.50, 124.93, 125.01, 125.43, 125.69, 126.05, 126.21, 126.44, 126.55, 126.88, 127.64, 128.40, 128.53, 128.62, 128.97, 129.39, 131.38, 131.51, 131.61, 131.93, 133.04, 133.84, 133.86, 135.06, 136.70, 143.35. HRMS (ESI) *m/z* calcd. for C₂₈H₁₉N₂O₂ [M + H]⁺: 415.1447, found 415.1446.

6-nitro-4,7-di(2-thienyl)-1H-indole 57e

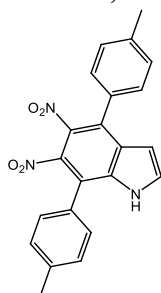
Yellow solid, mp 190–191 °C (ethanol). ¹H NMR (CDCl₃, 600 MHz): δ (ppm) 7.07 (dd, *J* = 3.2, 2.2 Hz, 1H), 7.18–7.22 (m, 3H), 7.46 (dd, *J* = 5.1, 1.0 Hz, 1H), 7.48 (t, *J* = 2.8 Hz, 1H), 7.50–7.56 (m, 2H), 8.02 (s, 1H), 8.64 (br s, 1H). ¹³C NMR (CDCl₃, 151 MHz): δ (ppm) 103.92, 113.19, 115.59, 126.31, 126.40, 127.61, 127.75, 127.95, 128.07, 128.17, 128.28, 129.65, 133.34, 135.92, 141.13, 144.01. HRMS (ESI) *m/z* calcd. for C₁₆H₁₁N₂O₂S₂ [M + H]⁺: 327.0262, found 327.0264.

4,7-dimethyl-6-nitro-1H-indole 57f

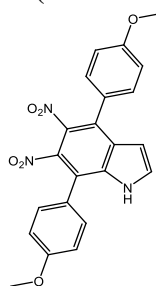
Yellow solid, mp 160–161 °C (ethanol). ¹H NMR (CDCl₃, 300 MHz): δ (ppm) 2.56 (s, 3H), 2.74 (s, 3H), 6.64 (dd, *J* = 3.2, 2.1 Hz, 1H), 7.46 (t, *J* = 3.2 Hz, 1H), 7.66 (s, 1H), 8.58 (br s, 1H). ¹³C NMR (CDCl₃, 75 MHz): δ (ppm) 14.41, 18.51, 102.74, 116.15, 116.93, 128.37, 128.42, 131.15, 134.81 (two carbons are accidentally isochronous). HRMS (ESI) *m/z* calcd. for C₁₀H₁₁N₂O₂ [M + H]⁺: 191.0821, found 191.0822.

4,7-diethyl-6-nitro-1H-indole 57g

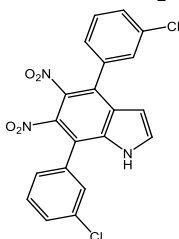
Yellow solid, mp 120–122 °C (ethanol). ¹H NMR (CDCl₃, 300 MHz): δ (ppm) 1.39 (t, *J* = 7.6 and 7.5 Hz, 6H, two part. overlapped), 2.94 (q, *J* = 7.6 Hz, 2H), 3.15 (q, *J* = 7.5 Hz, 2H), 6.67 (dd, *J* = 3.2, 2.0 Hz, 1H), 7.45 (dd, *J* = 3.2, 2.6 Hz, 1H), 7.65 (s, 1H), 8.53 (br s, 1H). ¹³C NMR (CDCl₃, 75 MHz): δ (ppm) 14.07, 14.26, 21.57, 25.81, 102.31, 102.41, 115.25, 121.80, 128.02, 130.42, 134.15, 134.62. HRMS (ESI) *m/z* calcd. for C₁₂H₁₅N₂O₂ [M + H]⁺: 219.1134, found 219.1135.

5,6-dinitro-4,7-di-*p*-tolyl-1H-indole 58a

Yellow solid, mp 292–293 °C (ethanol). ¹H NMR (CDCl₃, 600 MHz): δ (ppm) 2.44 (s, 3H), 2.45 (s, 3H), 6.57 (t, *J* = 2.3 Hz, 1H), 7.31 (d, *J* = 8.1 Hz, 2H), 7.32–7.43 (m, 6H), 7.43 (t, *J* = 2.3 Hz, 1H), 8.57 (br s, 1H). ¹³C NMR (CDCl₃, 151 MHz): δ (ppm) 21.52 (two isochronous carbons), 105.72, 120.26, 128.43, 128.48, 128.70, 128.74, 129.03, 129.74, 129.93, 130.46, 130.99, 133.63, 137.79, 138.76, 139.12, 139.97. HRMS (ESI) *m/z* calcd. for C₂₂H₁₈N₃O₄ [M + H]⁺: 388.1297, found 388.1298.

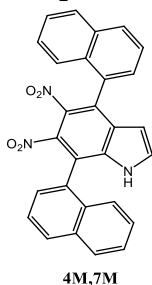
4,7-bis(4-methoxyphenyl)-5,6-dinitro-1H-indole 58b

Yellow solid, mp 253–254 °C (ethanol). ¹H NMR (Acetone-*d*₆, 300 MHz): δ (ppm) 3.90 (s, 6H), 6.57 (t, *J* = 3.2 Hz, 1H), 7.09–7.15 (m, 4H), 7.43–7.50 (m, 4H), 7.75 (t, *J* = 3.2 Hz, 1H), 11.06 (br s, 1H). ¹³C NMR (Acetone-*d*₆, 75 MHz): δ (ppm) 55.71, 55.76, 105.22, 115.20, 115.52, 121.10, 124.25, 127.00, 128.73, 129.41, 130.80, 131.25, 132.95, 134.63, 137.82, 139.22, 161.19, 161.48. HRMS (ESI) *m/z* calcd. for C₂₂H₁₈N₃O₆ [M + H]⁺: 420.1196, found 420.1198.

4,7-bis(3-chlorophenyl)-5,6-dinitro-1H-indole 58c

Yellow solid, mp 207–208 °C (ethanol). ¹H NMR (CDCl₃, 300 MHz): δ (ppm) 6.55 (dd, *J* = 3.3, 2.1 Hz, 1H), 7.32–7.39 (m, 2H), 7.42–7.56 (m, 7H), 8.65 (br s, 1H). ¹³C NMR (CDCl₃, 75 MHz): δ (ppm) 105.60, 119.30, 126.96, 127.13, 127.89, 128.54, 128.92, 128.93, 129.54, 130.27, 130.39, 130.97, 131.13, 132.87, 133.26, 134.97, 135.35, 135.74, 137.52, 138.39. HRMS (ESI) *m/z* calcd. for C₂₀H₁₂Cl₂N₃O₄ [M + H]⁺: 428.0205, found 428.0207.

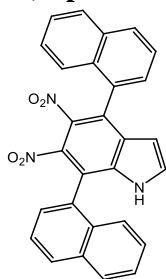
4,7-di(naphthalen-1-yl)-5,6-dinitro-1H-indole 58d(a)



4M,7M

¹H-NMR (600 MHz, CD₃CN, 1.96 ppm): δ 6.11 (d, *J* = 3.2 Hz, 1H), 7.42 (d, *J* = 3.2 Hz, 1H), 7.497.75 (m, 10H), 8.09 (d, *J* = 8.0 Hz, 1H), 8.12 (d, *J* = 8.0 Hz, 2H), 8.18 (d, *J* = 8.0 Hz, 1H), 9.84 (br s, 1H). ¹³C NMR (150.8 MHz, CD₃CN, 118.26 ppm): δ 105.6, 121.1, 125.9, 126.4, 126.5, 126.8, 127.4, 127.5, 127.6, 127.7, 128.1, 128.3, 129.0, 129.5, 129.6, 130.2, 130.3, 130.4, 130.9, 132.7, 132.8, 132.9, 133.1, 134.6, 134.9, 135.1, 138.9, 139.9. HRMS (ESI-QTOF) *m/z* calcd. for C₂₈H₁₈N₃O₄⁺ [M + H]⁺: 460.1292, found 460.1289.

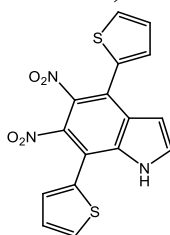
4,7-di(naphthalen-1-yl)-5,6-dinitro-1H-indole 58d(b)



4P,7M

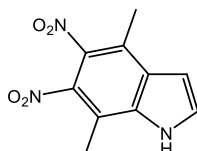
¹H-NMR (600 MHz, CD₃CN, 1.96 ppm): δ 6.18 (d, *J* = 3.2 Hz, 1H), 7.45 (d, *J* = 3.2 Hz, 1H), 7.497.58 (m, 2H), 7.60-7.76 (m, 8H), 8.08 (d, *J* = 8.3 Hz, 1H), 8.11₅ (d, *J* = 8.1 Hz, 1H), 8.12 (d, *J* = 8.3 Hz, 1H), 8.18 (d, *J* = 8.1 Hz, 1H), 9.90 (br s, 1H). ¹³C NMR (150.8 MHz, CD₃CN, 118.26 ppm): δ 105.6, 121.0, 125.8, 126.2, 126.5, 126.7, 127.5, 127.7, 127.8, 128.1₆, 128.2, 128.8₇, 128.9, 129.5, 129.6, 129.8, 130.3, 130.5, 130.9, 132.3, 132.5, 132.6, 133.2, 134.6, 134.9, 135.2, 138.8, 139.8. HRMS (ESI-QTOF) *m/z* calcd. for C₂₈H₁₈N₃O₄⁺ [M + H]⁺: 460.1292, found 460.1291.

5,6-dinitro-4,7-di(2-thienyl)-1H-indole (58e)



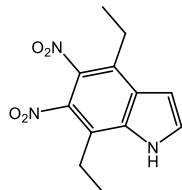
Yellow solid, mp 251–252 °C (ethanol). ¹H NMR (Acetone-d₆, 300 MHz): δ (ppm) 6.81 (m, 1H), 7.26-7.30 (m, 2H), 7.35 (dd, *J* = 3.6, 1.2 Hz, 1H), 7.43 (dd, *J* = 3.6, 1.2 Hz, 1H), 7.79-7.86 (m, 2H), 11.33 (br s, 1H). ¹³C NMR (Acetone-d₆, 75 MHz): δ (ppm) 104.56, 109.99, 113.90, 121.37, 127.77, 128.00, 128.54, 128.87, 129.00, 129.15, 129.68, 130.16, 132.74, 132.86, 132.91, 133.99. HRMS (ESI) *m/z* calcd. for C₁₆H₁₀N₃O₄S₂ [M + H]⁺: 372.0113, found 372.0116.

4,7-dimethyl-5,6-dinitro-1H-indole (58f)



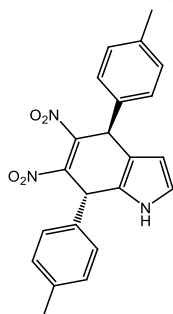
Yellow solid, mp 228–229 °C (ethanol). ¹H NMR (CDCl₃, 300 MHz): δ (ppm) 2.58 (s, 3H), 2.62 (s, 3H), 6.79 (dd, *J* = 3.3, 2.0 Hz, 1H), 7.53 (dd, *J* = 3.3, 2.6 Hz, 1H), 8.75 (br s, 1H). ¹³C NMR (Acetone-d₆, 75 MHz): δ (ppm) 12.17, 14.08, 103.90, 115.89, 123.78, 128.08, 130.77, 133.61, 137.69, 139.04. HRMS (ESI) *m/z* calcd. for C₁₀H₁₀N₃O₄ [M + H]⁺: 236.0666, found 236.0663.

4,7-diethyl-5,6-dinitro-1H-indole (58g)



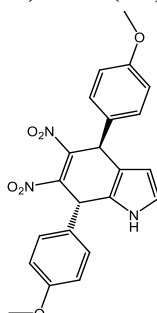
Yellow solid, mp 182–183 °C (ethanol). ¹H NMR (CDCl₃, 300 MHz): δ (ppm) 1.39 (t, *J* = 7.7 Hz, 6H, two part. overlapped), 2.96 (q, *J* = 7.6 Hz, 4H, two part. overlapped), 6.80 (dd, *J* = 3.3, 2.1 Hz, 1H), 7.53 (dd, *J* = 3.2, 2.7 Hz, 1H), 8.76 (br s, 1H). ¹³C NMR (CDCl₃, 75 MHz): δ (ppm) 14.18, 14.83, 21.21, 23.15, 104.41, 120.88, 127.65, 129.06, 130.33, 132.95, 137.81, 139.06. HRMS (ESI) *m/z* calcd. for C₁₂H₁₄N₃O₄ [M + H]⁺: 264.0984, found 264.0988.

(4*S*,7*S*)- and (4*R*,7*R*)-5,6-dinitro-4,7-di-*p*-tolyl-4,7-dihydro-1*H*-indole (59a)



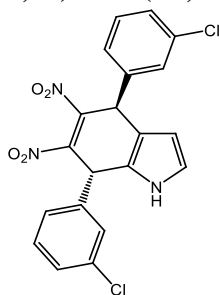
Yellow solid, mp 248–249 °C (petroleum ether/dichloromethane). ¹H NMR (Acetone-*d*₆, 300 MHz): δ (ppm) 2.29 (s, 3H), 2.30 (s, 3H), 5.68 (A of AB system, *J* = 7.2 Hz, 1H), 5.74 (t, *J* = 2.7 Hz, 1H), 5.82 (B of AB system, *J* = 7.2 Hz, 1H), 6.76 (td, *J* = 2.8, 0.6 Hz, 1H), 7.12 – 7.23 (m, 8H), 9.93 (br s, 1H). ¹³C NMR (Acetone-*d*₆, 75 MHz): δ (ppm) 21.06 (two isochronous carbons), 43.49, 44.44, 106.42, 116.24, 121.41, 123.33, 129.23, 129.38, 130.37, 130.54, 134.70, 136.59, 138.70, 139.25, 147.92, 149.69. HRMS (ESI) *m/z* calcd. for C₂₂H₂₀N₃O₄ [M + H]⁺: 390.1454, found 390.1458.

(4*S*,7*S*)- and (4*R*,7*R*)-4,7-bis(4-methoxyphenyl)-5,6-dinitro-4,7-dihydro-1*H*-indole (59b)



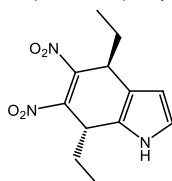
Yellow solid, mp 189–190 °C (petroleum ether/dichloromethane). ¹H NMR (CDCl₃, 300 MHz): δ (ppm) 3.78 (s, 6H, two part. overlapped), 5.51 (A of AB system, *J* = 7.2 Hz, 1H), 5.57 (B of AB system, *J* = 7.2 Hz, 1H), 5.84 (t, *J* = 2.7 Hz, 1H), 6.70 (t, *J* = 2.7 Hz, 1H), 6.82–6.89 (m, 4H), 7.09–7.15 (m, 4H), 7.71 (br s, 1H). ¹³C NMR (CDCl₃, 75 MHz): δ (ppm) 42.18, 43.19, 55.24, 55.32, 106.42, 114.48, 114.84, 116.02, 120.48, 122.47, 127.37, 129.41, 129.50, 129.61, 145.62, 148.30, 159.54, 160.05. HRMS (ESI) *m/z* calcd. for C₂₂H₂₀N₃O₆ [M + H]⁺: 422.1352, found 422.1356.

(4*S*,7*S*)- and (4*R*,7*R*)-4,7-bis(3-chlorophenyl)-5,6-dinitro-4,7-dihydro-1*H*-indole (59c)



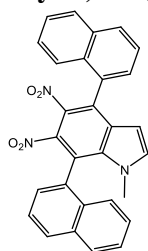
Yellow solid, mp 113–114 °C (petroleum ether/dichloromethane). ¹H NMR (CDCl₃, 300 MHz): δ (ppm) 5.56 (A of AB system, *J* = 7.2 Hz, 1H), 5.64 (B of AB system, *J* = 7.2 Hz, 1H), 5.85 (t, *J* = 2.7 Hz, 1H), 6.75 (t, *J* = 2.8 Hz, 1H), 7.09–7.13 (m, 2H), 7.17–7.18 (m, 2H), 7.26–7.33 (m, 4H), 7.75 (br s, 1H). ¹³C NMR (CDCl₃, 75 MHz): δ (ppm) 42.55, 43.59, 106.57, 115.43, 121.23, 121.51, 126.58, 126.61, 128.43, 128.50, 128.90, 129.56, 130.41, 130.82, 135.04, 135.50, 137.38, 139.30, 145.49, 148.17. HRMS (ESI) *m/z* calcd. for C₂₀H₁₄Cl₂N₃O₄ [M + H]⁺: 430.0361, found 430.0365.

(4*S*,7*S*)- and (4*R*,7*R*)-4,7-diethyl-5,6-dinitro-4,7-dihydro-1*H*-indole (59g)



Yellow solid, mp 117–119 °C (petroleum ether/dichloromethane). ¹H NMR (CDCl₃, 300 MHz): δ (ppm) 0.72 (t, *J* = 7.4 Hz, 6H, two part. overlapped), 1.68 – 1.88 (m, 4H), 4.41 (A of app ABX₂, ⁵*J* = 7.2, ³*J* = 4.0 Hz, 1H), 4.52 (B of app ABX₂, ⁵*J* = 7.2, ³*J* = 4.1 Hz, 1H), 6.05 (t, *J* = 2.6 Hz, 1H), 6.83 (t, *J* = 2.7 Hz, 1H), 7.98 (br s, 1H). ¹³C NMR (CDCl₃, 75 MHz): δ (ppm) 8.21, 8.24, 24.64, 25.11, 36.75, 37.69, 105.60, 115.04, 119.63, 122.00, 146.81, 150.19. HRMS (ESI) *m/z* calcd. for C₁₂H₁₆N₃O₄ [M + H]⁺: 266.1141, found 266.1138.

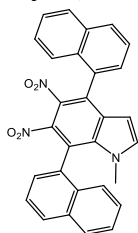
1-Methyl-4,7-di(naphthalen-1-yl)-5,6-dinitro-1*H*-indole 60a/60b



4*M*,7*M* / 4*P*,7*P*

¹H NMR (600 MHz, CDCl₃, 7.26 ppm): δ 2.87 (s, 3H), 6.10 (d, *J* = 3.2 Hz, 1H), 7.07 (d, *J* = 3.2 Hz, 1H), 7.44 (ddd, *J* = 8.4, 6.9, 1.0 Hz, 1H), 7.50–7.65 (m, 9H), 7.97 (d, *J* = 8.5 Hz, 2H), 8.00 (d, *J* = 8.5 Hz, 1H), 8.04 (d, *J* = 8.5 Hz, 1H). ¹³C NMR (150.8 MHz, CDCl₃, 77.36 ppm): δ 36.1, 104.6, 119.7, 125.3, 125.7, 126.0, 126.1, 126.7, 127.03, 127.06, 127.8, 128.8, 128.9, 129.0, 129.3, 129.8, 130.6, 130.7, 131.9, 132.1, 133.0, 133.4, 133.9, 134.0, 136.9, 137.7, 140.7. HRMS (ESI-QTOF) calcd. for C₂₉H₂₀N₃O₄ [M + H]⁺: 474.1448, found 470.1452.

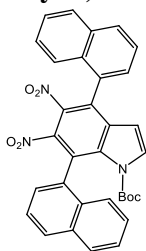
1-Methyl-4,7-di(naphthalen-1-yl)-5,6-dinitro-1H-indole 60c/60d



4M,7P / 4P,7M

¹H NMR (600 MHz, CD₃CN, 1.96 ppm): δ 2.9 (s, 3H), 6.14 (d, *J* = 3.2 Hz, 1H), 7.35 (d, *J* = 3.2 Hz, 1H), 7.52 (ddd, *J* = 8.5, 6.6, 1.1 Hz, 1H), 7.57-7.73 (m, 9H), 8.08 (d, *J* = 8.3 Hz, 1H), 8.10 (d, *J* = 8.3 Hz, 1H), 8.12 (d, *J* = 8.3 Hz, 1H), 8.17 (d, *J* = 8.3 Hz, 1H). ¹³C NMR (150.8 MHz, CD₃CN, 118.26 ppm): δ 36.3, 104.5, 120.5, 126.0, 126.5, 126.6, 127.5, 127.7, 127.8, 128.3, 128.4, 129.2, 129.4, 129.5, 129.8, 130.0, 130.2, 131.0, 131.6, 132.3, 132.4, 134.0, 134.0, 134.1, 134.6, 137.8, 139.1, 140.9. HRMS (ESI-QTOF) calcd. for C₂₉H₂₀N₃O₄ [M + H]⁺: 474.1448, found 470.1450.

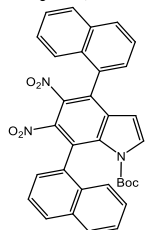
tert-Butyl 4,7-di(naphthalen-1-yl)-5,6-dinitro-1H-indole-1-carboxylate 61a/61c



4M,7M / 4P,7P

¹H NMR (600 MHz, CD₃CN, 1.96 ppm): δ 1.00 (s, 9H), 6.16 (d, *J* = 3.8 Hz, 1H), 7.47-7.51 (m, 2H), 7.53 (ddd, *J* = 8.5, 6.7, 1.2 Hz, 1H), 7.58 (ddd, *J* = 8, 4.9_s, 2.9 Hz, 1H), 7.61-7.66 (m, 5H), 7.69 (dd, *J* = 8.1, 7.1 Hz, 1H), 7.75 (d, *J* = 3.6 Hz, 1H), 8.04 (d, *J* = 8.2 Hz, 1H), 8.05 (dd, *J* = 7.4, 1.8 Hz, 1H), 8.09 (d, *J* = 8.3 Hz, 1H), 8.14 (d, *J* = 8.3 Hz, 1H). ¹³C NMR (150.8 MHz, CD₃CN, 118.26 ppm): δ 27.1, 86.2, 107.4, 122.7, 125.3, 126.2, 126.5, 126.6, 127.3, 127.4, 127.6, 127.8, 127.9, 128.0, 128.8, 129.5, 129.6, 130.2, 130.7, 131.7, 132.2, 132.6, 132.7, 133.6, 134.2, 134.3, 134.5, 135.1, 140.2, 142.5, 147.6. HRMS (ESI-QTOF) calcd. for C₃₃H₂₆N₃O₆ [M + H]⁺: 560.1816, found 560.1821.

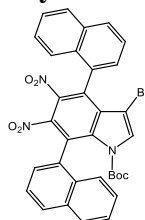
tert-Butyl 4,7-di(naphthalen-1-yl)-5,6-dinitro-1H-indole-1-carboxylate 61b/61d



4M,7P / 4P,7M

¹H NMR (600 MHz, CD₃CN, 1.96 ppm): δ 1.05 (s, 9H), 6.23 (d, *J* = 3.7 Hz, 1H), 7.49-7.68 (m, 9H), 7.70 (t, *J* = 7.7 Hz, 1H), 7.78 (d, *J* = 3.7 Hz, 1H), 8.04 (d, *J* = 8.3 Hz, 1H), 8.05 (d, *J* = 8.3 Hz, 1H), 8.09 (d, *J* = 8.3 Hz, 1H), 8.15 (d, *J* = 8.3 Hz, 1H). ¹³C NMR (150.8 MHz, CD₃CN, 118.26 ppm): δ 27.2, 86.3, 107.4, 122.8, 125.7, 126.1, 126.4, 126.4, 127.4, 127.6, 127.7, 127.8, 128.0, 128.6, 128.7, 129.5, 129.6, 130.2, 130.7, 131.5, 132.0, 132.3, 132.5, 133.8, 134.4, 134.5, 134.6, 135.3, 140.2, 142.2, 147.6. HRMS (ESI-QTOF) calcd. for C₃₃H₂₆N₃O₆ [M + H]⁺: 560.1816, found 560.1817.

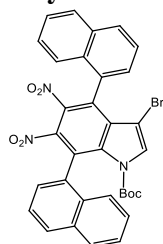
tert-Butyl 3-bromo-4,7-di(naphthalen-1-yl)-5,6-dinitro-1H-indole-1-carboxylate 62a/62c



4M,7M / 4P,7P

¹H NMR (600 MHz, CD₃CN, 1.96 ppm): δ 0.98 (s, 9H), 7.47-7.67 (m, 10H), 7.92 (s, 1H), 8.04 (d, *J* = 8.3 Hz, 1H), 8.05-8.08 (m, 2H), 8.14 (d, *J* = 8.0 Hz, 1H). ¹³C NMR (150.8 MHz, CD₃CN, 118.26 ppm): δ 27.0, 86.9, 95.7, 123.2, 125.2, 125.9, 126.5, 126.7, 127.4, 127.8, 127.9, 128.6, 128.9, 129.2, 129.4, 129.5, 129.7, 130.4, 130.9, 131.7, 132.3, 133.6, 133.9, 134.4, 134.8, 135.5, 141.1, 142.4, 146.6. HRMS (ESI-QTOF) calcd. for C₃₃H₂₅N₃O₆Br [M + H]⁺: 638.0921, found 638.0926.

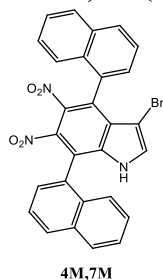
tert-Butyl 3-bromo-4,7-di(naphthalen-1-yl)-5,6-dinitro-1H-indole-1-carboxylate 62b/62d



4P,7M / 4M,7P

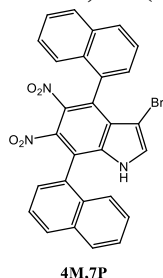
¹H NMR (600 MHz, CD₃CN, 1.96 ppm): δ 1.06 (s, 9H), 7.51-7.67 (m, 9H), 7.74 (d, *J* = 8.4 Hz, 1H), 7.95 (s, 1H), 8.02-8.08 (m, 3H), 8.14 (d, *J* = 8.2 Hz, 1H). ¹³C NMR (150.8 MHz, CD₃CN, 118.26 ppm): δ 27.1, 87.1, 95.7, 123.3, 125.6, 125.9, 126.5, 126.6, 127.4, 127.5, 127.8, 127.8, 127.9, 128.5, 129.2, 129.3, 129.5, 129.5, 129.7, 130.4, 130.9, 131.6, 132.1, 133.9, 134.0, 134.4, 134.6, 135.8, 141.2, 142.0, 146.7. HRMS (ESI-QTOF) calcd. for C₃₃H₂₅N₃O₆Br [M + H]⁺: 638.0921, found 638.0924.

3-Bromo-4,7-di(naphthalen-1-yl)-5,6-dinitro-1H-indoles 63a



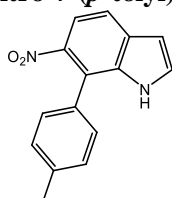
^1H NMR (600 MHz, CD_3CN , 1.96 ppm): δ 7.50-7.60 (m, 10H), 7.72 (dd, $J = 8.1$, 7.0 Hz, 1H), 8.06 (d, $J = 8.2$ Hz, 1H), 8.12 (d, $J = 8.2$ Hz, 2H), 8.19 (d, $J = 8.2$ Hz, 1H), 10.0 (br s, 1H). ^{13}C NMR (150.8 MHz, CD_3CN , 118.26 ppm): δ 92.9, 121.9, 125.7, 125.9, 126.0, 126.7, 126.8, 127.3, 127.6, 127.7, 128.2, 128.3, 128.5, 128.8, 129.2, 129.4, 129.6, 130.5₂, 130.5₄, 131.1, 132.8, 133.8, 134.0, 134.8, 134.9, 135.0, 139.8, 139.9. HRMS (ESI-QTOF) calcd. for $\text{C}_{28}\text{H}_{17}\text{N}_3\text{O}_4\text{Br}$ [$\text{M} + \text{H}$] $^+$: 538.0397, found 538.0401.

3-Bromo-4,7-di(naphthalen-1-yl)-5,6-dinitro-1H-indoles 63d



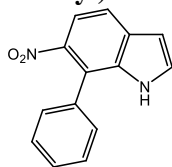
^1H NMR (600 MHz, CD_3CN , 1.96 ppm): δ 7.51-7.59 (m, 3H), 7.59-7.68 (m, 6H), 7.70 (dd, $J = 7.2$, 1.0 Hz, 1H), 7.74 (dd, $J = 8.0$, 7.0 Hz, 1H), 8.06 (d, $J = 8.0$ Hz, 1H), 8.12 (t, $J = 8.0$ Hz, 2H), 8.19 (d, $J = 8.0$ Hz, 1H), 10.19 (br s, 1H). ^{13}C NMR (150.8 MHz, CD_3CN , 118.26 ppm): δ 92.9, 121.8, 125.7, 125.7, 125.9, 126.7, 126.8, 127.3, 127.7, 127.7, 128.3, 128.7, 129.0, 129.1, 129.3, 129.5, 129.6, 130.1, 130.5, 131.1, 132.4, 134.0, 134.1, 134.3, 134.9, 135.1, 139.7. HRMS(ESI-QTOF) calcd. for $\text{C}_{28}\text{H}_{17}\text{N}_3\text{O}_4\text{Br}$ [$\text{M} + \text{H}$] $^+$: 538.0397, found 538.0403.

6-Nitro-7-(*p*-tolyl)-1H-indole (64a)



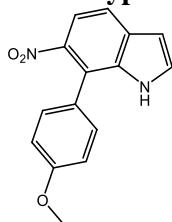
Waxy solid. ^1H NMR (CDCl_3 , 300 MHz): δ (ppm) 2.43 (s, 3H), 6.67 (dd, $J = 3.2$, 2.1 Hz, 1H), 7.29 (AA'BB', 4H), 7.37 (dd, $J = 3.2$, 2.6 Hz, 1H), 7.66 (d, $J = 8.7$ Hz, 1H), 7.85 (d, $J = 8.7$ Hz, 1H), 8.28 (br s, 1H). ^{13}C NMR (CDCl_3 , 75 MHz): δ (ppm) 21.30, 103.55, 116.61, 119.59, 122.02, 128.25, 129.31, 129.84, 130.99, 131.14, 134.57, 138.21, 142.57. HRMS (ESI) m/z calcd. for $\text{C}_{15}\text{H}_{13}\text{N}_2\text{O}_2$ [$\text{M} + \text{H}$] $^+$: 253.0972, found 253.0993.

7-(4-Phenyl)-6-nitro-1H-indole (64b)



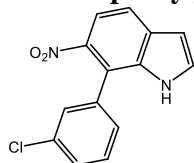
Orange oil. ^1H NMR (CDCl_3 , 300 MHz): δ (ppm) 6.68 (dd, $J = 3.2$, 2.1 Hz, 1H), 7.35-7.42 (m, 3H), 7.43-7.56 (m, 3H), 7.67 (d, $J = 8.7$ Hz, 1H), 7.87 (d, $J = 8.7$ Hz, 1H), 8.30 (br s, 1H). ^{13}C NMR (CDCl_3 , 75 MHz): δ (ppm) 103.62, 116.64, 119.80, 121.99, 128.38, 128.43, 129.13, 129.41, 131.13, 134.32, 134.51, 142.48. HRMS (ESI) m/z calcd. for $\text{C}_{14}\text{H}_{11}\text{N}_2\text{O}_2$ [$\text{M} + \text{H}$] $^+$: 239.0815, found 239.0873.

7-(4-Methoxyphenyl)-6-nitro-1H-indole (64c)



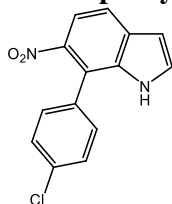
Yellow solid, mp 175-177 °C (taken-up with petroleum ether/DCM). ^1H NMR (CDCl_3 , 300 MHz): δ (ppm) 3.87 (s, 3H), 6.67 (dd, $J = 3.2$, 2.1 Hz, 1H), 7.03 (half AA'BB', 2H), 7.32 (half AA'BB', 2H), 7.37 (dd, $J = 3.2$, 2.6 Hz, 1H), 7.65 (d, $J = 8.7$ Hz, 1H), 7.82 (d, $J = 8.7$ Hz, 1H), 8.32 (br s, 1H). ^{13}C NMR (CDCl_3 , 75 MHz): δ (ppm) 55.33, 103.62, 114.64, 116.65, 119.57, 121.67, 126.10, 129.23, 129.70, 130.93, 134.77, 142.77, 159.62. HRMS(ESI) m/z calcd. for $\text{C}_{15}\text{H}_{13}\text{N}_2\text{O}_3$ [$\text{M} + \text{H}$] $^+$: 269.0921, found 269.0997.

7-(3-Chlorophenyl)-6-nitro-1H-indole (64d)



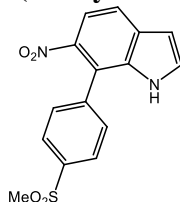
Yellowish solid, mp 122-125 °C (taken-up with petroleum ether/DCM). ^1H NMR (CDCl_3 , 300 MHz): δ (ppm) 6.70 (dd, $J = 3.2$, 2.0 Hz, 1H), 7.28 (td, 1H), 7.40-7.50 (m, 4H), 7.70 (d, $J = 8.7$ Hz, 1H), 7.91 (d, $J = 8.7$ Hz, 1H), 8.23 (br s, 1H). ^{13}C NMR (CDCl_3 , 75 MHz): δ (ppm) 103.85, 116.75, 120.32, 120.51, 126.82, 128.55, 128.63, 129.67, 130.45, 131.42, 134.34, 135.02, 136.23, 142.26. HRMS (ESI) m/z calcd. for $\text{C}_{14}\text{H}_{10}\text{ClN}_2\text{O}_2$ [$\text{M} + \text{H}$] $^+$: 273.0425, found 273.0615.

7-(4-Chlorophenyl)-6-nitro-1H-indole (64e)



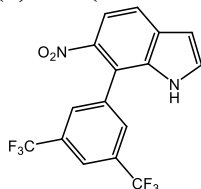
Yellow solid, mp 110-113 °C (taken-up with petroleum ether/DCM). ¹H NMR (CDCl₃, 300 MHz): δ (ppm) 6.69 (t, *J* = 2.5 Hz, 1H), 7.33 (d, *J* = 8.4 Hz, 2H), 7.40 (t, *J* = 2.9 Hz, 1H), 7.50 (d, *J* = 8.3 Hz, 2H), 7.70 (d, *J* = 8.7 Hz, 1H), 7.89 (d, *J* = 8.7 Hz, 1H), 8.23 (s, 1H). ¹³C NMR (CDCl₃, 75 MHz): δ (ppm) 103.79, 116.77, 120.19, 120.78, 129.44, 129.63, 129.92, 131.34, 132.81, 134.42, 134.55, 142.35. HRMS (ESI) *m/z* calcd. for C₁₄H₁₀ClN₂O₂ [M + H]⁺: 273.0425, found 273.0453.

7-(4-(Methylsulfonyl)phenyl)-6-nitro-1H-indole (64f)



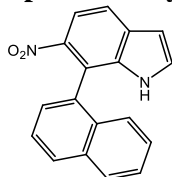
Yellow solid, mp 248-249 °C (taken-up with petroleum ether/DCM). ¹H NMR (CDCl₃, 300 MHz): δ (ppm) 3.17 (s, 3H), 6.72 (dd, *J* = 3.1, 2.0 Hz, 1H), 7.44 (dd, *J* = 3.2, 2.6 Hz, 1H), 7.62 (half AA'BB', *J* = 8.5 Hz, 2H), 7.75 (dd, *J* = 8.7, 0.8 Hz, 1H), 7.98 (d, *J* = 8.7 Hz, 1H), 8.10 (half AA'BB', *J* = 8.4 Hz, 2H), 8.24 (br s, 1H). ¹³C NMR (CDCl₃, 75 MHz): δ (ppm) 44.53, 104.01, 116.86, 120.13, 120.83, 128.23, 129.75, 130.17, 131.84, 134.14, 140.46, 140.88, 141.96. HRMS (ESI) *m/z* calcd. for C₁₅H₁₃N₂O₄S [M + H]⁺: 317.0591, found 317.0703.

7-(3,5-Bis(trifluoromethyl)phenyl)-6-nitro-1H-indole (64g)



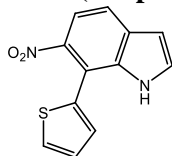
Yellow solid, mp 143-145 °C (taken-up with petroleum ether/DCM). ¹H NMR (CDCl₃, 300 MHz): δ (ppm) 6.75 (dd, *J* = 3.3, 2.1 Hz, 1H), 7.46 (dd, *J* = 3.3, 2.7 Hz, 1H), 7.78 (dd, *J* = 8.8, 0.8 Hz, 1H), 7.87 (s, 2H), 7.99-8.05 (m, 2H), 8.08 (br s, 1H). ¹³C NMR (CDCl₃, 75 MHz): δ (ppm) 104.28, 117.05, 118.89, 121.24, 122.45 (app quint, *J* = 3.72 Hz), 123.07 (q, *J* = 273.16 Hz), 129.06 (app d, *J* = 3.74 Hz), 130.34, 132.07, 132.58 (q, *J* = 33.30 Hz), 134.28, 137.13, 141.95. HRMS(ESI) *m/z* calcd. for C₁₆H₉F₆N₂O₂ [M + H]⁺: 375.0563, found 375.0635.

7-(Naphthalen-1-yl)-6-nitro-1H-indole (64h)



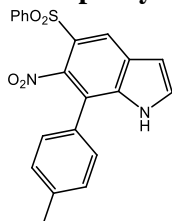
Orange oil. ¹H NMR (CDCl₃, 300 MHz): δ (ppm) 6.70 (dd, *J* = 3.2, 2.0 Hz, 1H), 7.30 (t, 1H), 7.34 (app.d, 2H), 7.43-7.54 (m, 3H), 7.58 (dd, *J* = 8.3, 7.0 Hz, 1H), 7.79 (dd, *J* = 8.7, 0.8 Hz, 1H), 7.93-7.99 (m, 2H), 8.05 (d, *J* = 8.7 Hz, 1H). ¹³C NMR (CDCl₃, 75 MHz): δ (ppm) 103.53, 116.77, 120.20, 120.42, 124.86, 125.65, 126.33, 126.37, 126.82, 128.58, 128.87, 129.55, 131.29, 131.42, 132.01, 133.80, 135.05, 143.25. HRMS (ESI) *m/z* calcd. for C₁₈H₁₃N₂O₂ [M + H]⁺: 289.0972, found 289.0792.

6-Nitro-7-(thiophen-2-yl)-1H-indole (64i)



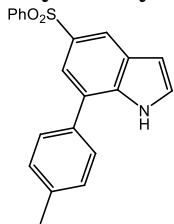
Yellow solid, mp 112-114 °C (taken-up with petroleum ether/DCM). ¹H NMR (CDCl₃, 300 MHz): δ (ppm) 6.68 (dd, *J* = 3.2, 2.1 Hz, 1H), 7.14-7.23 (m, 2H), 7.42 (t, *J* = 2.9 Hz, 1H), 7.53 (dd, *J* = 5.0, 1.4 Hz, 1H), 7.70 (d, *J* = 8.7 Hz, 1H), 7.82 (d, *J* = 8.7 Hz, 1H), 8.53 (br s, 1H). ¹³C NMR (CDCl₃, 75 MHz): δ (ppm) 103.77, 114.16, 116.60, 120.70, 127.42, 127.75, 127.92, 129.32, 130.92, 133.46, 135.13, 143.73. HRMS (ESI) *m/z* calcd. for C₁₂H₉N₂O₂S [M + H]⁺: 245.0379, found 245.0409.

6-Nitro-5-phenylsulfonyl-7-(p-tolyl)-1H-indole (65a)



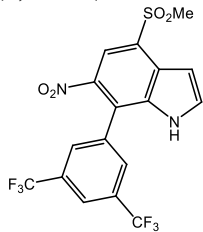
Yellow solid, mp 141-142 °C (ethanol). ¹H NMR (CDCl₃, 300 MHz): δ (ppm) 2.39 (s, 3H), 6.82 (dd, *J* = 3.3, 2.0 Hz, 1H), 7.26 (AA'BB', 4H), 7.42 (dd, *J* = 3.2, 2.5 Hz, 1H), 7.47-7.62 (m, 3H), 7.96-8.02 (m, 2H), 8.54 (br s, 1H), 8.55 (s, 1H). ¹³C NMR (CDCl₃, 75 MHz): δ (ppm) 21.34, 105.28, 116.15, 120.21, 123.79, 124.96, 127.29, 127.93, 128.68, 128.95, 129.29, 130.14, 133.17, 136.20, 139.75, 141.81, 149.47. HRMS (ESI) *m/z* calcd. for C₂₁H₁₇N₂O₄S [M + H]⁺: 393.0909, found 393.0993.

5-Phenylsulfonyl-7-(*p*-tolyl)-1*H*-indole (66a)



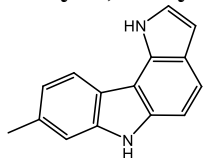
Yellow oil. ^1H NMR (CDCl_3 , 300 MHz): δ (ppm) 2.35 (s, 3H), 6.65 (dd, $J = 3.3, 2.1$ Hz, 1H), 7.15–7.30 (m, 4H), 7.35–7.49 (m, 4H), 7.65 (d, $J = 1.7$ Hz, 1H), 7.88–7.92 (m, 2H), 8.22 (d, $J = 1.6$ Hz, 1H), 8.60 (br s, 1H). ^{13}C NMR (CDCl_3 , 75 MHz): δ (ppm) 21.25, 104.66, 120.28, 120.81, 126.56, 126.66, 127.35, 127.95, 128.06, 129.08, 130.06, 132.54, 133.16, 134.37, 136.02, 138.28, 142.92. HRMS (ESI) m/z calcd. for $\text{C}_{21}\text{H}_{18}\text{NO}_2\text{S}$ [$\text{M} + \text{H}$] $^+$: 348.1053, found 348.1103.

7-(3,5-Bis(trifluoromethyl)phenyl)-2-methylsulfonyl-6-nitro-1*H*-indole (67g)



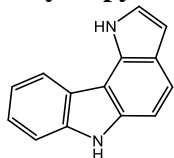
Brown solid, mp 222–224 °C (taken-up with petroleum ether/DCM). ^1H NMR (acetone- d_6 , 300 MHz): δ (ppm) 3.33 (s, 3H), 7.19 (dd, $J = 3.3, 1.8$ Hz, 1H), 7.97 (t, $J = 3.0$ Hz, 1H), 8.25 (q, $J = 0.8$ Hz, 1H), 8.29 (br s, 2H), 8.55 (s, 1H), 11.34 (br s, 1H). ^{13}C NMR (acetone- d_6 , 75 MHz): δ (ppm) 43.06, 102.68, 117.18, 122.52 (app. quint., $J = 3.77$ Hz), 123.50 (q, $J = 273.08$ Hz), 124.38, 128.23, 129.66 (app. d, $J = 3.64$ Hz), 131.36, 131.74 (q, $J = 33.33$ Hz), 134.69, 136.50, 136.89, 140.65. HRMS(ESI) m/z calcd. for $\text{C}_{17}\text{H}_{11}\text{F}_6\text{N}_2\text{O}_4\text{S}$ [$\text{M} + \text{H}$] $^+$: 453.0265, found 453.0289.

8-Methyl-1,6-dihydropyrrolo[3,2-*c*]carbazole (68a)



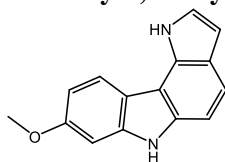
Grey solid, mp 238–240 °C (taken-up with petroleum ether/DCM). ^1H NMR (acetone- d_6 , 300 MHz): δ (ppm) 2.51 (3H, s), 6.62 (dd, $J = 3.1, 2.0$ Hz, 1H), 7.05 (ddt, $J = 8.0, 1.4, 0.7$ Hz, 1H), 7.23–7.30 (m, 2H), 7.35 (dt, $J = 1.5, 0.8$ Hz, 1H), 7.58 (dd, $J = 8.5, 0.8$ Hz, 1H), 8.30 (d, $J = 8.0$ Hz, 1H), 10.25 (br s, 1H), 10.68 (br s, 1H). ^{13}C NMR (acetone- d_6 , 75 MHz): δ (ppm) 22.12, 103.70, 105.52, 108.46, 111.65, 119.40, 120.60, 121.07, 121.36, 122.29, 122.45, 130.85, 134.29, 138.06, 140.34. HRMS (ESI) m/z calcd. for $\text{C}_{15}\text{H}_{13}\text{N}_2$ [$\text{M} + \text{H}$] $^+$: 221.1073, found 221.1125.

1,6-Dihydropyrrolo[3,2-*c*]carbazole (68b)



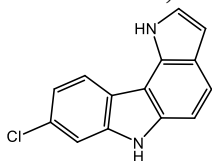
Grey glassy solid. ^1H NMR (acetone- d_6 , 300 MHz): δ (ppm) 6.63 (dd, $J = 3.2, 2.0$ Hz, 1H), 7.21 (ddd, $J = 8.1, 7.2, 1.1$ Hz, 1H), 7.28–7.32 (m, 2H), 7.35 (ddd, $J = 8.2, 7.2, 1.2$ Hz, 1H), 7.56 (dt, $J = 8.1, 1.0$ Hz, 1H), 7.64 (dd, $J = 8.5, 0.8$ Hz, 1H), 8.43 (ddd, $J = 7.8, 1.3, 0.7$ Hz, 1H), 10.38 (br s, 1H), 10.72 (br s, 1H). ^{13}C NMR (acetone- d_6 , 75 MHz): δ (ppm) 130.78, 105.51, 108.43, 111.54, 119.50, 120.03, 121.63, 122.47, 122.53, 122.75, 124.62, 130.94, 138.15, 139.82. HRMS (ESI) m/z calcd. for $\text{C}_{14}\text{H}_{11}\text{N}_2$ [$\text{M} + \text{H}$] $^+$: 207.0917, found 207.0975.

8-Methoxy-1,6-dihydropyrrolo[3,2-*c*]carbazole (68c)



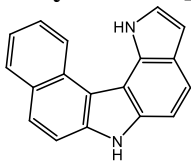
Whitish solid, mp 214–217 °C (taken-up with petroleum ether/DCM). ^1H NMR (acetone- d_6 , 300 MHz): δ (ppm) 3.88 (s, 3H), 6.61 (dd, $J = 3.2, 1.9$ Hz, 1H), 6.86 (dd, $J = 8.6, 2.3$ Hz, 1H), 7.09 (d, $J = 2.4$ Hz, 1H), 7.25 (d, $J = 8.7$ Hz, 1H), 7.28 (dd, $J = 3.0, 2.4$ Hz, 1H), 7.55 (dd, $J = 8.5, 0.7$ Hz, 1H), 8.30 (d, $J = 8.6$ Hz, 1H), 10.27 (br s, 1H), 10.68 (br s, 1H). ^{13}C NMR (acetone- d_6 , 75 MHz): δ (ppm) 55.78, 95.41, 103.63, 105.44, 107.52, 107.78, 116.80, 118.52, 122.21, 122.50, 122.62, 130.58, 137.97, 141.13, 158.86. HRMS (ESI) m/z calcd. for $\text{C}_{15}\text{H}_{13}\text{N}_2\text{O}$ [$\text{M} + \text{H}$] $^+$: 237.1022, found 237.1092.

8-Chloro-1,6-dihydropyrrolo[3,2-*c*]carbazole (68e)



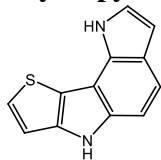
Yellow solid, mp 177–180 °C (taken-up with petroleum ether/DCM). ^1H NMR (CDCl_3 , 300 MHz): δ (ppm) 6.66 (dt, $J = 3.8, 2.0$ Hz, 1H), 7.22 (dt, $J = 8.4, 2.0$ Hz, 1H), 7.28–7.37 (m, 2H), 7.59 (t, $J = 1.7$ Hz, 1H), 7.68 (dd, $J = 8.5, 1.8$ Hz, 1H), 8.43 (dd, $J = 8.4, 1.5$ Hz, 1H), 10.55 (s, 1H), 10.81 (s, 1H). ^{13}C NMR (CDCl_3 , 75 MHz): δ (ppm) 103.85, 103.94, 105.56, 107.98, 111.37, 119.72, 120.64, 121.52, 122.64, 122.87, 129.82, 130.61, 138.61, 140.37. HRMS (ESI) m/z calcd. for $\text{C}_{14}\text{H}_{10}\text{ClN}_2$ [$\text{M} + \text{H}$] $^+$: 241.0527, found 241.0597.

1,6-Dihydrobenzo[c]pyrrolo[2,3-g]carbazole (68h)



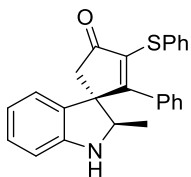
Grey solid, mp 227–230 °C (taken-up with petroleum ether/DCM). ¹H NMR (acetone-d₆, 300 MHz): δ (ppm) 6.74 (dd, *J* = 3.2, 1.8 Hz, 1H), 7.37 (dd, *J* = 3.2, 2.6 Hz, 1H), 7.43–7.50 (m, 2H), 7.65–7.72 (m, 2H), 7.84 (AB, *J* 17.6, 8.8 Hz, 2H), 8.05 (dm, *J* = 8.0 Hz, 1H), 9.06 (ddt, *J* = 8.4, 1.3, 0.7 Hz, 1H), 10.60 (br s, 1H), 10.99 (br s, 1H). ¹³C NMR (acetone-d₆, 75 MHz): δ (ppm) 104.61, 106.37, 109.87, 114.24, 116.12, 119.57, 122.56, 123.33, 123.67, 124.88, 126.52, 126.97, 130.11, 130.19, 130.30, 130.38, 137.09, 137.53. HRMS (ESI) *m/z* calcd. for C₁₈H₁₃N₂ [M + H]⁺: 257.1073, found 257.1097.

1,6-Dihydropyrrolo[2,3-e]thieno[3,2-b]indole (68i)



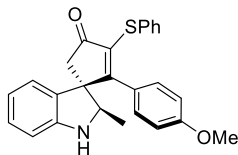
Whitish solid, mp 181–182 °C (taken-up with petroleum ether/DCM). ¹H NMR (CDCl₃, 300 MHz): δ (ppm) 6.59 (dd, *J* = 3.1, 2.0 Hz, 1H), 7.21 (d, *J* = 5.2 Hz, 1H), 7.24–7.30 (m, 2H), 7.42–7.48 (m, 2H), 10.51 (br s, 1H), 10.68 (br s, 1H). ¹³C NMR (CDCl₃, 300 MHz): δ (ppm) 103.77, 106.83, 108.46, 112.68, 115.34, 117.05, 122.00, 122.27, 126.26, 128.71, 139.53, 142.98. HRMS (ESI) *m/z* calcd. for C₁₂H₉N₂S [M + H]⁺: 213.0481, found 213.0499.

2'-Methyl-2-phenyl-3-(phenylthio)spiro[cyclopentane-1,3'-indolin]-2-en-4-one 76a



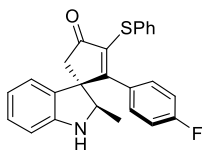
yellow solid, mp 155–157 °C. ¹H NMR (400 MHz, CDCl₃) δ 7.36–7.21 (m, 11H), 6.92 (t, *J* = 7.7 Hz, 1H), 6.62 (d, *J* = 7.8 Hz, 2H), 4.06 (q, *J* = 6.5 Hz, 1H), 3.78 (br s, 1H), 3.24 (d, *J* = 19.0 Hz, 1H), 2.67 (d, *J* = 19.0 Hz, 1H), 1.23 (d, *J* = 6.5 Hz, 3H). ¹³C NMR (100 MHz, CDCl₃) δ 202.6, 177.0, 151.6, 135.9, 135.3, 133.8, 131.2, 129.4, 129.2, 129.1, 128.8, 127.9, 127.6, 126.4, 123.4, 120.1, 110.6, 66.0, 58.5, 48.6, 14.2. HRMS (ESI⁺) *m/z* calcd. for C₂₅H₂₂NOS [MH]⁺: 384.1417, found: 384.1411 (1.6 ppm). $\tilde{\nu}_{\text{max}}$ (thin film)/cm⁻¹: 1711, 1605, 1480, 1439, 744, 698.

2-(4-Methoxyphenyl)-2'-methyl-3-(phenylthio)spiro[cyclopentane-1,3'-indolin]-2-en-4-one 76b



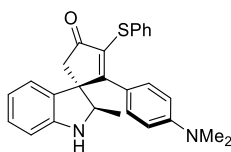
yellow solid, mp 59–61 °C. ¹H NMR (400 MHz, CDCl₃) δ 7.23–7.12 (m, 7H), 6.91 (t, *J* = 7.7 Hz, 1H), 6.70–6.65 (m, 5H), 4.09 (q, *J* = 6.7 Hz, 1H), 3.74 (s, 3H), 3.25 (d, *J* = 18.9 Hz, 1H), 2.67 (d, *J* = 19.0 Hz, 1H), 1.22 (d, *J* = 6.8 Hz, 3H). ¹³C NMR (100 MHz, CDCl₃) δ 202.7, 177.0, 160.3, 151.6, 134.6, 134.1, 131.5, 129.7, 129.3, 128.8, 127.5, 126.3, 123.5, 120.1, 113.0, 110.5, 66.1, 58.4, 55.0, 49.4, 14.4. HRMS (ESI⁺) calcd. for C₂₆H₂₄NO₂S [MH]⁺: 414.1522, found: 414.1526 (−1.0 ppm). $\tilde{\nu}_{\text{max}}$ (thin film)/cm⁻¹: 1707, 1604, 1504, 1250, 1179, 738.

2-(4-Fluorophenyl)-2'-methyl-3-(phenylthio)spiro[cyclopentane-1,3'-indolin]-2-en-4-one 76c

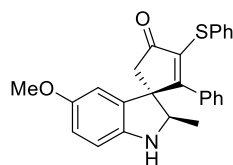


yellow solid, mp: 57–59 °C. ¹H NMR (400 MHz, CDCl₃) δ 7.23–7.12 (m, 7H), 6.91 (td, *J* = 7.4, 0.9 Hz, 1H), 6.85–6.80 (m, 2H), 6.66–6.63 (m, 3H), 4.08 (q, *J* = 6.7 Hz, 1H), 3.25 (d, *J* = 19.1 Hz, 1H), 2.68 (d, *J* = 19.1 Hz, 1H), 1.23 (d, *J* = 6.7 Hz, 3H). ¹³C NMR (100 MHz, CDCl₃) δ 202.5, 175.6, 162.9 (d, *J* = 249.7 Hz), 151.5, 136.2, 133.5, 130.1 (d, *J* = 3.2 Hz), 130.9, 130.0 (d, *J* = 8.5 Hz), 129.5, 129.3, 128.9, 126.6, 123.3, 120.1, 114.8 (d, *J* = 21.9 Hz, 1H), 110.5, 65.9, 58.4, 48.7, 14.3. ¹⁹F NMR (376 MHz, CDCl₃) δ −111.09 to −111.16 (m). HRMS (ESI⁺) calcd. for C₂₅H₂₀NNaOS [MNa]⁺: 424.1142, found: 424.1142 (0.0 ppm). $\tilde{\nu}_{\text{max}}$ (thin film)/cm⁻¹: 1710, 1602, 1502, 1481, 1160, 738.

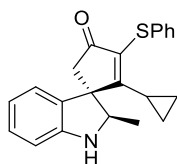
2-(4-(Dimethylamino)phenyl)-2'-methyl-3-(phenylthio)spiro[cyclopentane-1,3'-indolin]-2-en-4-one 76d



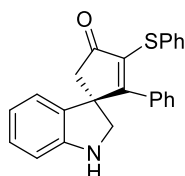
yellow solid, mp: 74–76 °C. ¹H NMR (400 MHz, CDCl₃) δ 7.26–7.12 (m, 5H), 7.13 (d, *J* = 7.9 Hz, 2H), 6.89 (t, *J* = 7.4 Hz, 1H), 6.74 (d, *J* = 9.0 Hz, 2H), 6.69 (d, *J* = 7.8 Hz, 1H), 6.45 (d, *J* = 9.0 Hz, 2H), 4.11 (q, *J* = 6.6 Hz, 1H), 3.24 (d, *J* = 18.8 Hz, 1H), 2.92 (s, 6H), 2.67 (d, *J* = 18.8 Hz, 1H), 1.20 (d, *J* = 6.6 Hz, 3H). ¹³C NMR (100 MHz, CDCl₃) δ 202.8, 178.2, 151.6, 150.9, 135.0, 132.4, 131.9, 130.0, 129.1, 128.8, 128.3, 128.0, 125.9, 123.7, 122.4, 120.1, 110.4, 66.3, 58.3, 50.5, 39.9, 14.6. HRMS (ESI⁺) calcd. for C₂₇H₂₇N₂OS [MH]⁺: 427.1839, found: 427.1840 (−0.3 ppm). $\tilde{\nu}_{\text{max}}$ (thin film)/cm⁻¹: 1702, 1604, 1509, 1482, 1199, 738.

5'-Methoxy-2'-methyl-2-phenyl-3-(phenylthio)spiro[cyclopentane-1,3'-indolin]-2-en-4-one 76e

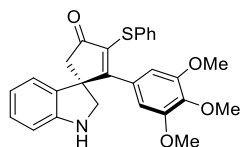
yellow solid, mp: 138–140 °C. ^1H NMR (400 MHz, CDCl_3) δ 7.35–7.33 (m, 2H), 7.28–7.23 (m, 6H), 6.88 (dd, $J = 8.5, 2.4$ Hz, 1H), 6.81 (d, $J = 2.4$ Hz, 1H), 6.74 (d, $J = 8.2$ Hz, 2H), 6.70 (d, $J = 8.2$ Hz, 2H), 4.13 (q, $J = 6.6$ Hz, 1H), 3.89 (s, 3H), 3.30 (d, $J = 19.1$ Hz, 1H), 2.76 (d, $J = 19.1$ Hz, 1H), 1.32 (d, $J = 6.8$ Hz, 3H). ^{13}C NMR (100 MHz, CDCl_3) δ 202.5, 177.1, 154.6, 145.4, 135.9, 135.2, 133.8, 133.0, 129.3, 129.2, 128.8, 128.0, 127.6, 126.5, 115.0, 112.0, 109.2, 66.4, 59.1, 56.0, 48.3, 14.2. HRMS (ESI $^+$) m/z calcd. for $\text{C}_{26}\text{H}_{23}\text{NNaO}_2\text{S}$ $[\text{MNa}]^+$: 436.1342, found: 436.1342 (0.0 ppm error). $\tilde{\nu}_{\text{max}}$ (thin film)/ cm^{-1} 1712, 1490, 1439, 1223, 738.

2-Cyclopropyl-2'-methyl-3-(phenylthio)spiro[cyclopentane-1,3'-indolin]-2-en-4-one 76f

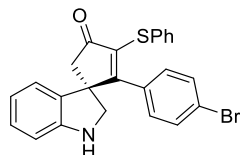
yellow solid, mp: 65–67 °C. ^1H NMR (400 MHz, CDCl_3) δ 7.36–7.32 (m, 2H), 7.26–7.21 (m, 4H), 7.09 (d, $J = 7.5$ Hz, 1H), 6.93 (*app* t, $J = 7.8$ Hz, 1H), 6.81 (d, $J = 7.8$ Hz, 1H), 4.19 (q, $J = 6.6$ Hz, 1H), 3.15 (d, $J = 19.1$ Hz, 1H), 2.58 (d, $J = 19.1$ Hz, 1H), 1.83–1.67 (m, 3H), 1.49 (d, $J = 6.5$ Hz, 3H), 1.18–1.13 (m, 1H), 0.98–0.94 (m, 1H). ^{13}C NMR (100 MHz, CDCl_3) δ 203.0, 189.6, 150.9, 135.7, 132.1, 129.0, 128.9, 127.1, 125.8, 125.8, 123.4, 120.0, 110.2, 65.9, 59.3, 48.7, 15.2, 14.4, 12.9, 12.3. HRMS (ESI $^+$) m/z calcd. for $\text{C}_{22}\text{H}_{21}\text{NNaOS}$ $[\text{MNa}]^+$: 370.1236, found: 370.1235 (0.2 ppm). $\tilde{\nu}_{\text{max}}$ (thin film)/ cm^{-1} 1702, 1568, 1480, 1238, 739.

2-Phenyl-3-(phenylthio)spiro[cyclopentane-1,3'-indolin]-2-en-4-one 76g

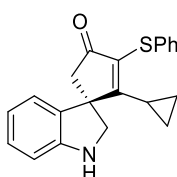
yellow solid, mp: 59–61 °C. ^1H NMR (400 MHz, CDCl_3) δ 7.13–7.02 (m, 10H), 6.99 (d, $J = 7.5$ Hz, 1H), 6.87 (s, 1H), 6.85 (s, 1H), 6.76 (t, $J = 7.5$ Hz, 1H), 6.56 (d, $J = 7.8$ Hz, 1H), 3.69 (d, $J = 9.8$ Hz, 1H), 3.61 (br, 1H), 3.51 (d, $J = 9.8$ Hz, 1H), 2.96 (d, $J = 18.8$ Hz, 1H), 2.85 (d, $J = 18.8$ Hz, 1H). ^{13}C NMR (100 MHz, CDCl_3) δ 203.2, 176.8, 151.1, 134.8, 134.0, 133.55, 131.8, 129.8, 129.5, 129.3, 129.0, 128.3, 128.1, 126.8, 122.8, 119.9, 110.5, 57.6, 56.4, 52.4. HRMS (ESI $^+$) m/z calcd. for $\text{C}_{24}\text{H}_{19}\text{NNaOS}$ $[\text{MNa}]^+$: 392.1080, found: 392.1077 (0.7 ppm). $\tilde{\nu}_{\text{max}}$ (thin film)/ cm^{-1} 1710, 1603, 1486, 742, 697.

3-(Phenylthio)-2-(3,4,5-trimethoxyphenyl)spiro[cyclopentane-1,3'-indolin]-2-en-4-one 76h

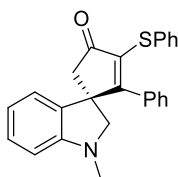
yellow solid, mp: 58–60 °C. ^1H NMR (400 MHz, CDCl_3) δ 7.57–7.39 (m, 7H), 7.14 (t, $J = 7.3$ Hz, 1H), 6.97 (d, $J = 7.8$ Hz, 1H), 6.53 (s, 2H), 4.11 (d, $J = 9.9$ Hz, 1H), 4.10 (s, 3H), 3.94 (d, $J = 9.9$ Hz, 1H), 3.82 (s, 6H), 3.39 (d, $J = 18.8$ Hz, 1H), 3.25 (d, $J = 18.8$ Hz, 1H). ^{13}C NMR (100 MHz, CDCl_3) δ 203.1, 175.7, 152.4, 151.2, 145.1, 138.7, 133.8, 133.5, 132.1, 129.4, 129.2, 128.8, 126.6, 122.9, 119.6, 110.2, 105.8, 60.8, 57.8, 56.3, 55.6, 52.6. HRMS (ESI $^+$) m/z calcd. for $\text{C}_{27}\text{H}_{26}\text{NO}_4\text{S}$ $[\text{MH}]^+$: 460.1577, found: 460.1578 (–0.2 ppm). $\tilde{\nu}_{\text{max}}$ (thin film)/ cm^{-1} : 1709, 1582, 1501, 1488, 1464, 1412, 1337, 1233, 737.

2-(4-bromophenyl)-3-(phenylthio)spiro[cyclopentane-1,3'-indolin]-2-en-4-one 76i

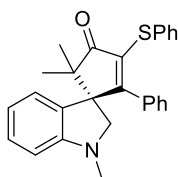
yellow solid, mp: 139–140 °C. ^1H NMR (400 MHz, CDCl_3) δ 7.32 (d, $J = 8.4$ Hz, 2H), 7.21–7.13 (m, 6H), 7.04 (d, $J = 7.5$ Hz, 1H), 6.83 (t, $J = 7.4$ Hz, 1H), 6.78 (d, $J = 8.4$ Hz, 2H), 6.64 (d, $J = 7.8$ Hz, 1H), 3.73 (d, $J = 9.9$ Hz, 1H), 3.62 (d, $J = 9.9$ Hz, 1H), 3.06 (d, $J = 18.9$ Hz, 1H), 2.91 (d, $J = 18.9$ Hz, 1H). ^{13}C NMR (100 MHz, CDCl_3) δ 202.8, 174.8, 151.0, 135.2, 132.9, 132.7, 131.2, 131.1, 130.0, 129.7, 129.3, 128.9, 126.9, 123.8, 122.6, 119.8, 110.4, 57.4, 56.1, 51.9. HRMS (ESI $^+$) m/z calcd. for $\text{C}_{24}\text{H}_{19}\text{BrNOS}$ $[\text{MH}]^+$: 448.0365, found: 448.0365 (0.1 ppm). $\tilde{\nu}_{\text{max}}$ (thin film)/ cm^{-1} : 1712, 1603, 1483, 1009, 742, 697.

2-Cyclopropyl-3-(phenylthio)spiro[cyclopentane-1,3'-indolin]-2-en-4-one 76j

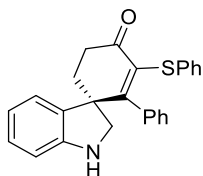
yellow soli, mp: 62–63 °C. ^1H NMR (400 MHz, CDCl_3) δ 7.60–7.4 (m, 6H), 7.27 (d, $J = 7.2$ Hz, 1H), 7.11 (t, $J = 7.3$ Hz, 1H), 7.03 (d, $J = 7.8$ Hz, 1H), 4.39 (d, $J = 9.9$ Hz, 1H), 4.26 (br s, 1H), 3.95 (d, $J = 9.8$ Hz, 1H), 3.15 (*app* s, 2H), 2.10–1.97 (m, 2H), 1.72–1.66 (m, 1H), 1.41–1.34 (m, 1H), 1.28–1.18 (m, 1H). ^{13}C NMR (100 MHz, CDCl_3) δ 203.1, 188.3, 151.1, 135.3, 131.8, 129.0, 128.9, 127.4, 127.2, 125.9, 123.0, 119.6, 110.2, 58.6, 56.9, 51.4, 13.8, 12.2, 10.7. HRMS (ESI $^+$) m/z calcd. for $\text{C}_{21}\text{H}_{20}\text{NOS}$ $[\text{MH}]^+$: 334.1260, found: 334.1262 (–0.6 ppm error). $\tilde{\nu}_{\text{max}}$ (thin film)/ cm^{-1} 1703, 1604, 1579, 1488, 1237, 740.

1'-Methyl-2-phenyl-3-(phenylthio)spiro[cyclopentane-1,3'-indolin]-2-en-4-one 76k

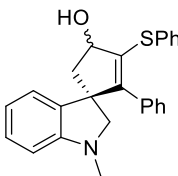
yellow solid, mp 140–142 °C. ^1H NMR (400 MHz, CDCl_3) δ 7.35–7.18 (m, 8H), 7.08 (d, $J = 7.5$ Hz, 1H), 7.04–7.02 (m, 2H), 6.84 (t, $J = 7.5$ Hz, 1H), 6.55 (d, $J = 7.9$ Hz, 1H), 3.56 (d, $J = 9.3$ Hz, 1H), 3.45 (d, $J = 9.3$ Hz, 1H), 3.05 (d, $J = 18.2$ Hz, 1H), 2.99 (d, $J = 18.2$ Hz, 1H), 2.71 (s, 3H). ^{13}C NMR (100 MHz, CDCl_3) δ 203.0, 176.2, 152.5, 135.0, 133.9, 133.5, 132.4, 129.6, 129.3, 129.2, 128.8, 128.4, 127.9, 126.6, 122.3, 118.6, 107.7, 65.6, 55.1, 52.1, 35.4. HRMS (ESI $^+$) m/z calcd. for $\text{C}_{25}\text{H}_{21}\text{NNaOS}$ [MNa] $^+$: 406.1236, found: 406.1231 (1.2 ppm error). $\tilde{\nu}_{\text{max}}$ (thin film)/ cm^{-1} : 1713, 1604, 1490, 740, 697.

1',5,5-Trimethyl-2-phenyl-3-(phenylthio)spiro[cyclopentane-1,3'-indolin]-2-en-4-one 76l

yellow oil. ^1H NMR (400 MHz, CDCl_3) δ 7.29–7.15 (m, 9H), 7.03 (s, 1H), 6.99 (s, 1H), 6.73–6.68 (m, 2H), 6.51 (d, $J = 8.0$ Hz, 1H), 3.52 (d, $J = 11.1$ Hz, 1H), 3.35 (d, $J = 11.1$ Hz, 1H), 2.07 (s, 3H), 1.33 (s, 3H), 0.91 (s, 3H). ^{13}C NMR (100 MHz, CDCl_3) δ 208.6, 174.1, 152.7, 134.2, 133.8, 131.8, 131.0, 129.8, 129.2, 129.1, 128.8, 128.1, 128.0, 126.7, 124.1, 118.1, 107.8, 63.8, 58.6, 53.2, 35.7, 26.9, 19.2. HRMS (ESI $^+$) m/z calcd. for $\text{C}_{27}\text{H}_{26}\text{NNaOS}$ [MNa] $^+$: 434.1544, found: 434.1549 (1.1 ppm). $\tilde{\nu}_{\text{max}}$ (thin film)/ cm^{-1} : 2970, 1713, 1491, 739, 697.

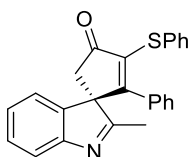
2-Phenyl-3-(phenylthio)spiro[cyclohexane-1,3'-indolin]-2-en-4-one 76m

yellow oil. ^1H NMR (400 MHz, CDCl_3) δ 7.24–7.10 (m, 11H), 6.82 (t, $J = 7.1$ Hz, 2H), 6.63 (d, $J = 7.8$ Hz, 2H), 3.61 (d, $J = 9.3$ Hz, 1H), 3.35 (d, $J = 9.3$ Hz, 1H), 2.88 (ddd, $J = 17.5, 12.5, 4.8$ Hz, 1H), 2.65 (dt, $J = 17.5, 4.8$ Hz, 1H), 2.50 (dt, $J = 12.5, 4.8$ Hz, 1H), 2.39 (td, $J = 12.5, 4.8$ Hz, 1H). ^{13}C NMR (100 MHz, CDCl_3) δ 194.3, 168.1, 150.9, 138.7, 136.5, 134.1, 129.8, 129.1, 128.7, 128.7, 127.9, 127.8, 127.0, 125.9, 124.4, 118.8, 110.7, 58.9, 53.4, 34.84, 34.80. HRMS (ESI $^+$) m/z calcd. for $\text{C}_{25}\text{H}_{21}\text{NNaOS}$ [MNa] $^+$: 406.1236, found: 406.1236 (0.1 ppm error). ν_{max} (thin film)/ cm^{-1} : 1682, 1485, 740, 698.

1'-Methyl-2-phenyl-3-(propylthio)spiro[cyclopentane-1,3'-indolin]-2-en-4-ol 76n

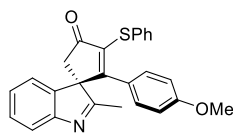
yellow oil. Diastereoisomer I: ^1H NMR (400 MHz, CDCl_3) δ 7.40–7.11 (m, 10H), 6.97 (d, $J = 7.5$ Hz, 2H), 6.76 (td, $J = 7.5, 2.0$ Hz, 1H), 6.42 (d, $J = 7.8$ Hz, 1H), 4.80 (d, $J = 7.0$ Hz, 1H), 3.40 (d, $J = 9.0$ Hz, 1H), 3.25 (d, $J = 9.0$ Hz, 1H), 2.62 (s, 3H), 2.52 (dd, $J = 14.2, 7.0$ Hz, 1H), 2.38 (dd, $J = 14.2, 2.8$ Hz, 1H), 2.17 (d, $J = 2.8$ Hz, 1H). ^{13}C NMR (100 MHz, CDCl_3) δ 152.3, 152.0, 135.0, 134.6, 133.6, 130.4, 129.1, 128.6, 128.3, 127.8, 127.7, 127.0, 124.3, 118.3, 107.3, 99.9, 74.8, 66.3, 59.9, 48.1, 35.7. HRMS (ESI) m/z calcd. for $\text{C}_{25}\text{H}_{24}\text{NOS}$ [MH] $^+$: 386.1574, found: 386.1573 (0.2 ppm). $\tilde{\nu}_{\text{max}}$ (thin film)/ cm^{-1} : 2925, 1603, 1490, 741, 697.

Distereoisomer II: ^1H NMR (400 MHz, CDCl_3) δ 7.43–7.40 (m, 2H), 7.33–7.13 (m, 7H), 7.08 (dd, $J = 7.3, 1.1$ Hz, 1H), 7.01–6.97 (m, 2H), 6.74 (td, $J = 7.3, 1.1$ Hz, 1H), 6.46 (d, $J = 8.0$ Hz, 1H), 4.93 (app t, $J = 5.6$ Hz, 1H), 3.43 (d, $J = 9.4$ Hz, 1H), 3.31 (d, $J = 9.4$ Hz, 1H), 2.80 (dd, $J = 13.5, 7.0$ Hz, 1H), 2.64 (s, 3H), 2.22 (dd, $J = 13.5, 5.8$ Hz, 1H), 2.14 (s broad, 1H). ^{13}C NMR (100 MHz, CDCl_3) δ 152.5, 150.6, 135.9, 134.84, 134.79, 133.0, 131.1, 129.2, 129.0, 128.5, 127.8, 127.7, 127.3, 122.5, 117.9, 107.5, 74.6, 66.8, 59.2, 49.3, 35.5. HRMS (APCI) m/z calcd. for $\text{C}_{25}\text{H}_{24}\text{NOS}$ [MH] $^+$: 386.1572, found: 386.1573 (0.4 ppm). $\tilde{\nu}_{\text{max}}$ (thin film)/ cm^{-1} : 2855, 1604, 1491, 742, 696.

2'-Methyl-2-phenyl-3-(phenylthio)spiro[cyclopentane-1,3'-indol]-2-en-4-one 78a

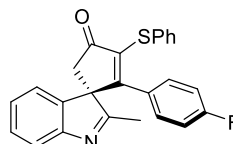
yellow solid, mp: 59–60 °C. ^1H NMR (400 MHz, CDCl_3) δ 7.47 (d, $J = 7.7$ Hz, 1H), 7.33–7.27 (m, 1H), 7.21–7.07 (m, 7H), 7.01 (app t, $J = 7.7$ Hz, 2H), 6.74 (d, $J = 7.8$ Hz, 2H), 2.85 (d, $J = 19.2$ Hz, 1H), 2.77 (d, $J = 19.2$ Hz, 1H), 2.13 (s, 3H). ^{13}C NMR (100 MHz, CDCl_3) δ 201.2, 181.4, 171.5, 155.1, 140.7, 137.2, 132.6, 132.4, 130.3, 130.1, 129.2, 129.0, 128.3, 127.1, 127.0, 126.5, 121.7, 120.7, 67.1, 43.3, 16.0. HRMS (ESI $^+$) m/z calcd. for $\text{C}_{25}\text{H}_{19}\text{NNaOS}$ [MNa] $^+$: 404.1080, found: 404.1079 (0.1 ppm error). $\tilde{\nu}_{\text{max}}$ (thin film)/ cm^{-1} : 1716, 1580, 1461, 1441, 740, 697.

2-(4-Methoxyphenyl)-2'-methyl-3-(phenylthio)spiro[cyclopentane-1,3'-indol]-2-en-4-one 78b



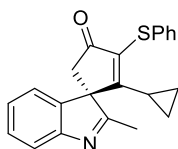
yellow solid, mp 64–65 °C. ^1H NMR (400 MHz, CDCl_3) δ 7.50 (d, J = 7.7 Hz, 1H), 7.31 (td, J = 6.8, 2.2 Hz, 1H), 7.22–7.07(m, 7H), 6.80 (*app* d, J = 8.9 Hz, 2H), 6.54 (*app* d, J = 8.9 Hz, 2H), 3.61 (s, 3H), 2.81 (d, J = 18.5 Hz, 1H), 2.72 (d, J = 18.5 Hz, 1H), 2.10 (s, 3H). ^{13}C NMR (100 MHz, CDCl_3) δ 201.1, 182.2, 171.3, 161.3, 155.0, 141.4, 134.9, 133.1, 129.5, 129.2, 129.1, 129.0, 126.9, 126.6, 124.8, 121.7, 120.8, 113.8, 67.0, 55.2, 43.6, 15.9. HRMS (ESI^+) m/z calcd. for $\text{C}_{26}\text{H}_{21}\text{NNaO}_2\text{S}$ [MNa] $^+$: 434.1185, found: 434.1180 (1.2 ppm error). $\tilde{\nu}_{\text{max}}$ (thin film)/ cm^{-1} : 1711, 1603, 1578, 1505, 1253, 1178, 1025, 907, 726, 688.

2-(4-Fluorophenyl)-2'-methyl-3-(phenylthio)spiro[cyclopentane-1,3'-indol]-2-en-4-one 78c



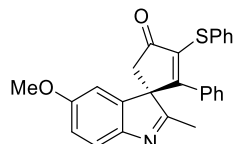
yellow solid, mp: 54–56 °C. ^1H NMR (400 MHz, CDCl_3) δ 7.43 (d, J = 7.6 Hz, 1H), 7.26 (dt, J = 6.6, 2.2 Hz, 1H), 7.15–7.03 (m, 7H), 6.71–6.63 (m, 4H), 2.80 (d, J = 18.5 Hz, 1H), 2.72 (d, J = 18.5 Hz, 1H), 2.08 (s, 3H). ^{13}C NMR (100 MHz, CDCl_3) δ 201.0, 181.3, 169.7, 163.5 (d, J^1 = 252.4 Hz), 155.0, 140.6, 137.3, 132.2, 130.2, 129.3, 129.3, 129.2 (d, J^3 = 9.0 Hz), 128.4 (d, J^4 = 3.5 Hz), 127.3, 126.6, 121.7, 120.8, 115.5 (d, J^2 = 22.0 Hz, 1H), 67.1, 43.2, 15.9. ^{19}F NMR (376 MHz, CDCl_3) δ (-108.63)–(-108.70) (m, 1F). HRMS (ESI^+) m/z calcd. for $\text{C}_{25}\text{H}_{19}\text{FNOS}$ [MH] $^+$: 400.1166, found: 400.1168 (-0.5 ppm error). $\tilde{\nu}_{\text{max}}$ (thin film)/ cm^{-1} : 1716, 1602, 1580, 1503, 1236, 1161, 757, 739.

2-Cyclopropyl-2'-methyl-3-(phenylthio)spiro[cyclopentane-1,3'-indol]-2-en-4-one 78d



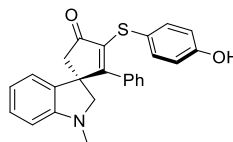
yellow solid, mp: 60–62 °C. ^1H NMR (400 MHz, CDCl_3) δ 7.57 (d, J = 7.9 Hz, 1H), 7.38 (dt, J = 7.4, 1.5, 1H), 7.27–7.16 (m, 7H), 2.74 (d, J = 19.0 Hz, 1H), 2.69 (d, J = 19.0 Hz, 1H), 2.25 (s, 3H), 1.26–1.16 (m, 2H), 0.93–0.73 (m, 3H). ^{13}C NMR (100 MHz, CDCl_3) δ 201.1, 182.9, 182.0, 155.2, 140.6, 134.3, 132.2, 129.2, 129.2, 128.3, 126.6, 126.5, 121.9, 120.7, 67.3, 42.4, 15.9, 14.0, 11.5, 10.0. HRMS (ESI^+) m/z calcd. for $\text{C}_{22}\text{H}_{20}\text{NOS}$ [MH] $^+$: 346.1260, found: 346.1261 (-0.2 ppm error). $\tilde{\nu}_{\text{max}}$ (thin film)/ cm^{-1} : 1713, 1579, 741.

5'-Methoxy-2'-methyl-2-phenyl-3-(phenylthio)spiro[cyclopentane-1,3'-indol]-2-en-4-one 78e



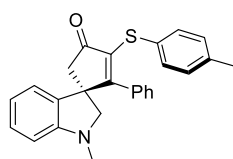
a yellow solid, mp: 59–61 °C. ^1H NMR (400 MHz, CDCl_3) δ 7.33 (d, J = 8.5 Hz, 1H), 7.18–7.01 (m, 7H), 6.78–6.74 (m, 3H), 6.66 (d, J = 2.4 Hz, 1H), 3.67 (s, 3H), 2.81 (d, J = 19.1 Hz, 1H), 2.70 (d, J = 19.1 Hz, 1H), 2.06 (s, 3H). ^{13}C NMR (100 MHz, CDCl_3) δ 201.2, 179.0, 171.6, 158.8, 148.7, 142.4, 137.0, 132.6, 132.4, 130.4, 130.1, 129.0, 128.3, 127.1, 127.1, 121.1, 113.8, 108.1, 67.2, 55.7, 43.6, 15.8. HRMS (ESI^+) m/z calcd. for $\text{C}_{26}\text{H}_{21}\text{NO}_2\text{S}$ [MH] $^+$: 412.1366, found: 412.1368 (-0.6 ppm error). ν_{max} (thin film)/ cm^{-1} : 1716, 1581, 1473, 1440, 1284, 739, 690.

3-((4-Hydroxyphenyl)thio)-1'-methyl-2-phenylspiro[cyclopentane-1,3'-indolin]-2-en-4-one 79a

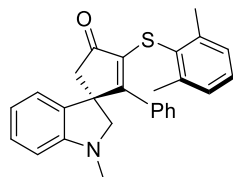


yellow solid, mp: 168–170 °C. ^1H NMR (400 MHz, CDCl_3) δ 7.30–7.16 (m, 7H), 6.96–6.93 (m, 3H), 6.75 (t, J = 7.1 Hz, 1H), 6.63 (d, J = 8.7 Hz, 2H), 6.47 (d, J = 7.1 Hz, 1H), 5.16 (s, 1H), 3.46 (d, J = 9.6 Hz, 1H), 3.36 (d, J = 9.6 Hz, 1H), 2.94 (d, J = 18.8 Hz, 1H), 2.89 (d, J = 18.8 Hz, 1H), 2.64 (s, 3H). ^{13}C NMR (100 MHz, CDCl_3) δ 203.7, 174.6, 173.3, 155.3, 152.4, 136.4, 134.0, 133.4, 132.5, 129.2, 128.4, 127.9, 123.3, 122.2, 118.5, 116.0, 107.7, 65.5, 54.9, 52.2, 35.4. HRMS (ESI^+) m/z calcd. for $\text{C}_{25}\text{H}_{22}\text{NO}_2\text{S}$ [MH] $^+$: 400.1366, found: 400.1365 (0.3 ppm error). $\tilde{\nu}_{\text{max}}$ (thin film)/ cm^{-1} : 3372, 1697, 1602, 1582, 1493, 1268, 1218, 830, 743, 697.

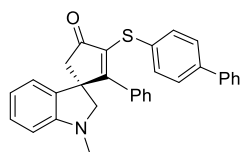
1'-Methyl-2-phenyl-3-(p-tolylthio)spiro[cyclopentane-1,3'-indolin]-2-en-4-one 79b



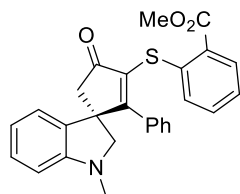
yellow solid, mp: 125–127 °C. ^1H NMR (400 MHz, CDCl_3) δ 7.24–7.10 (m, 6H), 6.97–6.91 (m, 5H), 6.72 (td, J = 7.6, 2.4 Hz, 1H), 6.57 (d, J = 7.9 Hz, 1H), 3.43 (d, J = 9.4 Hz, 1H), 3.33 (d, J = 9.4 Hz, 1H), 2.91 (d, J = 18.9 Hz, 1H), 2.84 (d, J = 18.9 Hz, 1H), 2.59 (s, 3H), 2.22 (s, 3H). ^{13}C NMR (100 MHz, CDCl_3) δ 203.1, 175.3, 152.4, 136.8, 135.5, 133.9, 132.5, 130.2, 129.8, 129.6, 129.2, 129.1, 128.4, 127.9, 122.2, 118.5, 107.6, 65.6, 54.9, 52.2, 35.4, 21.0. HRMS (ESI^+) m/z calcd. for $\text{C}_{26}\text{H}_{23}\text{NNaOS}$ [MNa] $^+$: 420.1393, found: 420.1389 (0.9 ppm error). $\tilde{\nu}_{\text{max}}$ (thin film)/ cm^{-1} : 1712, 1603, 1489, 804, 741, 697, 493.

3-((2,6-Dimethylphenyl)thio)-1'-methyl-2-phenylspiro[cyclopentane-1,3'-indolin]-2-en-4-one 79c

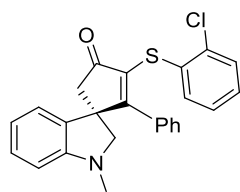
yellow solid, mp: 125–127 °C. ^1H NMR (400 MHz, CDCl_3) δ 7.18–7.15 (m, 2H), 7.12–7.08 (m, 2H), 7.05 (d, $J = 7.7$ Hz, 1H), 6.81 (d, $J = 7.3$ Hz, 2H), 6.77 (t, $J = 7.2$ Hz, 1H), 6.90 (d, $J = 7.5$ Hz, 2H), 6.83–6.75 (m, 3H), 6.43 (d, $J = 8.0$ Hz, 1H), 3.42 (d, $J = 8.9$ Hz, 1H), 3.31 (d, $J = 8.9$ Hz, 1H), 2.92 (d, $J = 19.1$ Hz, 1H), 2.86 (d, $J = 19.1$ Hz, 1H). ^{13}C NMR (100 MHz, CDCl_3) δ 202.9, 169.7, 152.6, 142.3, 135.8, 133.7, 132.4, 129.0, 128.9, 128.5, 128.4, 127.8, 127.6, 127.5, 122.4, 118.3, 107.6, 65.7, 54.8, 51.4, 35.3, 22.1. HRMS (ESI $^+$) m/z calcd. for $\text{C}_{27}\text{H}_{26}\text{NOS}$ $[\text{MH}]^+$: 412.1729, found: 412.1729 (0.2 ppm). $\tilde{\nu}_{\text{max}}$ (thin film)/ cm^{-1} : 1708, 1490, 1460, 773, 742, 699.

3-([1,1'-Biphenyl]-4-ylthio)-1'-methyl-2-phenylspiro[cyclopentane-1,3'-indolin]-2-en-4-one 79d

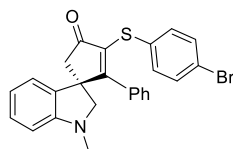
yellow solid, mp: 141–143 °C. ^1H NMR (400 MHz, CDCl_3) δ 7.55–7.50 (m, 2H), 7.46–7.39 (m, 4H), 7.37–7.24 (m, 4H), 7.24–7.16 (m, 3H), 7.04 (dd, $J = 7.4$, 1.0 Hz, 1H), 7.01–6.96 (m, 2H), 6.78 (td, $J = 7.4$, 0.8 Hz, 1H), 6.49 (d, $J = 7.9$ Hz, 1H), 3.51 (d, $J = 9.5$ Hz, 1H), 3.40 (d, $J = 9.5$ Hz, 1H), 3.03 (d, $J = 18.7$ Hz, 1H), 2.97 (d, $J = 18.7$ Hz, 1H), 2.65 (s, 3H). ^{13}C NMR (100 MHz, CDCl_3) δ 203.2, 176.2, 152.6, 140.4, 139.7, 135.0, 133.9, 132.5, 132.4, 130.1, 129.4, 129.3, 128.8, 128.5, 128.0, 127.6, 127.4, 127.0, 122.3, 118.6, 107.8, 65.7, 55.2, 52.2, 35.4. HRMS (ESI $^+$) calcd. for $\text{C}_{31}\text{H}_{25}\text{NNaOS}$ $[\text{MNa}]^+$: 482.1549, found: 482.1556 (-0.3 ppm error). $\tilde{\nu}_{\text{max}}$ (thin film)/ cm^{-1} : 1714, 1603, 1490, 1479, 760, 743, 697.

Methyl 2-((1'-methyl-4-oxo-2-phenylspiro[cyclopentane-1,3'-indolin]-2-en-3-yl)thio)benzoate 79e

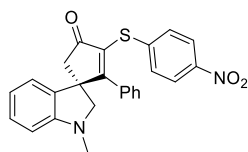
yellow solid, mp: 149–151 °C. ^1H NMR (400 MHz, CDCl_3) δ 7.97 (dd, $J = 7.7$, 1.6 Hz, 1H), 7.37 (td, $J = 7.6$, 1.6 Hz, 1H), 7.30–7.26 (m, 1H), 7.23–7.18 (m, 4H), 7.13 (d, $J = 7.6$ Hz, 1H), 7.08 (d, $J = 7.7$ Hz, 1H), 7.04–7.02 (m, 2H), 6.79 (app t, $J = 7.4$ Hz, 1H), 6.51 (t, $J = 7.7$ Hz, 1H), 3.89 (s, 3H), 3.55 (d, $J = 9.1$ Hz, 1H), 3.44 (d, $J = 9.1$ Hz, 1H), 3.05 (d, $J = 18.7$ Hz, 1H), 2.98 (d, $J = 18.7$ Hz, 1H), 2.67 (s, 3H). ^{13}C NMR (100 MHz, CDCl_3) δ 202.9, 179.2, 166.6, 152.5, 138.6, 134.3, 133.7, 132.3, 132.2, 131.5, 129.6, 129.3, 128.3, 128.0, 127.8, 127.4, 125.0, 122.3, 118.6, 107.8, 65.7, 55.4, 52.2, 52.2, 35.4. HRMS (ESI $^+$) m/z calcd. for $\text{C}_{27}\text{H}_{24}\text{NO}_3\text{S}$ $[\text{MH}]^+$: 442.1472, found: 442.1471 (0.2 ppm). $\tilde{\nu}_{\text{max}}$ (thin film)/ cm^{-1} : 1713, 1270, 1254, 741.

3-((2-Chlorophenyl)thio)-1'-methyl-2-phenylspiro[cyclopentane-1,3'-indolin]-2-en-4-one 79f

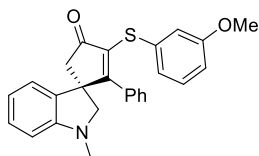
yellow solid, mp: 149–151 °C. ^1H NMR (400 MHz, CDCl_3) δ 7.29–7.22 (m, 2H), 7.21–7.15 (m, 4H), 7.11–7.05 (m, 3H), 6.98–6.93 (m, 2H), 6.77 (td, $J = 7.4$, 1.0 Hz, 1H), 6.47 (d, $J = 7.9$ Hz, 1H), 3.49 (d, $J = 9.4$ Hz, 1H), 3.38 (d, $J = 9.4$ Hz, 1H), 3.00 (d, $J = 18.7$ Hz, 1H), 2.94 (d, $J = 18.7$ Hz, 1H), 2.63 (s, 3H). ^{13}C NMR (100 MHz, CDCl_3) δ 202.6, 175.9, 152.6, 134.5, 134.0, 133.8, 132.3, 132.1, 131.3, 129.9, 129.4, 129.3, 128.2, 128.0, 128.0, 126.9, 122.6, 118.7, 107.9, 65.8, 55.3, 52.1, 35.5. HRMS (ESI $^+$) m/z calcd. for $\text{C}_{25}\text{H}_{20}\text{ClNNaOS}$ $[\text{MNa}]^+$: 440.0846, found: 440.0833 (2.8 ppm error). $\tilde{\nu}_{\text{max}}$ (thin film)/ cm^{-1} : 1714, 1604, 1490, 1451, 743, 698.

3-((4-Bromophenyl)thio)-1'-methyl-2-phenylspiro[cyclopentane-1,3'-indolin]-2-en-4-one, 19g

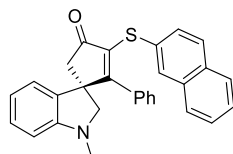
yellow solid, mp: 120–122 °C. ^1H NMR (400 MHz, CDCl_3) δ 7.32–7.25 (m, 3H), 7.23–7.16 (m, 3H), 7.12–7.07 (m, 2H), 6.98 (dd, $J = 7.4$, 1.0 Hz, 1H), 6.95–6.91 (m, 2H), 6.77 (td, $J = 7.4$, 0.9 Hz, 1H), 6.48 (d, $J = 7.9$ Hz, 1H), 3.49 (d, $J = 9.5$ Hz, 1H), 3.38 (d, $J = 9.5$ Hz, 1H), 2.98 (d, $J = 18.7$ Hz, 1H), 2.91 (d, $J = 18.7$ Hz, 1H), 2.64 (s, 3H). ^{13}C NMR (100 MHz, CDCl_3) δ 202.9, 176.6, 152.6, 134.6, 133.8, 132.7, 132.2, 132.0, 131.5, 129.6, 129.4, 128.4, 128.1, 122.3, 120.8, 118.7, 107.8, 65.6, 55.2, 52.1, 35.4. HRMS (ESI $^+$) m/z calcd. for $\text{C}_{25}\text{H}_{20}\text{BrNNaOS}$ $[\text{MNa}]^+$: 484.0341, found: 484.0343 (-0.7 ppm error). $\tilde{\nu}_{\text{max}}$ (thin film)/ cm^{-1} : 1715, 1604, 1490, 1472, 743, 697.

1'-Methyl-3-((4-nitrophenyl)thio)-2-phenylspiro[cyclopentane-1,3'-indolin]-2-en-4-one 79h

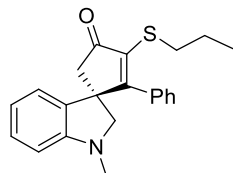
yellow oil. ^1H NMR (400 MHz, CDCl_3) δ 8.05–8.02 (m, 2H), 7.30–7.17 (m, 6H), 7.00 (app t, $J = 7.5$ Hz, 1H), 6.94–6.91 (m, 2H), 6.78 (dt, $J = 7.4$, 1.0 Hz, 1H), 3.51 (d, $J = 9.6$ Hz, 1H), 3.41 (d, $J = 9.6$ Hz, 1H), 3.04 (d, $J = 18.6$ Hz, 1H), 2.95 (d, $J = 18.6$ Hz, 1H), 2.63 (s, 3H). ^{13}C NMR (100 MHz, CDCl_3) δ 202.2, 179.5, 152.5, 145.8, 143.7, 133.3, 132.1, 131.6, 130.0, 129.6, 128.2, 128.1, 127.8, 124.0, 122.1, 118.7, 107.9, 65.5, 55.5, 51.9, 35.3. HRMS (ESI $^+$) m/z calcd. for $\text{C}_{25}\text{H}_{21}\text{N}_2\text{O}_3\text{S}$ $[\text{MH}]^+$: 429.1267, found: 429.1266 (0.4 ppm error). $\tilde{\nu}_{\text{max}}$ (thin film)/ cm^{-1} : 1714, 1513, 1490, 852, 740, 697.

3-((3-Methoxyphenyl)thio)-1'-methyl-2-phenylspiro[cyclopentane-1,3'-indolin]-2-en-4-one 79i

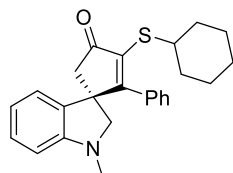
yellow oil. ^1H NMR (400 MHz, CDCl_3) δ 7.51–7.47 (m, 3H), 7.4 (app t, $J = 7.8$ Hz, 1H), 7.32 (d, $J = 7.8$ Hz, 1H), 7.32 (app d, $J = 7.8$ Hz, 1H), 7.12–7.04 (m, 3H), 6.97 (dd, $J = 8.4$, 2.0 Hz, 1H), 6.78 (d, $J = 8.4$ Hz, 1H), 4.02 (s, 3H), 3.80 (d, $J = 9.3$ Hz, 1H), 3.69 (d, $J = 9.3$ Hz, 1H), 3.29 (d, $J = 18.9$ Hz, 1H), 3.23 (d, $J = 18.9$ Hz, 1H), 2.94 (s, 3H). ^{13}C NMR (100 MHz, CDCl_3) δ 203.0, 176.5, 159.6, 152.4, 134.7, 133.8, 132.3, 129.6, 129.3, 129.2, 128.3, 127.9, 122.2, 121.7, 118.5, 114.8, 112.5, 107.7, 35.3. HRMS (ESI $^+$) m/z calcd. for $\text{C}_{26}\text{H}_{23}\text{NNaO}_2\text{S}$ $[\text{MNa}]^+$: 436.1341, found: 436.1342 (0.3 ppm). $\tilde{\nu}_{\text{max}}$ (thin film)/ cm^{-1} : 1712, 1589, 1477, 1245, 1229, 728, 696.

1'-Methyl-3-(naphthalen-2-ylthio)-2-phenylspiro[cyclopentane-1,3'-indolin]-2-en-4-one 79j

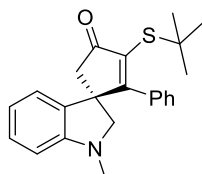
yellow solid, mp: 129–133 $^{\circ}\text{C}$. ^1H NMR (400 MHz, CDCl_3) δ 7.74 (d, $J = 7.5$ Hz, 1H), 7.71–7.64 (m, 3H), 7.49–7.37 (m, 3H), 7.31 (dd, $J = 8.7$, 1.2 Hz, 1H), 7.26–7.12 (m, 4H), 7.07 (d, $J = 7.3$ Hz, 1H), 7.03–6.94 (m, 2H), 6.79 (t, $J = 7.4$ Hz, 1H), 6.49 (d, $J = 7.9$ Hz, 1H), 3.52 (d, $J = 9.3$ Hz, 1H), 3.41 (d, $J = 9.3$ Hz, 1H), 3.02 (d, $J = 18.7$ Hz, 1H), 2.95 (d, $J = 18.7$ Hz, 1H), 2.65 (s, 3H). ^{13}C NMR (100 MHz, CDCl_3) δ 203.2, 176.6, 152.6, 135.0, 133.9, 133.6, 132.5, 132.1, 130.8, 129.4, 129.3, 128.6, 128.6, 128.4, 128.0, 127.7, 127.5, 127.3, 126.5, 126.0, 122.4, 118.6, 107.8, 65.6, 55.2, 52.2, 35.4. HRMS (ESI $^+$) m/z calcd. for $\text{C}_{29}\text{H}_{23}\text{NNaOS}^+$ $[\text{MNa}]^+$: 456.1393, found: 456.1395 (–1.0 ppm error). $\tilde{\nu}_{\text{max}}$ (thin film)/ cm^{-1} : 1714, 1604, 1490, 742, 698.

5'-Methoxy-2'-methyl-2-phenyl-3-(phenylthio)spiro[cyclopentane-1,3'-indol]-2-en-4-one 79k

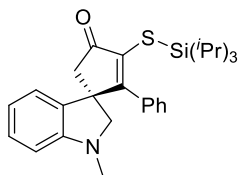
yellow solid, mp: 85–86 $^{\circ}\text{C}$. ^1H NMR (400 MHz, CDCl_3) δ 7.29–7.21 (m, 3H), 7.14 (t, $J = 7.6$ Hz, 1H), 6.97 (d, $J = 7.5$ Hz, 2H), 6.94 (d, $J = 7.5$ Hz, 1H), 6.71 (t, $J = 7.3$ Hz, 1H), 6.43 (d, $J = 7.9$ Hz, 1H), 3.39 (d, $J = 9.6$ Hz, 1H), 3.30 (d, $J = 9.6$ Hz, 1H), 2.89–2.82 (m, 3H), 2.75–2.70 (m, 1H), 2.60 (s, 3H), 1.53–1.42 (m, 2H), 0.84 (t, $J = 7.3$ Hz, 3H). ^{13}C NMR (100 MHz, CDCl_3) 204.4, 172.2, 152.4, 135.8, 134.4, 132.8, 129.1, 129.0, 128.4, 127.9, 122.2, 118.5, 107.6, 65.6, 54.7, 52.3, 35.4, 33.0, 23.3, 13.1. HRMS (ESI $^+$) m/z calcd. for $\text{C}_{22}\text{H}_{24}\text{NOS}$ $[\text{MH}]^+$: 350.1573, found: 350.1577 (–1.1 ppm error). $\tilde{\nu}_{\text{max}}$ (thin film)/ cm^{-1} : 1707, 1604, 1490, 743, 698.

3-(Cyclohexylthio)-1'-methyl-2-phenylspiro[cyclopentane-1,3'-indolin]-2-en-4-one 79l

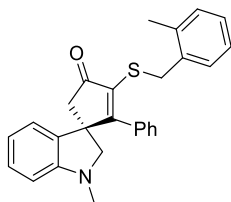
yellow oil. ^1H NMR (400 MHz, CDCl_3) δ 7.32–7.24 (m, 3H), 7.18 (t, $J = 7.6$ Hz, 1H), 7.00–6.97 (m, 3H), 6.75 (t, $J = 7.4$ Hz, 1H), 6.47 (d, $J = 7.9$ Hz, 1H), 3.57–3.50 (m, 1H), 3.43 (d, $J = 9.4$ Hz, 1H), 3.34 (d, $J = 9.4$ Hz, 1H), 2.92 (app s, 2H), 2.64 (s, 3H), 1.89–1.81 (m, 2H), 1.69–1.55 (m, 3H), 1.26–1.13 (m, 5H). ^{13}C NMR (100 MHz, CDCl_3) 204.6, 173.1, 152.4, 135.4, 134.5, 132.8, 129.0, 128.4, 127.9, 122.2, 118.5, 107.6, 65.6, 54.8, 52.2, 42.4, 35.4, 33.5, 33.3, 25.8, 25.6. HRMS (ESI $^+$) m/z calcd. for $\text{C}_{25}\text{H}_{27}\text{NNaOS}$ $[\text{MNa}]^+$: 412.1706, found: 412.1703 (0.6 ppm error). $\tilde{\nu}_{\text{max}}$ (thin film)/ cm^{-1} : 1704, 1603, 1489, 730, 696.

3-(tert-Butylthio)-1'-methyl-2-phenylspiro[cyclopentane-1,3'-indolin]-2-en-4-one 79m

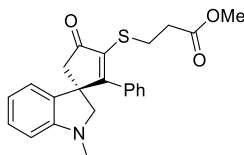
orange oil. ^1H NMR (400 MHz, CDCl_3) δ 7.34–7.20 (m, 4H), 7.05–6.99 (m, 3H), 6.80 (t, $J = 7.8$ Hz, 1H), 6.50 (d, $J = 7.9$ Hz, 1H), 3.47 (d, $J = 9.2$ Hz, 1H), 3.38 (d, $J = 9.2$ Hz, 1H), 3.03 (d, $J = 19.0$ Hz, 1H), 2.93 (d, $J = 19.0$ Hz, 1H), 2.65 (s, 3H), 1.22 (s, 9H). ^{13}C NMR (100 MHz, CDCl_3) δ 205.8, 182.5, 152.6, 134.8, 134.6, 132.5, 129.2, 129.1, 129.0, 127.6, 122.2, 118.4, 107.7, 65.6, 55.2, 51.6, 48.8, 35.3, 31.5. HRMS (ESI $^+$) m/z calcd. for $\text{C}_{23}\text{H}_{26}\text{NOS}$ $[\text{MH}]^+$: 364.1730, found: 364.1730 (–0.2 ppm error). $\tilde{\nu}_{\text{max}}$ (thin film)/ cm^{-1} : 1713, 1604, 1490, 742, 698.

1'-Methyl-2-phenyl-3-((triisopropylsilyl)thio)spiro[cyclopentane-1,3'-indolin]-2-en-4-one 79n

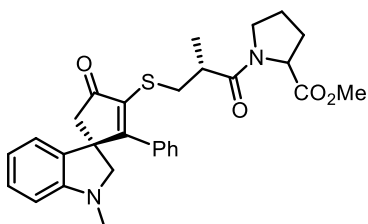
yellow oil. ^1H NMR (400 MHz, CDCl_3) δ 7.28–7.22 (m, 5H), 7.17 (td, J = 7.4, 1.1 Hz, 1H), 7.10–7.08 (m, 2H), 6.98 (dd, J = 7.4, 1.0 Hz, 1H), 6.73 (app t, J = 7.4 Hz, 1H), 6.45 (d, J = 7.8 Hz, 1H), 3.41 (d, J = 7.8 Hz, 1H), 3.30 (d, J = 9.4 Hz, 1H), 2.93 (d, J = 18.3 Hz, 1H), 2.88 (d, J = 18.3 Hz, 1H), 2.61 (s, 3H), 1.29–1.20 (m, 3H), 1.06 (d, J = 7.4 Hz, 9H), 1.01 (d, J = 7.4 Hz, 9H). ^{13}C NMR (100 MHz, CDCl_3) δ 204.5, 174.9, 152.6, 135.1, 134.9, 132.7, 128.9, 128.7, 128.7, 127.8, 122.5, 118.3, 107.6, 66.0, 55.1, 51.4, 35.4, 18.6, 18.5, 14.2. HRMS (APCI) m/z calcd. for $\text{C}_{28}\text{H}_{38}\text{NOSSi}$ $[\text{MH}]^+$: 464.2452, found: 464.2438 (3.0 ppm). $\tilde{\nu}_{\text{max}}$ (thin film)/ cm^{-1} : 2944, 2865, 1713, 1490, 1462, 742.

1'-Methyl-3-((2-methylbenzyl)thio)-2-phenylspiro[cyclopentane-1,3'-indolin]-2-en-4-one 79o

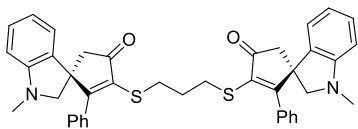
yellow solid, mp: 159–160 °C. ^1H NMR (400 MHz, CDCl_3) δ 7.25–7.01 (m, 9H), 6.66–6.61 (m, 3H), 6.54 (d, J = 7.4 Hz, 1H), 6.40 (d, J = 7.8 Hz, 1H), 4.18 (d, J = 12.9 Hz, 1H), 4.13 (d, J = 12.9 Hz, 1H), 3.30 (d, J = 9.6 Hz, 1H), 3.24 (d, J = 9.6 Hz, 1H), 2.85 (s, 2H), 2.58 (s, 3H), 2.19 (s, 3H). ^{13}C NMR (100 MHz, CDCl_3) δ 204.5, 175.7, 152.3, 137.3, 135.4, 135.0, 134.1, 132.3, 130.6, 129.9, 128.9, 128.3, 127.7, 127.4, 125.7, 122.5, 118.3, 107.5, 65.5, 54.8, 52.0, 35.4, 33.9, 19.0. HRMS (ESI $^+$) m/z calcd. for $\text{C}_{27}\text{H}_{25}\text{NNaOS}$ $[\text{MNa}]^+$: 434.1549, found: 434.1549 (0.1 ppm error). $\tilde{\nu}_{\text{max}}$ (thin film)/ cm^{-1} : 1705, 1604, 1490, 742, 730, 697.

Methyl-3-((1'-methyl-4-oxo-2-phenylspiro[cyclopentane-1,3'-indolin]-2-en-3-yl)thio)propanoate, 79p

orange oil. ^1H NMR (400 MHz, CDCl_3) δ 7.28–7.18 (m, 3H), 7.13 (td, J = 7.9, 1.3 Hz, 1H), 6.97 (d, J = 7.6 Hz, 1H), 6.94–6.91 (m, 2H), 6.42 (d, J = 8.1 Hz, 1H), 3.56 (s, 3H), 3.38 (d, J = 9.5 Hz, 1H), 3.28 (d, J = 9.5 Hz, 1H), 3.19 (dt, J = 13.6, 7.2 Hz, 1H), 3.05 (dt, J = 13.6, 7.2 Hz, 1H), 2.90 (d, J = 19.0 Hz, 1H), 2.85 (d, J = 19.0 Hz, 1H), 2.59 (s, 3H), 2.56–2.50 (m, 2H). ^{13}C NMR (100 MHz, CDCl_3) δ 204.1, 173.1, 172.0, 152.4, 134.8, 134.1, 132.5, 129.2, 129.1, 128.4, 128.0, 122.3, 118.5, 107.7, 65.6, 54.8, 52.3, 51.7, 35.4, 35.1, 26.1. HRMS (ESI $^+$) m/z calcd. for $\text{C}_{23}\text{H}_{24}\text{NO}_3\text{S}$ $[\text{MH}]^+$: 394.1471, found: 394.1469 (0.7 ppm). $\tilde{\nu}_{\text{max}}$ (thin film)/ cm^{-1} : 1735, 1706, 1603, 1245, 744, 699.

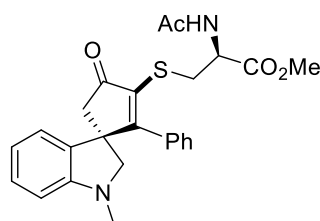
Methyl ((2R)-2-methyl-3-((1'-methyl-4-oxo-2-phenylspiro[cyclopentane-1,3'-indolin]-2-en-3-yl)thio)propanoyl)prolinate 79q

yellow oil. ^1H NMR (400 MHz, CDCl_3) δ 7.45–7.22 (m, 10H), 7.14–7.10 (m, 4H), 6.90 (td, J = 7.7, 1.2 Hz, 1H), 6.87 (td, J = 7.7, 1.2 Hz, 1H), 6.62 (s, 1H), 6.61 (s, 1H), 4.56–4.48 (m, 2H), 3.85 (s, 3H), 3.82 (s, 3H), 3.71–3.63 (m, 4H), 3.56 (d, J = 9.5 Hz, 1H), 3.54 (d, J = 9.5 Hz, 1H), 3.47 (d, J = 9.5 Hz, 1H), 3.44 (d, J = 9.5 Hz, 1H), 3.26–3.17 (m, 2H), 3.05–2.86 (m, 8H), 2.78 (s, 3H), 2.77 (s, 3H), 2.26–1.89 (m, 8H), 1.29 (d, J = 6.8 Hz, 3H), 1.23 (d, J = 6.8 Hz, 3H). ^{13}C NMR (100 MHz, CDCl_3) δ 204.30, 204.26, 173.54, 173.50, 172.79, 172.74, 172.65, 172.31, 152.44, 152.39, 135.95, 135.60, 134.20, 134.10, 132.70, 132.68, 129.22, 129.16, 129.12, 129.06, 128.62, 128.57, 127.9 (2xC), 122.51, 122.14, 118.55, 118.38, 107.65, 107.62, 65.82, 65.62, 58.54, 58.46, 54.64, 54.59, 52.50, 52.34, 52.11 (2xC), 46.84, 46.75, 39.66, 39.47, 35.40, 35.34, 34.69, 34.56, 29.03, 28.94, 24.70, 24.63, 16.97, 16.74. HRMS (APCI $^+$) m/z calcd. for $\text{C}_{29}\text{H}_{33}\text{N}_2\text{O}_4\text{S}$ $[\text{MH}]^+$: 505.2162, found: 505.2156 (1.7 ppm). $\tilde{\nu}_{\text{max}}$ (thin film)/ cm^{-1} : 2926, 1742, 1707, 1641, 1434, 1198, 1174, 731, 699.

3,3''-(Propane-1,3-diylbis(sulfanediy))bis(1'-methyl-2-phenylspiro[cyclopentane-1,3'-indolin]-2-en-4-one) 79r

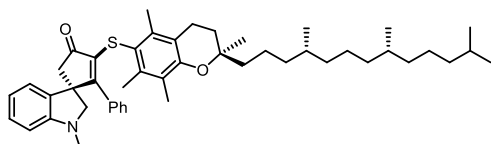
yellow solid, mp: 69–71 °C. ^1H NMR (400 MHz, CDCl_3) δ 7.29–7.20 (m, 6H), 7.14 (app t, J = 7.6 Hz, 2H), 6.93 (app t, J = 7.0 Hz, 6H), 6.69 (app t, J = 7.4 Hz, 2H), 6.44 (d, J = 7.9 Hz, 2H), 3.39 (d, J = 9.5 Hz, 2H), 3.29 (d, J = 9.5 Hz, 2H), 2.90–2.82 (m, 6H), 2.78–2.72 (m, 2H), 2.61 (s, 6H), 1.71–1.60 (m, 2H). ^{13}C NMR (100 MHz, CDCl_3) δ 204.2 (2xC), 173.0, 172.9, 152.4 (2xC), 135.0 (2xC), 134.2 (2xC), 132.5 (2xC), 129.1 (2xC), 129.0 (2xC), 128.3 (2xC), 128.0 (2xC), 122.3 (2xC), 118.6 (2xC), 107.6 (2xC), 65.6 (2xC), 54.8 (2xC), 52.2 (2xC), 35.4 (2xC), 30.0, 29.9, 29.3 (2xC). HRMS (ESI $^+$) m/z calcd. for $\text{C}_{41}\text{H}_{39}\text{N}_2\text{O}_2\text{S}_2$ $[\text{MH}]^+$: 655.2447, found: 655.2443 (0.7 ppm error). $\tilde{\nu}_{\text{max}}$ (thin film)/ cm^{-1} : 1706, 1603, 1490, 742, 698.

Methyl N-acetyl-S-(1'-methyl-4-oxo-2-phenylspiro[cyclopentane-1,3'-indolin]-2-en-3-yl)-D-cysteinate 79s



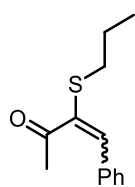
yellow oil. ^1H NMR (400 MHz, CDCl_3) δ 7.15–7.05 (m, 3H), 6.97 (app t, $J = 7.8$ Hz, 1H), 6.86 (dd, $J = 7.4, 1.1$ Hz, 0.5H), 6.81 (dd, $J = 7.4, 1.1$ Hz, 0.5H), 6.79–6.76 (m, 2H), 6.66 (d, $J = 7.8$ Hz, 1H), 6.56 (td, $J = 7.8, 2.3$ Hz, 1H), 6.26 (d, $J = 7.8$ Hz, 1H), 4.52–4.44 (m, 2H), 3.51 (s, 1.5 H), 3.47 (s, 1.5 H), 3.27–3.12 (m, 3H), 3.05 (dd, $J = 14.2, 5.1$ Hz, 0.5H), 2.99 (dd, $J = 14.2, 5.1$ Hz, 1H), 2.77 (dd, $J = 18.7, 2.5$ Hz, 1H), 2.70 (dd, $J = 18.7, 2.5$ Hz, 1H), 2.43 (s, 3H), 1.83 (s, 1.5 H), 1.79 (s, 1.5H). ^{13}C NMR (100 MHz, CDCl_3) δ 204.58, 204.51, 175.69, 175.60, 170.99, 170.05, 152.44, 152.39, 134.19, 134.12, 133.85 (2xC), 131.90, 131.84, 129.39, 129.35, 129.20, 129.18, 128.27 (2xC), 128.01 (2xC), 122.43, 122.36, 118.59 (2xC), 107.69 (2xC), 65.54, 65.46, 54.85, 54.78, 52.56, 52.51, 52.00, 51.95, 51.82 (2xC), 35.34 (2xC), 33.45, 33.32, 22.95, 22.92. HRMS (ESI $^+$) m/z calcd. for $\text{C}_{25}\text{H}_{27}\text{N}_2\text{NaO}_4\text{S}$ $[\text{MNa}]^+$: 473.1505, found: 473.1505 (0.1 ppm). $\tilde{\nu}_{\text{max}}$ (thin film)/ cm^{-1} : 1703, 1665, 1212, 908, 726, 697.

1'-Methyl-2-phenyl-3-(((R)-2,5,7,8-tetramethyl-2-((4R,8R)-4,8,12-trimethyltridecyl)chroman-6-yl)thio)spiro[cyclopentane-1,3'-indolin]-2-en-4-one 79t



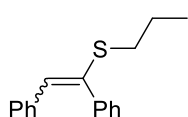
a yellow oil. ^1H NMR (400 MHz, CDCl_3) δ 7.15 (td, $J = 7.6, 1.7$ Hz, 1H), 7.04 (d, $J = 7.0$ Hz, 1H), 7.01–6.98 (m, 1H), 6.93–6.88 (m, 2H), 6.75 (t, $J = 7.6$ Hz, 1H), 6.59–6.55 (m, 2H), 6.31 (d, $J = 7.6$ Hz, 1H), 3.33 (d, $J = 9.0$ Hz, 1H), 3.28 (d, $J = 9.0$ Hz, 1H), 2.92 (app d, $J = 19.0$ Hz, 1H), 2.86 (d, 19.0 Hz, 1H), 2.54 (s, 3H), 2.45–2.34 (m, 2H), 2.29 (d, $J = 3.3$ Hz, 3H), 1.93 (d, $J = 4.6$ Hz, 3H), 1.67–1.06 (m, 26H), 0.89–0.84 (m, 12H). ^{13}C NMR (100 MHz, CDCl_3) δ 204.09, 204.05, 167.13, 167.06, 152.56 (2xC), 152.13 (2xC), 139.03, 139.00, 138.22, 138.18, 137.20, 137.17, 133.48, 133.46, 132.75(2xC), 128.82 (2XC), 127.68, 127.64, 127.19, 127.15, 126.61, 126.59, 122.80 (2xC), 122.35 (2xC), 118.28, 118.23, 118.15 (2xC), 117.21(2xC), 107.45 (2xC), 75.10 (2xC), 65.47, 65.46, 55.19, 55.18, 51.43 (2xC), 40.44, 40.40, 40.07, 40.01, 39.34 (2xC), 37.55, 37.42, 37.36, 37.26, 35.25 (2xC), 32.76, 32.70, 31.06, 31.03, 31.02, 30.96, 27.95 (2xC), 24.79, 24.42, 24.00, 23.72, 22.70, 22.61, 21.10, 21.01, 19.73, 19.66, 19.60, 19.57, 18.88 (2xC), 18.01 (2xC), 12.25 (2xC). HRMS (APCI $^+$) m/z calcd. for $\text{C}_{48}\text{H}_{66}\text{NO}_2\text{S}$ $[\text{MH}]^+$: 720.4809, found: 720.4781 (3.9 ppm). $\tilde{\nu}_{\text{max}}$ (thin film)/ cm^{-1} : 2943, 2866, 1711, 1605, 1490, 1460, 1102, 742, 698.

4-Phenyl-3-(propylthio)but-3-en-2-one 81



yellow oil. *E*-isomer: ^1H NMR (400 MHz, CDCl_3) δ 7.34–7.21 (m, 2H), 6.85 (s, 1H), 2.66 (app t, $J = 7.3$ Hz, 2H), 2.24 (s, 3H), 1.72–1.63 (m, 2H), 1.02 (t, $J = 7.3$ Hz, 3H); ^{13}C NMR for *E*-isomer (100 MHz, CDCl_3) δ 202.8, 137.3, 135.3, 132.0, 128.6, 128.4, 128.2, 34.7, 29.9, 22.5, 13.3; HRMS (ESI) m/z calcd. for $\text{C}_{13}\text{H}_{17}\text{OS}$ $[\text{MH}]^+$: 221.0994, found: 221.0995 (0.3 ppm); $\tilde{\nu}_{\text{max}}$ (thin film)/ cm^{-1} : 2962, 2927, 1694, 1354, 1172, 757, 699. *Z*-isomer: ^1H NMR (400 MHz, CDCl_3) δ 7.86–7.83 (m, 2H), 7.64 (s, 1H), 7.43–7.34 (m, 3H), 2.67 (app t, $J = 7.2$ Hz, 2H), 2.55 (s, 3H), 1.56–1.47 (m, 2H), 0.90 (t, $J = 7.4$ Hz, 3H); ^{13}C NMR for *Z*-isomer (100 MHz, CDCl_3) δ 198.6, 141.6, 136.3, 134.7, 130.9, 129.5, 128.3, 35.9, 27.5, 23.2, 13.3; HRMS (ESI) m/z calcd. for $\text{C}_{13}\text{H}_{17}\text{OS}$ $[\text{MH}]^+$: 221.0995, found: 221.0995 (0.3 ppm); $\tilde{\nu}_{\text{max}}$ (thin film)/ cm^{-1} : 2963, 2929, 1677, 1204, 1219, 1181, 755, 691.

(1,2-Diphenylvinyl)(propyl)sulfane 83



yellow oil. ^1H NMR (400 MHz, CDCl_3) δ 7.77 (d, $J = 7.2$ Hz, 2H), 7.63 (d, $J = 7.8$ Hz, 2H), 7.42–7.29 (m, 12H), 7.13–7.08 (m, 4H), 6.96 (d, $J = 7.6$ Hz, 2H), 6.83 (s, 1H, major), 6.17 (s, 1H, minor), 2.54 (t, $J = 7.2$ Hz, 2H, minor), 2.42 (t, $J = 7.2$ Hz, 2H, major), 1.68–1.69 (m, 2H, minor), 1.52–1.43 (m, 2H, major), 0.99 (t, $J = 7.4$ Hz, 3H, minor), 0.85 (t, $J = 7.4$ Hz, 3H, major). ^{13}C NMR (100 MHz, CDCl_3) δ 141.2, 138.3, 138.1, 137.8, 137.1, 136.8, 131.9, 129.6, 129.5, 128.8, 128.6, 128.3, 128.0, 127.9, 127.9(3), 127.8, 127.1, 126.6, 126.4, 34.8, 33.8, 23.2, 22.5, 13.4, 13.2. HRMS (APCI) m/z calcd. for $\text{C}_{17}\text{H}_{19}\text{S}$ $[\text{MH}]^+$: 255.1187, found: 255.1202 (5.7 ppm). $\tilde{\nu}_{\text{max}}$ (thin film)/ cm^{-1} : 2961, 1444, 763, 692.

7. ABBREVIATION LIST

° C	Celsius degrees
µm	Micrometers
4-DMAP	4-Dimethylaminopyridine
Å	Ångstrom
AC	Absolute Configuration
B3LYP	Becke, 3-parameter, Lee–Yang–Parr
BET	Back electron transfer
BH&H-LYP	Becke-Half-and-Half, Lee–Yang–Parr
br s	Broad singlet
calcd.	Calculated
CAM	Coulomb-attenuating method
CFL	Compact Fluorescent Lamp
cm	Centimeter
COSY	CORrelated SpectroscopY
CSP	Chiral Stationary Phase
d	Doublet
DA	Diels Alder
DABCO	1,4-Diazabicyclo[2.2.2]octane
DBU	1,5-Diazabicyclo(5.4.0)undec-7-ene
DCE	1,2-Dichloroethane
DCM	Dichloromethane
dd	Double doublet
ddd	Doublet of doublets of doublets
DDQ	2,3-Dichloro-5,6-dicyano-1,4-benzoquinone
DEPT	Distortionless Enhancement by Polarization Transfer
DFT	Density Functional Theory
DMF	<i>N,N</i> -dimethylformamide
DMSO	Dimethylsulfoxide
dq	Double quartet
ECD	Electronic Circular Dichroism
EDA	Electron Donor Acceptor
EDG	Electron Donating Group
equiv.	Equivalents
ESI	Electrospray Ionisation
eV	Electronvolt
EWG	Electron Withdrawing Group
GHD	Glucose Dehydrogenase
h	Hour(s)
HAT	Hydrogen Atom Transfer
HFIP	1,1,1,3,3,3-Hexafluoro-2-propanol
HMQC	Heteronuclear Multiple-Quantum Correlation
HPLC	High Performance Liquid Chromatography
HRMS	High-Resolution Mass Spectrometry
Hz	Herz
h _{CT}	Charge-Transfer Band
ICD	Intramolecular Conjugate Displacement
IR	InfraRed
<i>J</i>	Coupling constants

K	Kelvin
LED	Light Emitting Diode
M	Molar
m	multiplet
<i>m</i> -	<i>Meta</i> -
m/z	Mass-to-charge ratio
MHz	Mega-Hertz
mins.	Minutes
Mol.	Mole
mp	Melting point
MSD	Mass Selective Detector
<i>n</i> -	<i>Normal</i>
NADP+	Oxidized form of Nicotinamide Adenine Dinucleotide phosphate
NADPH	Reduced form of Nicotinamide Adenine Dinucleotide phosphate
NBS	<i>N</i> -Bromosuccinimide
nm	Nanometers
NMR	Nuclear Magnetic Resonance
NOESY	Nuclear Overhauser Effect Spectroscopy
<i>o</i> -	<i>Ortho</i> -
ORSA	Organic Reactions for Synthetic Applications
ORTEP	Oak Ridge Thermal-Ellipsoid Plot Program
<i>p</i> -	<i>Para</i> -
PCM	Polarizable Continuum Model
ppm	Parts per million
PTFE	Polytetrafluoroethylene
Pyr	Pyridine
q	Quartet
qd	Doublet of quartets
QTOF	Quadrupole Time of Flight
r.t.	Room temperature
<i>s</i>	Seconds
s	Singlet
SET	Single Electron Transfer
S _N V	Nucleophilic Vinylic Substitution
t	Time
T	Temperature
TBN	<i>Tert</i> -butylnitrite
td	Triplet of doublets
TD-DFT	Time dependent - Density Functional Theory
TFA	Trifluoroacetic acid
TFE	2,2,2-Trifluoroethanol
THF	Tetrahydrofuran
TLC	Thin Layer Chromatography
TOF	Time of Flight
tt	Triplet of triplets
UV-Vis	Ultraviolet–visible
W	Watt
λ	Wavelength
$\tilde{\nu}_{\max}$	Maximum frequencies
φ or Φ	Quantum yield

8. REFERENCES

- [1] G. W. Gribble, in *Prog. Heterocycl. Chem.*, Vol. 31, Elsevier, **2020**, pp. 83-117.
- [2] A. Pagano, M. Mancinelli, L. Bianchi, G. Giorgi, M. Maccagno, G. Petrillo, C. Tavani, *Tetrahedron* **2019**, 75, 4506-4515.
- [3] A. Benzi, L. Bianchi, M. Maccagno, A. Pagano, G. Petrillo, C. Tavani, *Molecules* **2019**, 24, 3802.
- [4] A. Pagano, E. Marotta, A. Mazzanti, G. Petrillo, C. Tavani, M. Mancinelli, *Synlett* **2018**, 29, 2161-2166.
- [5] H. E. Ho, A. Pagano, J. A. Rossi-Ashton, J. R. Donald, R. G. Epton, M. J. James, P. O'Brien, R. J. K. Taylor, W. P. Unsworth., *Chem. Sci.* **2020**, DOI: 10.1039/c9sc05311e.
- [6] J. A. Joule, K. Mills, *Heterocyclic chemistry*, John Wiley & Sons, **2008**.
- [7] C. Cabrele, O. Reiser, *J. Org. Chem.* **2016**, 81, 10109-10125.
- [8] B. B. Mishra, D. Kumar, A. Mishra, P. P. Mohapatra, V. K. Tiwari, in *Adv. Heterocycl. Chem.*, Vol. 107, Elsevier, **2012**, pp. 41-99.
- [9] A. R. Katritzky, C. A. Ramsden, E. Scriven, R. Taylor, *Comprehensive heterocyclic chemistry III*, Vol. 4, Elsevier Amsterdam, **2008**.
- [10] R. Dua, S. Shrivastava, S. Sonwane, S. Srivastava, *Adv. Biol. Res.* **2011**, 5, 120-144.
- [11] (a) T. Eicher, S. Hauptmann, A. Speicher, *The Chemistry of Heterocycles: Structures, Reactions, Synthesis, and Applications*, John Wiley & Sons, **2013**; (b) R. V. Orru, M. de Greef, *Synthesis* **2003**, 2003, 1471-1499.
- [12] A. Baeyer, *Ber. Dtsch. Chem. Ges.* **1880**, 13, 2254-2263.
- [13] G. W. Gribble, *Indole ring synthesis: From natural products to drug discovery*, John Wiley & Sons, **2016**.
- [14] (a) D. A. Horton, G. T. Bourne, M. L. Smythe, *Chem. Rev.* **2003**, 103, 893-930; (b) N. K. Kaushik, N. Kaushik, P. Attri, N. Kumar, C. H. Kim, A. K. Verma, E. H. Choi, *Molecules* **2013**, 18, 6620-6662.
- [15] R. R. King, L. A. Calhoun, *Phytochemistry* **2009**, 70, 833-841.
- [16] P. P. Molesworth, M. G. Gardiner, R. C. Jones, J. A. Smith, R. S. Tegg, C. Wilson, *Aust. J. Chem.* **2010**, 63, 813-820.
- [17] H. Zhang, Q. Wang, X. Ning, H. Hang, J. Ma, X. Yang, X. Lu, J. Zhang, Y. Li, C. Niu, *J. Agric. Food. Chem.* **2015**, 63, 3734-3741.
- [18] H. Zhang, X. Ning, H. Hang, X. Ru, H. Li, Y. Li, L. Wang, X. Zhang, S. Yu, Y. Qiao, *Org. Lett.* **2013**, 15, 5670-5673.
- [19] W. Al-Zereini, I. Schuhmann, H. Laatsch, E. Helmke, H. Anke, *J. Antibiot.* **2007**, 60, 301.
- [20] (a) M. Chakrabarty, T. Kundu, S. Arima, Y. Harigaya, *Tetrahedron Lett.* **2005**, 46, 2865-2868; (b) J. E. Macor, R. Post, K. Ryan, *Synth. Commun.* **1993**, 23, 65-72; (c) M. Rakshit, T. Kundu, G. K. Kar, M. Chakrabarty, *Monatsh. Chem. Chem. Mon.* **2013**, 144, 717-724; (d) P. Zajdel, N. Masurier, V. Canale, P. Verdie, M. Amblard, M. Pawłowski, J. Martinez, G. Subra, *Tetrahedron Lett.* **2013**, 54, 998-1002.
- [21] M. G. Ferlin, G. Chiarello, S. Dall'Acqua, E. Maciocco, M. P. Mascia, M. G. Pisu, G. Biggio, *Biorg. Med. Chem.* **2005**, 13, 3531-3541.
- [22] L. Birbaum, L. Gillard, H. Gérard, H. Oulyadi, G. Vincent, X. Moreau, M. De Paolis, I. Chataigner, *Chem. Eur. J.* **2019**, 25, 13688-13693.
- [23] P. Santhini, S. A. Babu, A. Krishnan R, E. Suresh, J. John, *Org. Lett.* **2017**, 19, 2458-2461.
- [24] E. Garcia, L. Benjamin, R. I. Fryer, *J. Heterocycl. Chem.* **1973**, 10, 51-53.

- [25] M. Sulur, P. Sharma, R. Ramakrishnan, R. Naidu, E. Merifield, D. M. Gill, A. M. Clarke, C. Thomson, M. Butters, S. Bachu, *Org. Process Res. Dev.* **2012**, *16*, 1746-1753.
- [26] H. Xu, Z. Pan, L. Dai, K. Mao, L. Rong, *Appl. Organomet. Chem.* **2019**, *33*, e4653.
- [27] L. Sternbach, R. I. Fryer, O. Keller, W. Metlesics, G. Sach, N. Steiger, *J. Med. Chem.* **1963**, *6*, 261-265.
- [28] S. Nakahara, T. Sadachi, A. Kubo, *Heterocycles* **2010**, *81*, 145-148.
- [29] (a) G. Chauvière, B. Bouteille, B. Enanga, C. de Albuquerque, S. L. Croft, M. Dumas, J. Périé, *J. Med. Chem.* **2003**, *46*, 427-440; (b) M. M. Ramla, M. A. Omar, A.-M. M. El-Khamry, H. I. El-Diwani, *Biorg. Med. Chem.* **2006**, *14*, 7324-7332; (c) A. Romero-Castro, I. León-Rivera, L. C. Ávila-Rojas, G. Navarrete-Vázquez, A. Nieto-Rodríguez, *Arch. Pharm. Res.* **2011**, *34*, 181-189; (d) N. R. Tawari, M. S. Degani, *Chem. Biol. Drug Des.* **2011**, *78*, 408-417; (e) J. H. Tocher, *Gen. Pharmacol.* **1997**, *28*, 485-487.
- [30] F. Hayat, A. N. I. Viswanath, A. N. Pae, H. Rhim, W.-K. Park, H.-Y. P. Choo, *Biorg. Med. Chem.* **2015**, *23*, 1313-1320.
- [31] (a) D. E. Bergstrom, P. Zhang, W. T. Johnson, *Nucleic Acids Res.* **1997**, *25*, 1935-1942; (b) C. Ceballos, S. Khiati, C. A. Prata, X.-X. Zhang, S. Giorgio, P. Marsal, M. W. Grinstaff, P. Barthélémy, M. Camplo, *Bioconjugate Chem.* **2010**, *21*, 1062-1069; (c) H. Challa, M. L. Styers, S. A. Woski, *Org. Lett.* **1999**, *1*, 1639-1641; (d) S. A. Ingale, P. Leonard, H. Yang, F. Seela, *Org. Biomol. Chem.* **2014**, *12*, 8519-8532.
- [32] (a) Z. Le, L. Zeng, J. Xu, H. Liu, M. Ma, *J. Appl. Polym. Sci.* **2008**, *107*, 2793-2801; (b) H. Talbi, D. Billaud, *Synth. Met.* **1998**, *97*, 239-244.
- [33] J. Xu, W. Zhou, J. Hou, S. Pu, L. Yan, J. Wang, *J. Polym. Sci. Pol. Chem.* **2005**, *43*, 3986-3997.
- [34] J. Xu, W. Zhou, J. Hou, S. Pu, L. Yan, J. Wang, *Mater. Lett.* **2005**, *59*, 2412-2417.
- [35] (a) A. Da Settimo, M. Saettone, *Tetrahedron* **1965**, *21*, 1923-1929; (b) Y. Miki, M. Umemoto, H. Maruyama, *Heterocycles* **2007**, *71*, 2457-2463; (c) W. E. Noland, K. R. Rush, *J. Org. Chem.* **1966**, *31*, 70-77; (d) W. E. Noland, L. R. Smith, D. C. Johnson, *J. Org. Chem.* **1963**, *28*, 2262-2266; (e) E. T. Pelkey, G. W. Gribble, *Synthesis* **1999**, *1999*, 1117-1122.
- [36] (a) S. N. Lavrenov, S. A. Lakatosh, L. N. Lysenkova, A. M. Korolev, M. N. Preobrazhenskaya, *Synthesis* **2002**, *2002*, 0320-0322; (b) W. E. Noland, K. R. Rush, *J. Org. Chem.* **1964**, *29*, 947-948.
- [37] D. Tu, J. Luo, C. Jiang, *Chem. Commun.* **2018**, *54*, 2514-2517.
- [38] P. Saxena, M. Kapur, *Chem. Asian J.* **2018**, *13*, 861-870.
- [39] B. P. Fors, S. L. Buchwald, *J. Am. Chem. Soc.* **2009**, *131*, 12898-12899.
- [40] A. Shoberu, C. K. Li, Z. K. Tao, G. Y. Zhang, J. P. Zou, *Adv. Synth. Catal.* **2019**, *361*, 2255-2261.
- [41] S. M. Barry, J. A. Kers, E. G. Johnson, L. Song, P. R. Aston, B. Patel, S. B. Krasnoff, B. R. Crane, D. M. Gibson, R. Loria, *Nat. Chem. Biol.* **2012**, *8*, 814.
- [42] R. Zuo, Y. Ding, *ACS Synth. Biol.* **2019**, *8*, 857-865.
- [43] R. J. Sundberg, *Indoles*, Elsevier, **1996**.
- [44] E. Fischer, F. Jourdan, *Ber. Dtsch. Chem. Ges.* **1883**, *16*, 2241-2245.
- [45] S. M. Parmerter, A. G. Cook, W. B. Dixon, *J. Am. Chem. Soc.* **1958**, *80*, 4621-4622.
- [46] (a) P. Fludzinski, L. A. Wittenauer, K. W. Schenck, M. L. Cohen, *J. Med. Chem.* **1986**, *29*, 2415-2418; (b) A. R. Katritzky, S. Rachwal, S. Bayyuk, *Org. Prep. Proced. Int.* **1991**, *23*, 357-363; (c) H. Singer, W. Shive, *J. Org. Chem.* **1957**, *22*, 84-85.
- [47] B. Narayana, B. Ashalatha, K. V. Raj, J. Fernandes, B. Sarojini, *Biorg. Med. Chem.* **2005**, *13*, 4638-4644.
- [48] A. El Kihel, A. Lagnaoui, T. Harjane, Y. Kattir, S. Guesmi, P. Bauchat, *Arab. J. Chem.* **2013**, *6*, 173-176.

- [49] (a) M. Mąkosza, *Chem. Soc. Rev.* **2010**, 39, 2855-2868; (b) M. Makosza, K. Wojciechowski, *Heterocycles* **2001**, 54, 445-474; (c) M. Mąkosza, K. Wojciechowski, *Chem. Rev.* **2004**, 104, 2631-2666.
- [50] K. Liu, D. Yin, *Org. Lett.* **2008**, 11, 637-639.
- [51] K. Wojciechowski, M. Makosza, *Tetrahedron Lett.* **1984**, 25, 4793-4794.
- [52] R. Bujok, Z. Wróbel, K. Wojciechowski, *Synlett* **2012**, 23, 1315-1320.
- [53] (a) N. Moskalev, M. Barbasiewicz, M. Mąkosza, *Tetrahedron* **2004**, 60, 347-358; (b) N. Moskalev, M. Makosza, *Tetrahedron Lett.* **1999**, 40, 5395-5398.
- [54] N. Moskalev, M. Makosza, *Heterocycles* **2000**, 52, 533-536.
- [55] T. Zieliński, P. Dydio, J. Jurczak, *Tetrahedron* **2008**, 64, 568-574.
- [56] (a) V. V. Rozhkov, A. M. Kuvshinov, V. I. Gulevskaya, I. I. Chervin, S. A. Shevelev, *Synthesis* **1999**, 1999, 2065-2070; (b) V. V. Rozhkov, A. M. Kuvshinov, S. A. Shevelev, *Org. Prep. Proced. Int.* **2000**, 32, 94-96; (c) V. V. Rozhkov, A. M. Kuvshinov, S. A. Shevelev, *Synth. Commun.* **2002**, 32, 1465-1474.
- [57] (a) O. M. Petruk, Y. A. Kyriukha, A. V. Bezudny, V. V. Rozhkov, *J. Fluorine Chem.* **2015**, 175, 176-179; (b) V. V. Rozhkov, *Tetrahedron* **2014**, 70, 3595-3600.
- [58] E. T. Pelkey, G. W. Gribble, *Tetrahedron Lett.* **1997**, 38, 5603-5606.
- [59] B. J. Stokes, S. Liu, T. G. Driver, *J. Am. Chem. Soc.* **2011**, 133, 4702-4705.
- [60] T.-S. Zhang, R. Wang, P.-J. Cai, W.-J. Hao, S.-J. Tu, B. Jiang, *Org. Chem. Front.* **2019**, 6, 2968-2973.
- [61] J. Bergman, P. Sand, U. Tilstam, *Tetrahedron Lett.* **1983**, 24, 3665-3668.
- [62] J. Bergman, P. Sand, *Tetrahedron* **1990**, 46, 6085-6112.
- [63] (a) R. Bernini, G. Fabrizi, A. Sferrazza, S. Cacchi, *Angew. Chem. Int. Ed.* **2009**, 48, 8078-8081; (b) Z.-H. Guan, Z.-Y. Yan, Z.-H. Ren, X.-Y. Liu, Y.-M. Liang, *Chem. Commun.* **2010**, 46, 2823-2825; (c) Z. Shi, F. Glorius, *Angew. Chem. Int. Ed.* **2012**, 51, 9220-9222.
- [64] (a) X.-L. Lian, Z.-H. Ren, Y.-Y. Wang, Z.-H. Guan, *Org. Lett.* **2014**, 16, 3360-3363; (b) J. J. Neumann, S. Rakshit, T. Droege, S. Würtz, F. Glorius, *Chem. Eur. J.* **2011**, 17, 7298-7303; (c) S. Würtz, S. Rakshit, J. J. Neumann, T. Dröge, F. Glorius, *Angew. Chem. Int. Ed.* **2008**, 47, 7230-7233.
- [65] G.-B. Deng, J.-L. Zhang, Y.-Y. Liu, B. Liu, X.-H. Yang, J.-H. Li, *Chem. Commun.* **2015**, 51, 1886-1888.
- [66] R. Sundberg, *J. Org. Chem.* **1965**, 30, 3604-3610.
- [67] G. A. Russell, C. F. Yao, H. I. Tashtoush, J. E. Russell, D. F. Dedolph, *J. Org. Chem.* **1991**, 56, 663-669.
- [68] (a) A. K. Clarke, J. M. Lynam, R. J. Taylor, W. P. Unsworth, *ACS Catal.* **2018**, 8, 6844-6850; (b) S. G. Dawande, V. Kanchupalli, J. Kalepu, H. Chennamsetti, B. S. Lad, S. Katukojvala, *Angew. Chem. Int. Ed.* **2014**, 53, 4076-4080; (c) Y. Li, J. Waser, *Angew. Chem. Int. Ed.* **2015**, 54, 5438-5442; (d) C. Liu, W. Huang, M. Wang, B. Pan, Y. Gu, *Adv. Synth. Catal.* **2016**, 358, 2260-2266; (e) Y. Matsuda, S. Naoe, S. Oishi, N. Fujii, H. Ohno, *Chem. Eur. J.* **2015**, 21, 1463-1467; (f) N. Thies, C. G. Hrib, E. Haak, *Chem. Eur. J.* **2012**, 18, 6302-6308.
- [69] S. Sampaolesi, S. Gabrielli, R. Ballini, A. Palmieri, *Adv. Synth. Catal.* **2017**, 359, 3407-3413.
- [70] (a) L. Bianchi, G. Giorgi, M. Maccagno, G. Petrillo, C. Scapolla, C. Tavani, *Tetrahedron* **2016**, 72, 7050-7058; (b) C. Tavani, L. Bianchi, G. Giorgi, M. Maccagno, G. Petrillo, *Eur. J. Org. Chem.* **2018**, 2018, 126-136.
- [71] (a) L. Bianchi, G. Giorgi, M. Maccagno, G. Petrillo, C. Scapolla, C. Tavani, *Tetrahedron Lett.* **2012**, 53, 752-757; (b) L. Bianchi, M. Maccagno, M. Pani, G. Petrillo, C. Scapolla, C. Tavani, *Tetrahedron* **2015**, 71, 7421-7435.

- [72] L. Bianchi, A. Carloni-Garaventa, M. Maccagno, M. Pani, G. Petrillo, C. Scapolla, C. Tavani, *Tetrahedron* **2015**, *71*, 7550-7561.
- [73] F. Hu, J. P. Ng, P. Chiu, *Synthesis* **2019**, *51*, 1073-1086.
- [74] (a) C. Della Rosa, M. Kneeteman, P. Mancini, *Tetrahedron Lett.* **2007**, *48*, 1435-1438; (b) J. H. Li, J. K. Snyder, *J. Org. Chem.* **1993**, *58*, 516-519; (c) E. Wenkert, P. D. Moeller, S. R. Piettre, *J. Am. Chem. Soc.* **1988**, *110*, 7188-7194.
- [75] D. Giomi, M. Cecchi, *Tetrahedron* **2002**, *58*, 8067-8071.
- [76] C. C. Loh, D. Enders, *Angew. Chem. Int. Ed.* **2012**, *51*, 46-48.
- [77] (a) J.-P. Begue, D. Bonnet-Delpon, B. Crousse, *Synlett* **2004**, *2004*, 18-29; (b) I. A. Shuklov, N. V. Dubrovina, A. Boerner, *Synthesis* **2007**, *2007*, 2925-2943.
- [78] G. H. Christie, J. Kenner, *J. Chem. Soc., Trans.* **1922**, *121*, 614-620.
- [79] M. Ōki, *Top. Stereochem.* **1983**, 1-81.
- [80] (a) A. Miyashita, A. Yasuda, H. Takaya, K. Toriumi, T. Ito, T. Souchi, R. Noyori, *J. Am. Chem. Soc.* **1980**, *102*, 7932-7934; (b) H. Takaya, K. Mashima, K. Koyano, M. Yagi, H. Kumobayashi, T. Taketomi, S. Akutagawa, R. Noyori, *J. Org. Chem.* **1986**, *51*, 629-635.
- [81] (a) G. Bringmann, C. Günther, M. Ochse, O. Schupp, S. Tasler, in *Prog. Chem. Org. Nat. Prod.*, Springer, **2001**, pp. 1-249; (b) A. R. d. Santos, A. C. Pinheiro, A. C. R. Sodero, A. S. d. Cunha, M. C. Padilha, P. M. d. Sousa, S. P. Fontes, M. P. Veloso, C. A. M. Fraga, *Quím.* **2007**, *30*, 125-135.
- [82] (a) J. Clayden, W. J. Moran, P. J. Edwards, S. R. LaPlante, *Angew. Chem. Int. Ed.* **2009**, *48*, 6398-6401; (b) S. R. LaPlante, P. J. Edwards, L. D. Fader, A. Jakalian, O. Hucke, *Chem. Med. Chem.* **2011**, *6*, 505-513.
- [83] (a) J.-C. Kizirian, *Chem. Rev.* **2008**, *108*, 140-205; (b) D. Lucet, T. Le Gall, C. Mioskowski, *Angew. Chem. Int. Ed.* **1998**, *37*, 2580-2627; (c) R. Noyori, *Angew. Chem. Int. Ed.* **2002**, *41*, 2008-2022.
- [84] M. Frisch, G. Trucks, H. Schlegel, G. Scuseria, M. Robb, J. Cheeseman, G. Scalmani, V. Barone, B. Mennucci, G. Petersson, *Gaussian 09 Revision D. 01*, Gaussian Inc. Wallingford CT. See also: URL: <http://www.gaussian.com> **2009**.
- [85] A. Mazzanti, L. Lunazzi, M. Minzoni, J. E. Anderson, *J. Org. Chem.* **2006**, *71*, 5474-5481.
- [86] G. S. Kottas, L. I. Clarke, D. Horinek, J. Michl, *Chem. Rev.* **2005**, *105*, 1281-1376.
- [87] R. Akué-Gédu, L. Nauton, V. Théry, J. Bain, P. Cohen, F. Anizon, P. Moreau, *Biorg. Med. Chem.* **2010**, *18*, 6865-6873.
- [88] (a) C. Dell'Erba, F. Gasparrini, S. Grilli, L. Lunazzi, A. Mazzanti, M. Novi, M. Pierini, C. Tavani, C. Villani, *J. Org. Chem.* **2002**, *67*, 1663-1668; (b) L. Lunazzi, M. Mancinelli, A. Mazzanti, *J. Org. Chem.* **2007**, *72*, 5391-5394; (c) L. Lunazzi, M. Mancinelli, A. Mazzanti, *J. Org. Chem.* **2008**, *73*, 5354-5359.
- [89] J. Bouchard, S. Wakim, M. Leclerc, *J. Org. Chem.* **2004**, *69*, 5705-5711.
- [90] F. Giraud, E. Pereira, F. Anizon, P. Moreau, *Eur. J. Org. Chem.*
- [91] W. Zhang, J. M. Ready, *Nat. Prod. Rep.* **2017**, *34*, 1010-1034.
- [92] (a) D. L. Clive, Z. Li, M. Yu, *J. Org. Chem.* **2007**, *72*, 5608-5617; (b) L. Wang, B. Prabhudas, D. L. Clive, *J. Am. Chem. Soc.* **2009**, *131*, 6003-6012.
- [93] J. E. Baldwin, *J. Chem. Soc., Chem. Commun.* **1976**, 734-736.
- [94] J. Bariwal, L. G. Voskressensky, E. V. Van der Eycken, *Chem. Soc. Rev.* **2018**, *47*, 3831-3848.
- [95] M. E. Welsch, S. A. Snyder, B. R. Stockwell, *Curr. Opin. Chem. Biol.* **2010**, *14*, 347-361.
- [96] E. D. Cox, J. M. Cook, *Chem. Rev.* **1995**, *95*, 1797-1842.
- [97] (a) P. Fedoseev, E. Van der Eycken, *Chem. Commun.* **2017**, *53*, 7732-7735; (b) Q.-F. Wu, H. He, W.-B. Liu, S.-L. You, *J. Am. Chem. Soc.* **2010**, *132*, 11418-11419.

- [98] M. J. James, P. O'Brien, R. J. Taylor, W. P. Unsworth, *Chem. Eur. J.* **2016**, *22*, 2856-2881.
- [99] M. J. James, J. D. Cuthbertson, P. O'Brien, R. J. Taylor, W. P. Unsworth, *Angew. Chem. Int. Ed.* **2015**, *54*, 7640-7643.
- [100] H. E. Ho, T. C. Stephens, T. J. Payne, P. O'Brien, R. J. Taylor, W. P. Unsworth, *ACS Catal.* **2018**, *9*, 504-510.
- [101] L. Buzzetti, G. E. Crisenza, P. Melchiorre, *Angew. Chem. Int. Ed.* **2019**, *58*, 3730-3747.
- [102] (a) H. Cui, W. Wei, D. Yang, J. Zhang, Z. Xu, J. Wen, H. Wang, *RSC Advances* **2015**, *5*, 84657-84661; (b) H. L. Hua, Y. T. He, Y. F. Qiu, Y. X. Li, B. Song, P. Gao, X. R. Song, D. H. Guo, X. Y. Liu, Y. M. Liang, *Chem. Eur. J.* **2015**, *21*, 1468-1473; (c) D.-P. Jin, P. Gao, D.-Q. Chen, S. Chen, J. Wang, X.-Y. Liu, Y.-M. Liang, *Org. Lett.* **2016**, *18*, 3486-3489; (d) Y. Liu, Q.-L. Wang, C.-S. Zhou, B.-Q. Xiong, P.-L. Zhang, C.-a. Yang, K.-W. Tang, *J. Org. Chem.* **2018**, *83*, 2210-2218; (e) C. Pan, B. Huang, W. Hu, X. Feng, J.-T. Yu, *J. Org. Chem.* **2016**, *81*, 2087-2093; (f) W. Wei, H. Cui, D. Yang, H. Yue, C. He, Y. Zhang, H. Wang, *Green Chem.* **2017**, *19*, 5608-5613; (g) J. Wen, W. Wei, S. Xue, D. Yang, Y. Lou, C. Gao, H. Wang, *J. Org. Chem.* **2015**, *80*, 4966-4972; (h) X. H. Yang, X. H. Ouyang, W. T. Wei, R. J. Song, J. H. Li, *Adv. Synth. Catal.* **2015**, *357*, 1161-1166; (i) Y. Zhang, J. Zhang, B. Hu, M. Ji, S. Ye, G. Zhu, *Org. Lett.* **2018**, *20*, 2988-2992.
- [103] (a) M. Feng, B. Tang, S. H. Liang, X. Jiang, *Curr. Top. Med. Chem.* **2016**, *16*, 1200-1216; (b) A. Gangjee, Y. Zeng, T. Talreja, J. J. McGuire, R. L. Kisliuk, S. F. Queener, *J. Med. Chem.* **2007**, *50*, 3046-3053; (c) E. A. Ilardi, E. Vitaku, J. T. Njardarson, *J. Med. Chem.* **2013**, *57*, 2832-2842; (d) B. Le Grand, C. Pignier, R. Létienne, F. Cuisiat, F. Rolland, A. Mas, B. Vacher, *J. Med. Chem.* **2008**, *51*, 3856-3866.
- [104] R. S. Mulliken, *J. Am. Chem. Soc.* **1952**, *74*, 811-824.
- [105] R. Foster, *J. Phys. Chem.* **1980**, *84*, 2135-2141.
- [106] (a) E. Hilinski, J. Masnovi, C. Amatore, J. Kochi, P. Rentzepis, *J. Am. Chem. Soc.* **1983**, *105*, 6167-6168; (b) S. V. Rosokha, J. K. Kochi, *Acc. Chem. Res.* **2008**, *41*, 641-653; (c) J. O. Singh, J. D. Anunziata, J. J. Silber, *Can. J. Chem.* **1985**, *63*, 903-907.
- [107] (a) M. A. Fox, J. Younathan, G. E. Fryxell, *J. Org. Chem.* **1983**, *48*, 3109-3112; (b) T. Gotoh, A. B. Padias, H. Hall Jr, *J. Am. Chem. Soc.* **1991**, *113*, 1308-1312; (c) R. Rathore, J. K. Kochi, **2000**; (d) S. Sankararaman, W. Haney, J. Kochi, *J. Am. Chem. Soc.* **1987**, *109*, 7824-7838.
- [108] (a) C. G. Lima, T. de M. Lima, M. Duarte, I. D. Jurberg, M. W. Paixao, *ACS Catal.* **2016**, *6*, 1389-1407; (b) L. Marzo, S. Wang, B. König, *Org. Lett.* **2017**, *19*, 5976-5979; (c) V. Quint, F. Morlet-Savary, J.-F. o. Lohier, J. Lalevee, A.-C. Gaumont, S. Lakhdar, *J. Am. Chem. Soc.* **2016**, *138*, 7436-7441; (d) M. L. Spell, K. Deveau, C. G. Bresnahan, B. L. Bernard, W. Sheffield, R. Kumar, J. R. Ragains, *Angew. Chem. Int. Ed.* **2016**, *55*, 6515-6519; (e) J. Zhang, Y. Li, R. Xu, Y. Chen, *Angew. Chem. Int. Ed.* **2017**, *56*, 12619-12623.
- [109] Z.-Y. Cao, T. Ghosh, P. Melchiorre, *Nat. Commun.* **2018**, *9*, 3274.
- [110] L. Bianchi, M. Maccagno, G. Petrillo, F. Sancassan, D. Spinelli, C. Tavani, *Targets in heterocyclic systems: chemistry and properties* **2006**, *10*, 1-23.
- [111] S. Superchi, P. Scafato, M. Gorecki, G. Pescitelli, *Curr. Med. Chem.* **2018**, *25*, 287-320.
- [112] C. E. Check, T. M. Gilbert, *J. Org. Chem.* **2005**, *70*, 9828-9834.
- [113] O. P. a. P. International, *In Gaussian 09 the BH&HLYP functional has the form: 0.5*EXHF + 0.5*EXLSDA + 0.5*ΔEXBecke88 + ECLYP.*
- [114] Y. Zhao, D. G. Truhlar, *Theor. Chem. Acc.* **2008**, *120*, 215-241.
- [115] J.-D. Chai, M. Head-Gordon, *Phys. Chem. Chem. Phys.* **2008**, *10*, 6615-6620.
- [116] T. Yanai, D. P. Tew, N. C. Handy, *Chem. Phys. Lett.* **2004**, *393*, 51-57.

- [117] (a) M. Ambrogi, A. Ciogli, M. Mancinelli, S. Ranieri, A. Mazzanti, *J. Org. Chem.* **2013**, 78, 3709-3719; (b) G. Cera, M. Chiarucci, A. Mazzanti, M. Mancinelli, M. Bandini, *Org. Lett.* **2012**, 14, 1350-1353; (c) E. Martinelli, A. C. Vicini, M. Mancinelli, A. Mazzanti, P. Zani, L. Bernardi, M. Fochi, *Chem. Commun.* **2015**, 51, 658-660.
- [118] M. A. Cismesia, T. P. Yoon, *Chem. Sci.* **2015**, 6, 5426-5434.
- [119] K. Liang, N. Li, Y. Zhang, T. Li, C. Xia, *Chem. Sci.* **2019**, 10, 3049-3053.
- [120] T. J. Fyfe, B. Zarzycka, H. D. Lim, B. Kellam, S. N. Mistry, V. Katrich, P. J. Scammells, J. R. Lane, B. Capuano, *J. Med. Chem.* **2018**, 62, 174-206.